Copolymerization of Norbornene with Conjugated Hydrocarbon Monomers using Anilinonaphthoquinone-ligated Nickel Complexes

（アニリノナフトキノン配位子を有するニッケル錯体によるノルボルネンと共役系炭化水素モノマーとの共重合）

MD. SAMIUL ISLAM CHOWDHURY

Polymer Chemistry Laboratory

Hiroshima University

March 2020

Contents

Abbreviation

AIBN	2,2′-azobisisobutyronitrile
Al	aluminum
Ar	aryl
atm	atmospheric pressure
BD	butadiene
m-CPBA	3-chloroperoxybenzoic acid
CDN	conjugated diene
COP	cyclic olefin polymer
COC	cyclic olefin copolymer
^{o}C	degree Celsius
DSC	differential scanning calorimetry
dMAO	dried methylaluminoxane
DVB	divinylbenzene
ENC	ethylene-norbornene copolymer
g	gram(s)
GPC	gel permeation chromatography
GPa	gigapascal
h	hour (s)
Hz	hertz
IBAO	isobutylaluminoxane
IP	isoprene
^{i}Pr	isopropyl
L	liter (s)
m	milli
MAO	methylaluminoxane
MMAO	modified methylaluminoxane

Me	methyl
min	minute (s)
μ	micro
M_n	number-average molecular weight
M_w	weight-average molecular weight
MMA	methyl methacrylate
mol	mole(s)
M_w/M_n	molecular weight distributions
MPa	megapascal
N	number of polymer chains
NMR	nuclear magnetic resonance
NB	norbornene
ODCB	*ortho*-dichlorobenzene
ppm	parts per million
PNB	polynorbornene
R	alkyl
RATRP	reverse atom transfer radical polymerization
ROMP	ring opening metathesis polymerization
s	second
St	styrene
THF	tetrahydrofuran
T_g	glass transition temperature
XSt	*para*-substituted-styrene (X: -OMe, -Me, -F, -Cl and -Br)

Chapter I

General Introduction

1-1. Cyclic Olefin Polymers

Cyclic olefin polymers (COPs) are attracting great attention because they possess unique structures with attractive properties. Their application expands from optical accessories to medical equipment.[1-3] Among various performance parameters of COPs, a high glass transition temperature (T_g) is the most attractive one as its thermal stability of COPs. A monomer with a large steric hindrance is necessary to achieve high T_g. Cyclic olefins are commercially available from a handful of pilot-scale plants around the world. Current world production of these resins is around 20 million lb/yr. The three most important cycloolefin monomers are norbornene, cyclopentadiene, and dicyclopentadiene. Norbornene is highly used monomer among the cyclic olefins because of their high homo- and copolymerization ability to exposed diverse application.

1-2. Norbornene (NB)

Bicyclo [2.2.1]hept-2-ene, known as NB is usually produced by the Diels-Alder reaction of cyclopentadiene and ethylene (**Scheme 1-1**). It

possesses ring strain that causes the double bond highly active. It is colorless substance, melts at 46 °C and boils at 96 °C. It is commercially available.

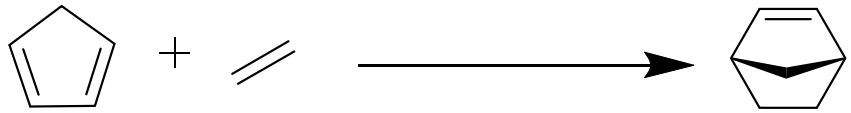

Scheme 1-1: Synthesis of NB.

1-3. Types of NB Polymerization

NB can be polymerized in three different types of mechanism, that is, (i) ring opening metathesis polymerization (ROMP), (ii) cationic or radical polymerization and (iii) coordination-insertion polymerization (**Scheme 1-2**).[4] Each route through the choice of catalyst leads to its own polymer type which is different in structure and properties from the other two.

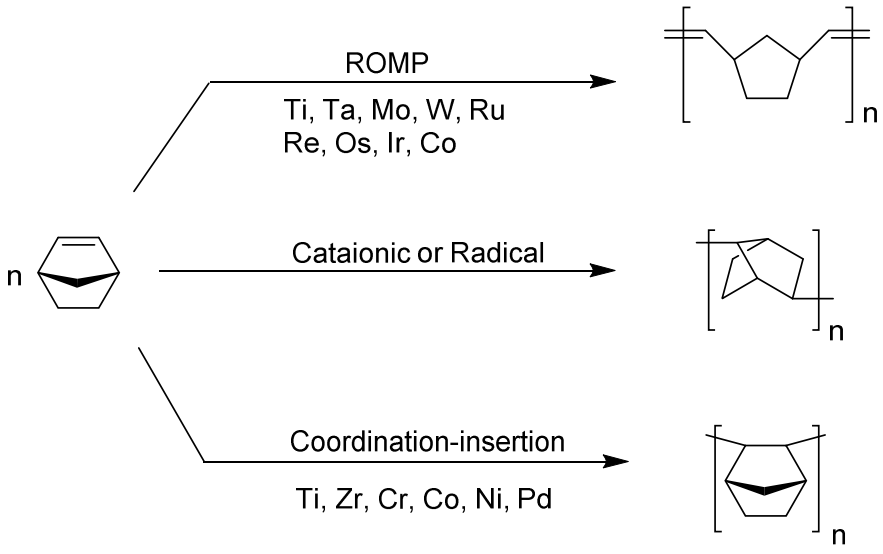

Scheme 1-2. Different methods of polymerization of NB.

1-3-1. Ring Opening Metathesis Polymerization (ROMP)

In 1984, a COP is obtained by ROMP of NB derivative followed by hydrogenation was carried out by Yamazaki and collaborators from Zeon Company in Japan.[1]

Ring opening metathesis polymerization (ROMP) is one of the well-known methods for NB polymerization.[5] The polymer obtained by ROMP is a polyalkenamer which contains double bonds in the polymer backbone (**Scheme 1-3**). The double bonds of the polymer chains can be cross linked through vulcanization. The vulcanized polynorbornene (PNB) product is used as an elastomeric material for vibration and sound damping. This product has varieties of applications such as engine mounts, shock-proof bumpers, and flexible couplings. In addition, porous PNB is a good soaking material for oil spills and absorbing capacity up to 400% of their own mass.

In general, $RuCl_3$/HCl in butanol used as a catalyst for commercial polymerization. While the heterogeneous catalysts are usually used in industry. Academic research has focused on molecular single-site catalysts with metal–carbene complexes, for example, W,[6,7] Mo[8,9] and Ru[10,11] complexes. A variety of transition metal catalyst systems based on Ti, Zr, Hf, V, Nb, Ta, Os and Rh has been reported for ROMP of NB.[12-18]

The control of stereochemistry in PNB depend on the reaction conditions such as catalyst, activator, solvent and temperature. The $ReCl_5$/$EtAlCl_2$/ethyl

acrylate catalyst system produced *cis*-PNB and *trans*-PNB was obtained with the system of $IrCl_3 \cdot xH_2O/EtAlCl_2$. The T_g value increases with increasing the stereoregularity in PNB. The introduction of tacticity increased the permeability coefficient and improved stability of the polymer.[19]

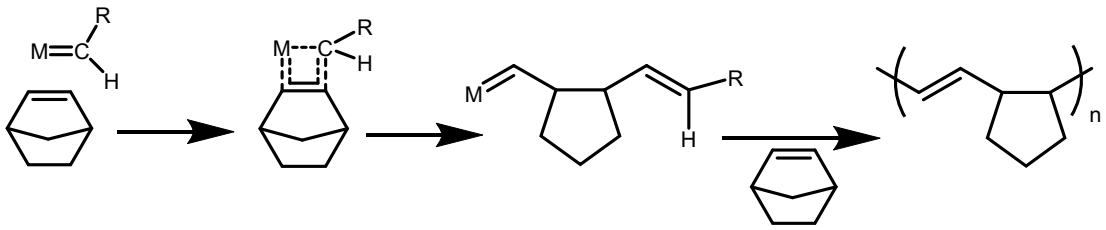

Scheme 1-3. Mechanism of ROMP

1-3-2. Cationic and Radical Polymerization

Some research works have reported on the cationic and radical polymerization of NB. This first report on PNB was described in 1967.[20] The low molar mass oligomeric material was obtained with 2,7-connectivity of the monomer. Initiators such as azoisobutyronitrile (AIBN), tert-butyl peracetate or tert-butyl peroxypivalate were used for the radical polymerization and cationic polymerization started with $EtAlCl_2$.[20-23]

1-3-3. Coordination-insertion Polymerization

NB can be polymerized with adding only the double bond of the component and the bicyclic structural unit remains unchanged (**Scheme 1-4**). The polymerization is such like the vinyl polymerization of olefin via coordination-insertion mechanism and the polymer chain does not contain any double bonds.[24-26] The coordination-insertion polymerization of NB can take place as a homo- and copolymerization.

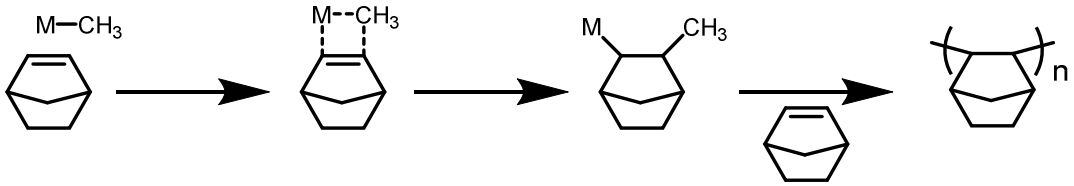

Scheme 1-4. Mechanism of coordination-insertion polymerization of NB.

These PNBs possess high glass transition and decomposition temperatures which comprise good adhesion to films and substrates, thermal stability, high elongation-to-break values, and low stress.[27] Furthermore, the polymeric films show low water uptake, good heat resistance, excellent in transparency, unchanged viscoelastic, low optical birefringence and dielectric loss.[28] Films are also applied as cover layers for liquid-crystal displays. Some polymers designed as promising materials for future photoresist resins.[29,30]

1-3-3-1. Metal Complexes

A large number of metal catalysts are used for coordination-insertion polymerization of NB. According to their metal composition, the catalysts are divided into two groups: (a) the early transition (e. g. Ti and Zr) metal complexes and (b) late transition metal (e. g. Co, Cu, Fe, Ni and Pd) complexes.

1-3-3-2. Activators for Catalysts

Trialkylaluminium and alkylaluminium chloride are significant components in classical heterogeneous Ziegler-Natta coordination polymerization catalysis. The highly efficient activator known as "methylaluminoxane" (MAO) is the hydrolysis product of trimethylaluminium discovered by Kaminsky and Shin (**Scheme 1-5**).[31]

MAO increases the activity of metallocene catalysts up to six order of magnitude relative to alkylaluminiums. MAO obtained from a controlled hydrolysis of Me_3Al by crystal water of $CuSO_4 \cdot 5H_2O$, $MgCl_2 \cdot 6H_2O$ or $Al_2(SO_4)_3 \cdot$14-18 H_2O is a mixture of oligomeric product $[\text{-Al(Me)O-}]_n$ (n = 5-20) and residual Me_3Al.[32] Despite of extensive research, the exact composition and the structure of MAO are still not clear.[33] It is difficult to clarify the structure of MAO because of the presence of multiple equilibriums in MAO solution. Two types of Me_3Al are detected in MAO solution, i.e., free Me_3Al and associated Me_3Al.

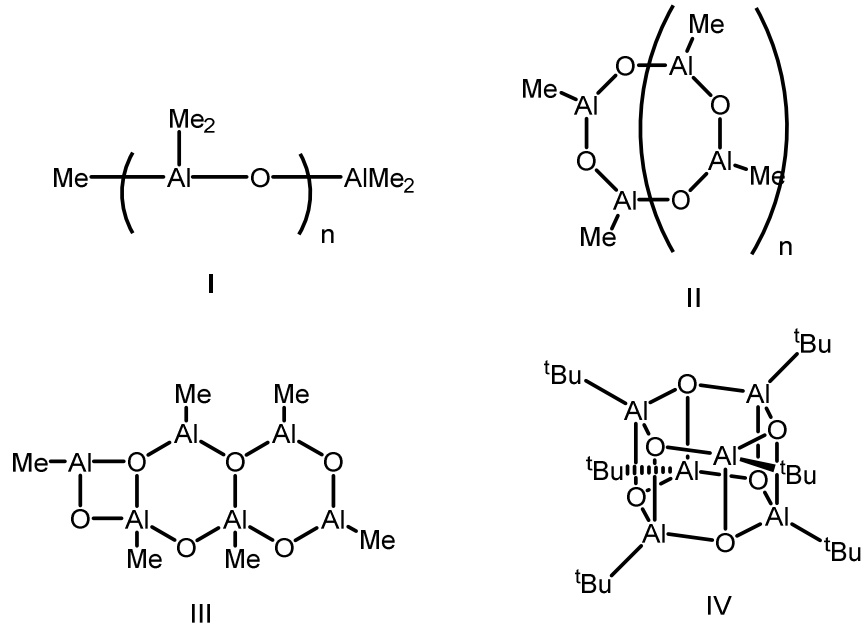

Scheme 1-5. Proposed structures of methylaluminoxane (MAO): (I) linier; (II) cyclic; (III) two-dimensional; (IV) three-dimensional cage.

MAO is an expensive material. It is normally stored in toluene or other hydrocarbon solvents. It tends to precipitate in solution over time and form gels. In the MAO solution, the residual Me_3Al appears to interconvert various MAO oligomers, which is the problem of this material.

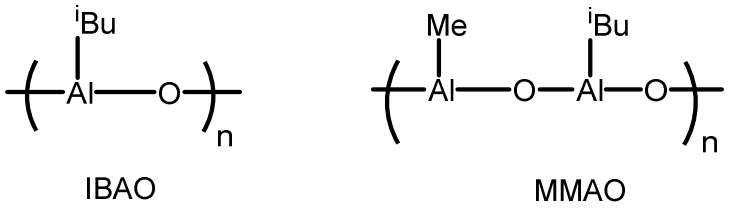

Scheme 1-6. Structures of isobutylaluminoxane (IBAO) and modified methylaluminoxane (MMAO).

Isobutylaluminoxane (IBAO) was synthesized from $^{i}Bu_3Al$ and H_2O in order to reduce the cost and improve the solubility. The modified methylaluminoxane (MMAO) was synthesized from the hydrolysis of the mixture of $^{i}Bu_3Al$ and Me_3Al to reduce the residual Me_3Al and production cost (**Scheme 1-6**). MMAO has better solubility and stability than MAO.

Except organoaluminium compounds described above, boron-based compounds have been discovered as activators for metallocene catalyst, and many of them contain fluorinated aromatic groups. Pentafluorophenyl-substituted activators such as tris(pentafluorophenyl)borane and various salts of tetrakis(pentafluorophenyl)borate are used for metallocene catalysts (**Scheme 1-7**).

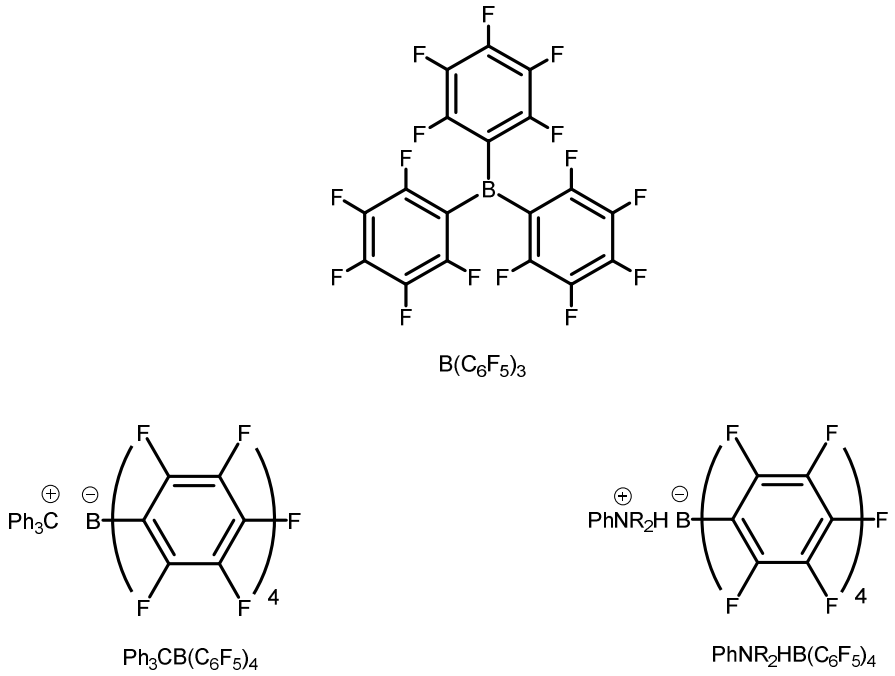

Scheme 1-7. Structures of borane and borates.

Role of Activators

The activators play the key role in the polymerization of olefins with transition metal complexes. MAO is the most used activator.

Firstly, MAO alkylates a halogenated metallocene complex. Monomethylation takes place within second and an excess MAO leads to dimethylated species (**Scheme 1-8**).

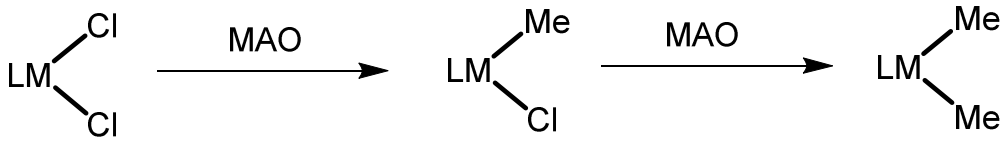

Scheme 1-8. Reaction of metallocene and MAO.

Secondly, MAO abstracts a methyl anion from the metallocene, forming a $(MeMAO)^-$ anion which can distribute the electron over the whole cage, and thus stabilizes the metal cation (**Scheme 1-9**).[34]

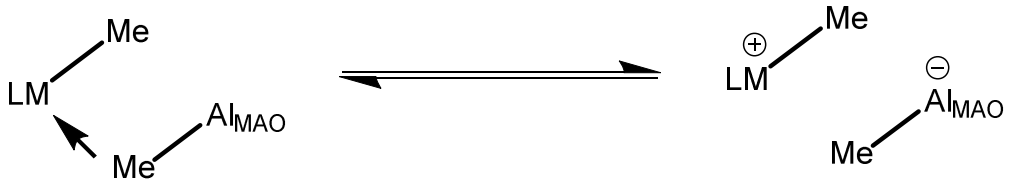

Scheme 1-9. Plausible ion-pair of metal cation and anion produced by MAO.

The metal cation of $LM(CH_3)^+$ formed is weakly coordinated with the anion and shows activity for olefin polymerization. MAO can also work as a scavenger to remove water and oxygen from the reaction mixture.

In the case of boron compounds, the cationic species is formed by abstraction of CH_3^- from a dimethyl metal complex with a strong Lewis acid like $B(C_6F_5)_3$. The labile cation-anion ion-pair allows olefin for insertion.[35] Trityl cation (Ph_3C^+) and ammonium cation (HNR_3^+) are powerful alkyl abstracting and protonolysis reagents, respectively, which give the cation with the non-coordinating and/or weakly coordinating anion $B(C_6F_5)_4^-$. Therefore, several borates have been developed as an effective activator (**Scheme 1-10**).

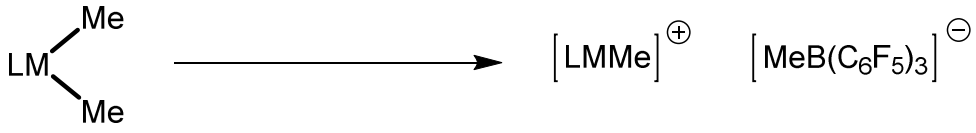

Scheme 1-10. Plausible ion-pair of metal cation and methylborate anion produced by $B(C_6F_5)_3$.

The ratio of MAO to metallocene is around 5000:1 for highly active systems, whereas the ratio of borate to metallocene is 1:1. The borate system is very sensitive to moisture and oxygen. As a result, highly pure system or a scavenger is necessary.

1-3-3-3. Early Transition Metal Catalysts

Titanium Catalysts

The first coordination polymerization of NB was carried out with a $TiCl_4$-Al^iBu_3 catalyst with an Al:Ti ratio of 1:2 in the early 1960's.[36] The high molecular weight of PNB was obtained using the $TiCl_4$-$LiAl(C_7H_{15})_4$ catalytic system.[36]

PNB was obtained with the series of β-diketonate titanium complexes activated by MAO in the highest activity of 8.4 x 10^3 $g_{polymer}$ mol_{Ti}^{-1} h^{-1}.[37]

The half-sandwich titanocene catalysts (^{t}BuN-Me_2Si-Flu)$TiMe_2$ (**Ti-1**) and (^{t}BuN-Me_2Si-Me_4Cp)$TiMe_2$ (**Ti-2**) was activated with Me_3Al-free MAO (dried MAO, dMAO) for the coordination-insertion polymerization of NB (**Scheme 1-11**).[38] **Ti-1** showed high activity at 20 and 40 °C but low activity at 0 °C, and **Ti-2** showed very low activity even at 40 °C.

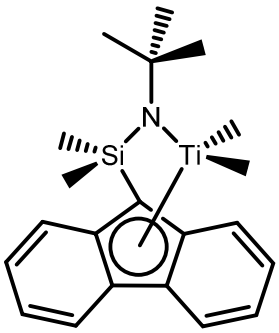

Ti-1

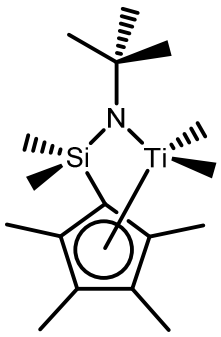

Ti-2

Scheme 1-11. Half-sandwich titanocene catalysts.

Each catalytic system such as **Ti-1**/dMAO, **Ti-1**/MMAO, and **Ti-1**/borate/Oct_3Al showed good activity over a wide range of reaction temperatures. The **Ti-1**/borate/R_3Al system showed the overall highest activities up to 4.8×10^6 $g_{polymer}$ mol_{Ti}^{-1} h^{-1} compared to the dMAO and MMAO system.[38] The highest conversion of 69 % PNB was obtained by $CpTi(OBz)_3$/MAO catalytic system at 60 °C.[39]

Zirconium Catalysts

A number of zirconocenes, Cp_2ZrCl_2, *rac*-$Et(Ind)_2ZrCl_2$, *rac*-$Et(H_4Ind)_2ZrCl_2$, *rac*-$Me_2Si(Ind)_2ZrCl_2$, *meso*-$Me_2Si(Ind)_2ZrCl_2$, $Me_2C(flu)(Cp)ZrCl_2$, and $Ph_2C(flu)(Cp)ZrCl_2$, showed very low activity for coordination-insertion polymerization of NB, and the PNBs produced were insoluble in common organic solvent.[40]

The coordination-insertion polymerization of NB with zirconocenes in the presence of methylaluminoxane or borate has also been described in several patents.[41]

1-3-3-4. Late Transition Metal Catalysts

Chromium Catalysts

Coordination-insertion polymerization of NB using the chromium(III) complex bearing a bulky bis(imino)pyridyl ligand activated with MAO (Al/Cr ratio = 500) showed moderate activity of 3.5×10^2 $g_{polymer}$ mol_{Cr}^{-1} h^{-1}.[42] The activity increased by binuclear chromium(III) complexes $[Cp'CrMeCl]_2$ activated with MAO up to 1.8×10^4 $g_{polymer}$ mol_{Cr}^{-1} h^{-1}.[43] The same activity obtained for the coordination-insertion polymerization of NB when the polynuclear cage-type heterometallic carboxylate complexes were used.[44]

Iron Catalysts

Only a few studies were reported regarding the iron complexes used as catalysts for the coordination-insertion polymerization of NB. Iron complexes bearing bulky chelating tridentate bis(imino)pyridyl ligands gave activity of 9.25×10^3 $g_{polymer}$ mol_{Fe}^{-1} h^{-1} once activated with MAO.[45] Furthermore, polynuclear homo- and heterometallic carboxylate complexes were used for the coordination polymerization of NB and the highest activity was obtained around 10^7 $g_{polymer}$ mol_{Fe}^{-1} h^{-1} after activation with MAO. [44]

Cobalt Catalysts

A series of cobalt(II) complexes having terpyridine derivatives as tridentate *N*-donor ligands showed very low conversions when activated with

MMAO. Thus, dMAO was chosen as cocatalyst and applied as a solution in chlorobenzene which led to a drastic increase of the conversion up to > 99% and activities calculated as 6.7 $\times 10^3$ $g_{polymer}$ mol_{Co}^{-1} h^{-1}.[46] The complexes bearing bulky bis(imino)pyridyl ligands with different substituents were introduced on the aryl groups of the imine functions. The closely related precatalysts which was modified either the electron density at the metal atom or the steric demand around the catalytic center.[47,48] The polymerization activity increased up to 10^4. Co complexes with *N*,*O*-chelating trans bis(*β*-ketoiminato) ligands was activated with MAO towards coordination polymerization of NB.[47,48] The obtained polymer was of high molecular weight of around 10^6 g mol^{-1}.[49] The iminato-R substituent had a strong influence on the catalytic activity of the order of **Co-5** > **Co-4** ≥ **Co-3** > **Co-2** > **Co-1** (**Scheme 1-12**).[50]

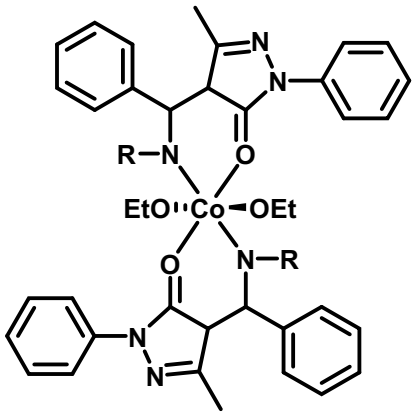

Co-1 R= *p*-fluorophenyl
Co-2 R= phenyl
Co-3 R= *o*-tolyl
Co-4 R= *p*-nitrophenyl
Co-5 R= 1-napthyl

Scheme 1-12. Bis(*β*-ketoiminato) cobalt complexes.

Palladium Catalysts

In 1966, the first coordination-insertion polymerization of NB was reported with palladium catalysts using $PdCl_2$.[51] The coordination-insertion polymerization of NB was conducted with $[Pd(CH_3CN)_4(BF_4)_2]$ in nitrobenzene at 25 °C and the yield was observed more than 90% after 5 min.[52] The living polymerization of NB proceeded with the same Pd(II) complex when a mixture of nitrobenzene and chlorobenzene was used as solvent.

The Pd(II) complexes with α-dioxime ligands were investigated with the different activators MAO, $B(C_6F_5)_3/Et_3Al$ and $B(C_6F_5)_3$ alone for NB polymerization. The activities covered a range between 1.2×10^4 and 3.2×10^7 $g_{polymer}$ mol_{Pd}^{-1} h^{-1}. The highest activity was obtained which similar for MAO or $B(C_6F_5)_3/Et_3Al$ but lower for the borane.[53] Pyrazolylpyridine Pd complexes in combination with MAO showed a moderate activity but the better activity obtained by the Pd complex with pyrrole-iminato and diamine ligand.[54]

Palladium methyl complexes bearing N-heterocyclic carbenesulfonate ligands with MAO exhibited high polymerization activities of up to 10^8 $g_{polymer}$ mol_{Pd}^{-1} h^{-1}.[55] Recently, aryloxide imidazolidin-2-imine bidentate bearing five and six-membered chelate neutral Pd(II) complexes with MAO showed high activity around 10^7 $g_{polymer}$ mol_{Pd}^{-1} h^{-1}.[56] The activity slightly reduced with $EtAlCl_2$ but the molecular weight increases up to 327000.

The neutral salicylaldiminato Pd(II) complexes (Pd-I, -II & -III) in combination with MMAO exhibited extremely high polymerization activities of

more than 10^8 $g_{polymer}$ mol_{Pd}^{-1} h^{-1}.[57] and the activity is the highest up to date among the Pd catalysts used for NB polymerization.

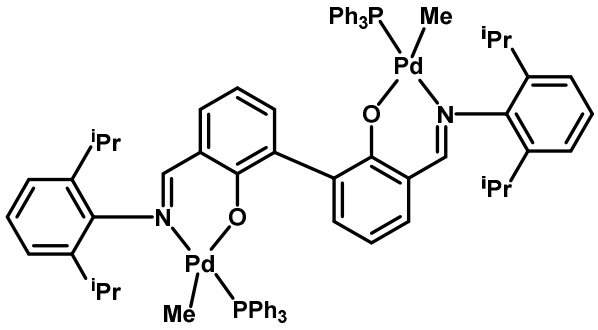

Pd-I

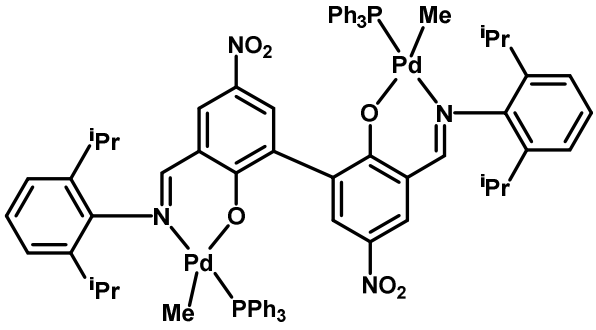

Pd-II

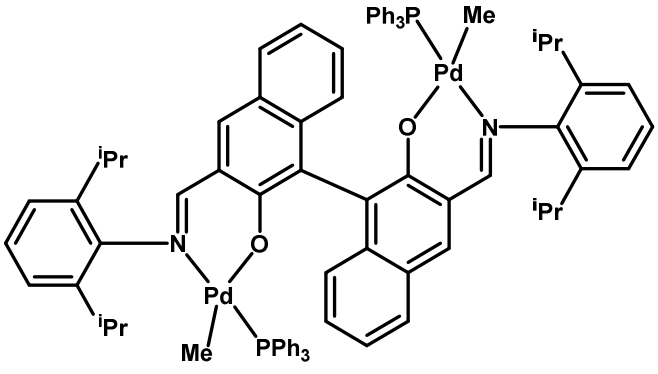

Pd-III

Scheme 1-13. Highly active salicylaldiminato Pd(II) complexes.

It was also found that the palladium complexes with pyridine exhibited much lower activities than those with PPh_3. Therefore, it was assumed that the bulky PPh_3 dissociates more easily than the small pyridine under activation with MMAO (**Scheme 1-13**).

Nickel Catalysts

The first studies Ni-based (**Ni-1**) catalytic systems were used without cocatalyst for the coordination polymerization of NB in 1993.[58]

The number of publications in this field has increased sharply. The simplest systems are composed of Ni(II) carboxylates or nickel acetylacetonate with MAO, and exhibit high initial activity more than 10^4 $kg_{polymer}$ mol_{Ni}^{-1} h^{-1}, which is several orders of magnitude higher than the activity of zirconocene systems.[59] $Ni(acac)_2$ was found to be more active than Ni(2-ethylhexanoate)$_2$, although the rate profiles were similar.

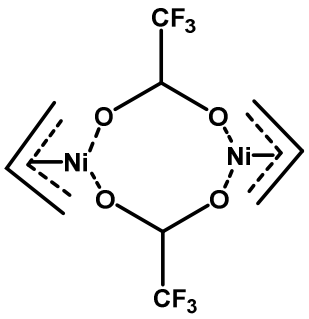

Ni-1

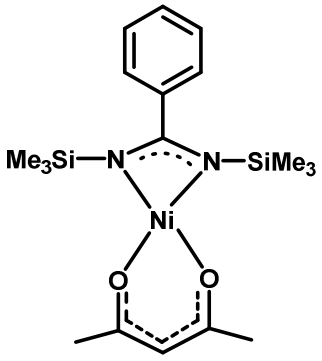

Ni-2

Precatalyst **Ni-2** was activated with MAO to show moderate activities around 10^5 $g_{polymer}$ mol_{Ni}^{-1} h^{-1} depending on the reaction conditions.[60] It was shown that the activities increased with rising a Al/Ni ratio up to 500 and then decreased again. The molecular weights of the PNBs increased up to a molar Al/Ni ratio of ~100. The effect of polymerization temperature was investigated from 70 to 0 °C. The resulted polymer yield and molecular weights showed maximum at 25 °C. These results indicated that higher temperatures induced some deactivation of the active sites in addition to more effective termination pathways.

The chiral benzamidinato nickel complexes (**Ni-3**) were activated with MAO and exhibited higher activities for NB polymerization of around 10^6 $g_{polymer}$ mol_{Ni}^{-1} h^{-1}.[61] The steric demand of the ligands slightly influenced the catalytic activities, which increased with increasing bulk in the substituents.

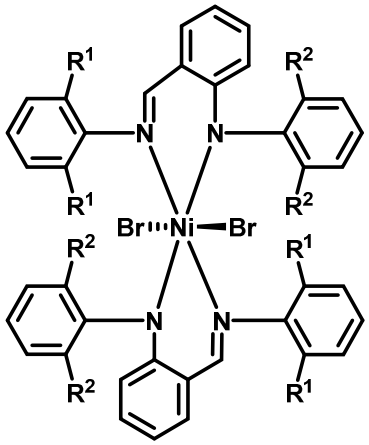

Ni-3

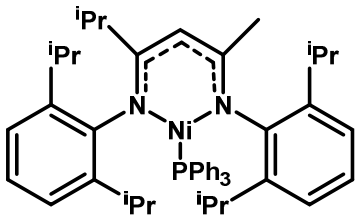

Ni-4

The nickel(I) complex (**Ni-4**) bearing a β-diketiminato ligand activated with MMAO was able to perform the polymerization with high activities of more than 10^7 $g_{polymer}$ mol_{Ni}^{-1} h^{-1}.[62] The catalyst was active over a wide range of temperatures. There was practically no loss in activity when the temperature was varied from 0 to 60 °C.

The nickel(II) imino-pyrrolylato chelate complexes (**Ni-5**) performed the coordination-insertion polymerization of NB with very high activities of more than 10^7 $g_{polymer}$ mol_{Ni}^{-1} h^{-1} in the presence of MMAO.[63] Bulky substituents in the *ortho*-position of nitrogen hindered the insertion of NB and lowered the activity.

Precatalysts (**Ni-6**) bearing bipyridine ligands were highly active in the presence of MMAO with activities in the range of 10^7–10^8 $g_{polymer}$ mol_{Ni}^{-1} h^{-1}. The activities increased slightly with increasing the bulkiness of the substituent.[64]

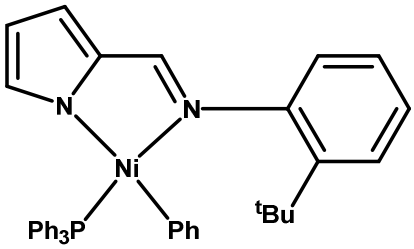

Ni-5

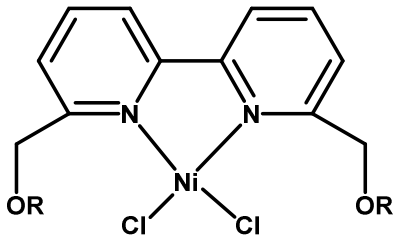

Ni-6

The nonchelating monodentate pseudo-tetrahedral benzimidazole nickel(II) catalysts (**Ni-7**)/MAO showed very high catalytic activities in a range of 5×10^8 (**Ni-7c**/MAO) to 1.7×10^9 $g_{polymer}$ mol_{Ni}^{-1} h^{-1} depending on the reaction conditions. The lower activity of the system **Ni-7c**/MAO was due to its lower steric demand and electronic poor nature.[65] The catalysts showed the highest activity and molecular weight up to 1.8×10^6 g/mol among the catalysts used for NB polymerization up to date.

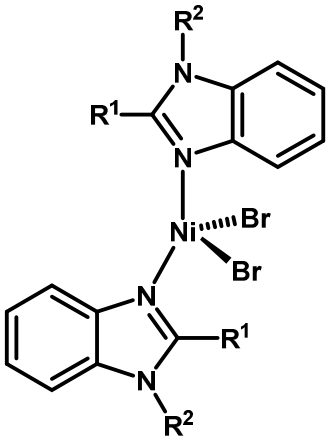

Ni-7

a; R^1 = 2,6-diflurophenyl, R^2 = H
b; R^1 = 2,6-diflurophenyl, R^2 = 2,6-diflurobenzyl
c; R^1 = Me, R^2 = H
d; R^1 = 2-methoxyphenyl, R^2 = 2-methoxybenzyl

Ni-8 with salicylaldiminato ligand afforded very high activities of more than 10^7 $g_{polymer}$ mol_{Ni}^{-1} h^{-1} activated with MMAO as cocatalyst.[66] High molecular weight PNBs were obtained in all conditions. **Ni-9** activated with MAO was a very efficient catalyst with activities of more than 10^8 $g_{polymer}$ mol_{Ni}^{-1} h^{-1} and there was no influence of the ligand with the similar structures.[67]

Complexes with higher steric hindrance can afford higher activities. Recently, novel aryloxide imidazolidin-2-imine bidentate bearing five and six-membered chelate neutral Ni (II) complexes with MAO showed high activity with very high molecular weight increases up to 745000.[56,68]

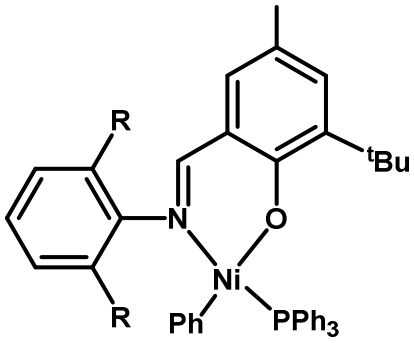

Ni-8

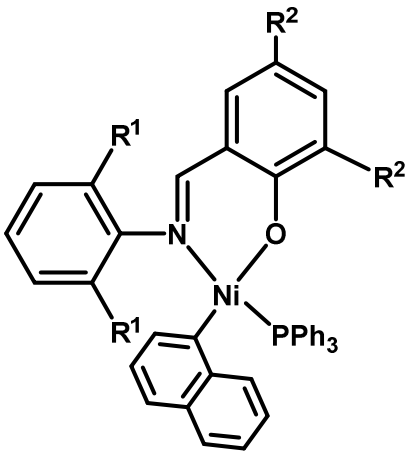

Ni-9

Activity Comparison

An overview of the catalytic systems used for NB polymerization is summarized in the review report of Blank *et. al.* [69] The report clears that the precatalysts based upon nickel and palladium show the highest activities. It is notable that the nickel catalysts deal with the largest number of publications. These nickel catalysts also reflected in the wide range of activity values. Most nickel catalysts exhibit activities of 10^5 $g_{polymer}$ mol_{Ni}^{-1} h^{-1}or higher (**Figure 1-1**). Precatalysts bearing *N*,*O*-coordinating salicylaldiminato or β-ketoiminato ligands show activities of at least 10^6 $g_{polymer}$ mol_{Ni}^{-1} h^{-1}.

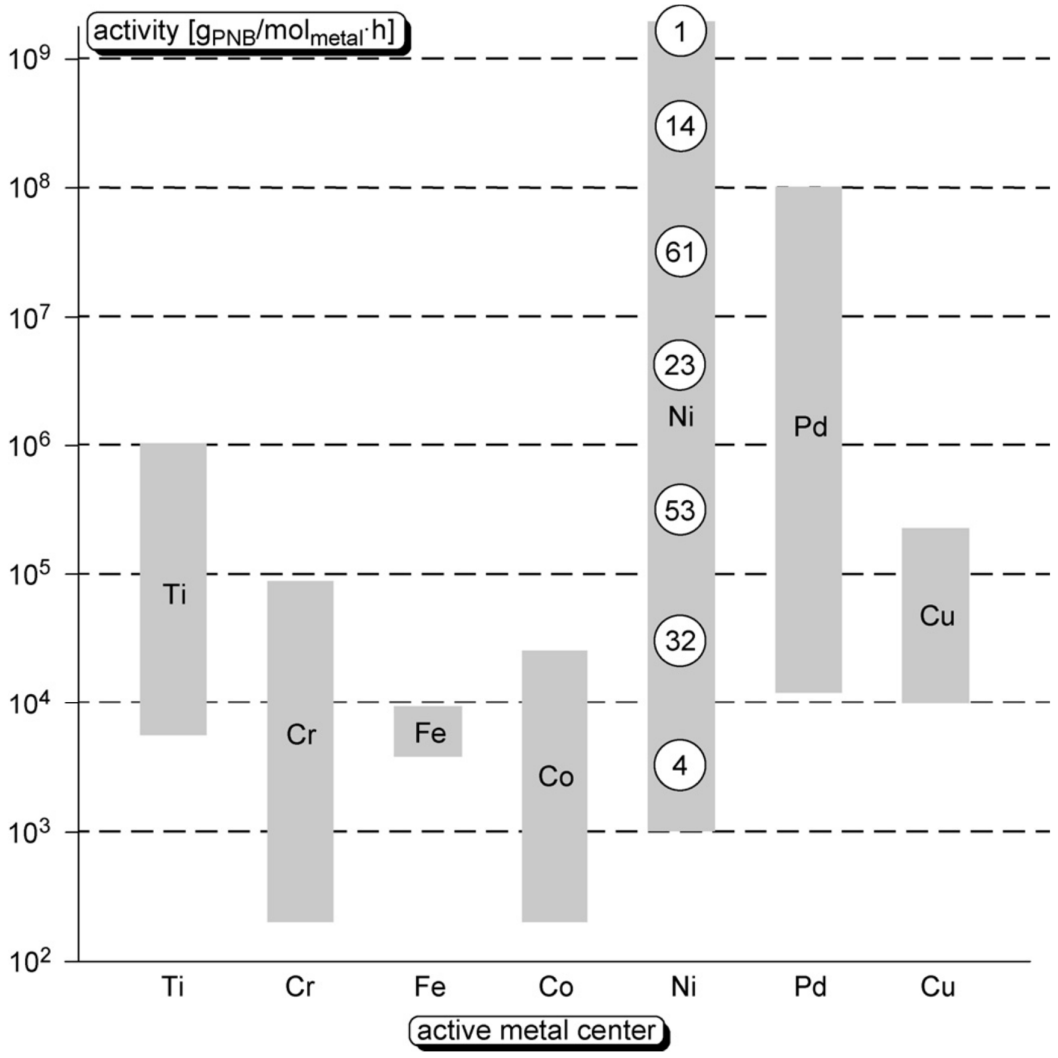

Figure 1-1: Activity ranges of the different metal catalysts for the coordination-insertion polymerization of NB. [69]

Homopolymerization of NB

Early Transition Metal Complexes ⟶ **Low activity**

Late Transition Metal Complexes ⟶ **High activity**

1-4. Cyclic Olefin Copolymers

The widespread application of PNB has some limitation by its low solubility, mechanical brittleness and poor processability because of high T_g close to the decomposition temperature. The inferior properties are improved in cyclic olefins copolymers (COCs).

COCs such as ethylene/norbornene copolymer (ENC) were firstly synthesized in the late 1950s but commercial productions are relatively new by copolymerization of a cyclic monomer (NB or 8,9,10-trinorborn-2-ene) and ethylene. They exhibit very potential physico-chemical properties such as high heat and chemical resistance, rigidity, glass-like transparency and low permeability to gas and water.[70-74] These features make interest of COC for many applications. COC is used in optics to make compact discs, magneto-optic storage discs, light grids and other optical devices due to their good optical and mechanical properties. COC can replace polypropylene in thin film capacitors because of their good dielectric resistance over a wide temperature range. COC is also used in housing, gears and colour toner binder resin. COC also focuses on medical and pharmaceutical applications: the primary packaging for drugs in solid form (blisters) and in liquid form of particularly for injectable formulations.[73,75] Additionally, they are extensively used in the field of diagnostics for microwell plates like microfluidic devices and bio diagnostic chips.[76] They have attracted considerable recent attention as substrate for biochips because COC has a low density and low autofluorescence.[76,77] COC is

also used for biosensor technology such as DNA immobilization, microarrays, nucleic acid purification and immunoassays.[78] The creation of bone replacement materials has also been reported using the blend of COC with polyethylene.[79] Studies have also been proceeded in other fields concerning the formation of COC nanoparticles, COC/silica nanocomposites foams and the processability of COC yarn by melt spinning.[80] Recently, a research work has been published concerning the modification of cyclic olefin copolymer in order to conduct to new electrochromatographic stationary phases.[81]

Generally, COC introduce the amorphous class of polymer. These materials are becoming economically important day by day. The first commercial products became available at the end of the 1980s using the Ziegler–Natta catalysts.[82]

The structure is shown in **Figure 1-2.** ENC is a 2,3-connected rotationally strongly constrained cyclic olefin copolymer. It possesses high thermal stability having high T_g with excellent optical transparency and low birefringence.

The nature and geometry of the catalyst used in the synthesis can control the microstructure of ENCs.[83] Copolymers with different properties were obtained by changing the catalyst system. To form blocks of cyclic monomer units and different stereoregularities within the NB blocks are depended on the ability of metallocene.[69]

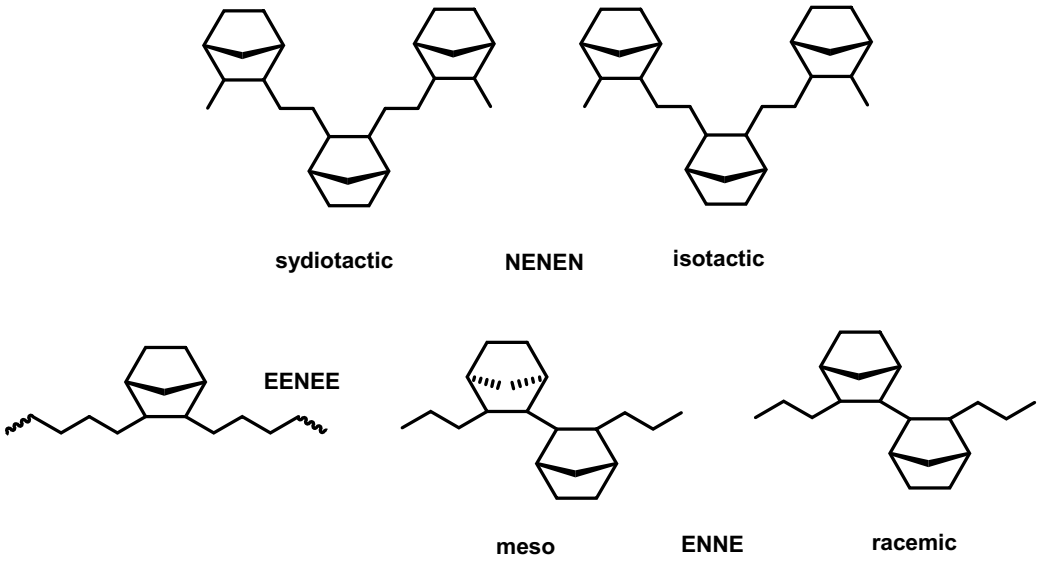

Figure 1-2. Different sequences of ENC copolymer.[70]

The copolymerization of ethylene and norbornene can produce copolymers with various types of sequences: alternate sequences (NENEN) or random sequences in blocks (isolated: EENEE, meso-dyads: ENNE or longer blocks: ENNNE).[70] The crystallinity of COC is controlled by the microstructure. It decreases and then disappears when the number of NB units increases in the copolymer. The copolymer with the NB unit greater than 14 mol% shows amorphous property. [84] The crystallinity also depends on the catalyst structure. Vinylic PNBs prepared with zirconocenes are partially crystalline but insoluble. Whereas, the soluble amorphous PNBs are obtained with late transition metals.[85]

Generally, a linear relationship is obtained between NB content and T_g value. Dyads and blocks of three or more NB units increase in the polymer backbone with increasing the NB contents. The high T_g associated with the inclusion of rigid NB units in the polymer chain leads to higher Young moduli and microhardness values in these COC. The stereoregular alternating copolymers were partially crystalline with T_g around 30 °C lower than their random content parts. The T_g value not only controlled by the NB content but also depends on the microstructure. As a result, the stereoregularity of the chain segments affects T_g value. Commercial grades of COC and COP are often given deflection temperature (HDT = heat deflection temperature). This temperature depends on the level of NB microstructure and influences the T_g value.[86] The grades that have the highest content of NB shows the highest T_g value and are more resistant to temperature.

The catalysts for copolymerization of NB and propylene are very limited. Living random copolymerization of NB and propylene using **Ti-1** activated by dMAO showed high activity and a good linear relationship between of T_g value and NB content in the copolymers. The activity increased by introducing the alkyl group on the fluorenyl ligand.[87] Poly(propylene-*ran*-norbornene) showed a higher T_g value than poly(ethylene-*ran*-norbornene) with the same NB content.[88] The same catalysts also used for copolymerization of NB with higher 1-alkene, styrene and functional ω-alkenes to give copolymers with good optical properties. [89]

Copolymerization of NB and higher 1-alkene has also been reported by a catalyst based on a late-transition-metal complex.

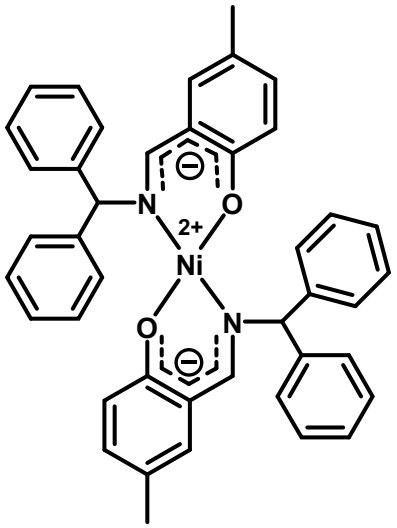

Ni-10

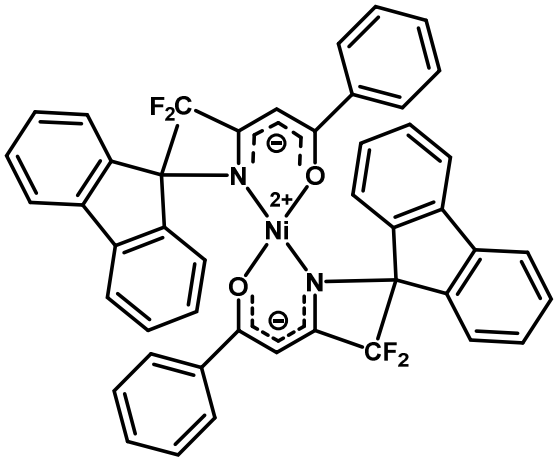

Ni11

Bis-(salicylaldehyde-benzhydrylimino)nickel complexes (**Ni-10**) exhibited high activities up to 2.40 x 10^5 $g_{polymer}$ mol_{Ni}^{-1} h^{-1} toward copolymerization of NB and 1-hexene in the presence of $B(C_6F_5)_3$. The produced copolymer showed good solubility, thermal stability and optical transparency. [90]

Recently, copolymerization of NB and styrene was conducted with Ni(II) complexes (**Ni-11**) bearing β-keto-9 fluorenyliminato ligands activated by $B(C_6F_5)_3$ to show high activity up to 10^5 $g_{polymer}$ mol_{Ni}^{-1} h^{-1}. [91]

Functional polymers are and will be in demand. Catalysts play the key role in functionalization of polyolefins by copolymerization. Nickel catalysts

have garnered much attention because of their low oxophilicity, and correspondingly the potential of realizing the copolymerizations of olefin with functionalized comonomers. A large number of nickel catalysts has been reported for the copolymerization of NB with functional monomer or NB derivatives with high activity. Even some are highly thermostable and can polymerize in a wide range of polymerization temperatures. [92] The nickel catalysts not only open the door for functional polymers in academic research but also opening the opportunity for industrial application in the nearest future.

1-5. Optical Plastics

The optical plastics commercially available are poly(methyl methacrylate) (PMMA), polycarbonate (PC), polystyrene (PS), styrene-methacrylate copolymer (NAS), Zeonex (hydrogenated product of PNB via ROMP commercialized by Zeon Co. Japan), ARTON (ROMP product commercialized by JSR Co. Japan), TOPAC (ENCs commercialized by Ticona), APEL (ENCs commercialized by Mitsui Co. Japan). PMMA and PC are widely used for CD, DVD, optical lens and glass substitutes, however they have poor humidity resistance. Compare to the other polymers, COC shows very good properties for use of optical plastics. **Table 1-1** compares the properties of various optical plastics.

Table 1-1. Properties of various optical plastics

Properties	**Unit**	**PMMA**	**PC**	**NAS**	**Zeonex**	**COC**
RI		1.49	1.58	1.56	1.53	1.51
Transmittance	%T	92	90	90	92	90
Birefringence	Qualitative	Low	High	High	High	Low
Water absorption (24 h, 23 °C)	wt %	0.3	0.2	0.15	0.01	0.01
Hardness	Rockwell M	90	50	80	75	
T_g	°C	105	145	100	140	70-170

Aim of this Work

Optical plastics are useful materials because of their high processability, and strength comparing to glass. An ideal optical plastic material has some requirement such as high thermal stability, high heat resistance, high transparency, high humidity resistance and low birefringence. PC and PMMA are widely used plastics. PC showed good heat resistivity and transparency, but it has poor humidity resistance. On the other hand, PMMA possesses good transparency with low birefringence. However, it has poor heat and humidity resistance.

NB-based polyolefins possess high thermal stability, heat resistance, transparency, chemical resistance, humidity resistance and low birefringence. The research on NB polymerization with late transition metal single-site catalysts has been directed to coordination-insertion polymerization rather than ROMP. The bicyclic structure in the main chain of vinyl added PNB retain excellent properties as optical plastic.

Since 1960, the coordination polymerization of NB was studied by traditional Ziegler-Natta catalysts and homogeneous metallocene catalysts. However, most of them showed very low activity and produced insoluble polymers. The late transition metals, for example, palladium, nickel and cobalt-based catalysts have been reported to produce PNB via coordination-insertion polymerization. Therefore, to find a suitable late transition metal catalyst for NB polymerization is an object in this field.

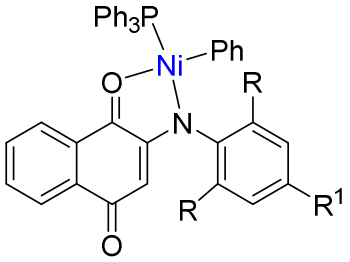

1a, R = $CH(CH_3)_2$, R^1 = H.
1b, R = R^1 = CH_3.
1c, R = R^1 = H.
1d, R = CH_3, R^1 = H.
1e, R = CH_2CH_3, R^1 = H.

Figure 1-3. Anilinonaphthoquinone-ligated nickel complexes.

Nickel metal has a great advantage in price among the late transition metals except iron. The designs of the ligands of nickel complexes are able to change their catalytic ability for NB polymerization. Considering the above point of view, anilinonapthoquinone ligated nickel complexes [Ni($C_{10}H_5O_2NAr$)(Ph)(PPh_3): **1a**, Ar = C_6H_3-2,6-^{i}Pr; **1b**, Ar = C_6H_2-2,4,6-Me; **1d,** Ar = C_6H_2-2,6-Me; **1e,** Ar = C_6H_2-2,6-Et;] (**Figure 1-3**) were selected, which were showed high activity and gave high molecular weight polymer in NB polymerization. The activity decreased according to the order: **1a** > **1e** > **1b** > **1d.** On the other hand, the number-average molecular weight (M_n) value was more than 5×10^5 g mol^{-1} irrespective of the complex used. The produced polymer is highly soluble in common organic solvents.

The author expected that the anilinonapthoquinone ligated nickel complexes should show the excellent catalytic abilities for copolymerization of NB and copolymerization of NB with conjugated hydrocarbon monomers were

conducted with **1a, 1b** and **1c** (bulky, less bulky and no substituent). In this thesis, the least bulky complex **1c** [Ar = C_6H_5] was newly synthesized with the purpose to investigate the ligand effects.

In Chapter II, NB/styrene (St) copolymerization was studied by complex **1a**-**1c** activated by MMAO and $B(C_6F_5)_3$ as a cocatalyst. The investigation focused the effects of ligand, reaction conditions and reactivity ratios of the catalyst on NB/St copolymerization. The physical properties of the obtained copolymers were also investigated.

In Chapter III, NB/*p*-substituted styrene (XSt) copolymerization was conducted by complex **1a**-**1c** activated by MMAO as a cocatalyst. The effect of ligand and reaction conditions on NB/XSt copolymerization were investigated. The physical and mechanical properties of the obtained copolymers were measured.

In Chapter IV, NB/divinylbenzene (DVB) copolymerization was conducted by complex **1a**-**1c** activated by MMAO as a cocatalyst. The effects of ligand, reaction conditions on NB/DVB copolymerization were investigated. The NB/DVB copolymer containing pendent styryl groups was modified to functional groups and also used as a macromonomer for graft polymerization of methyl methacrylate. The physical and mechanical properties of the obtained polymers were measured.

In Chapter V, copolymerization of NB with conjugated diene (CDN) i.e., butadiene (BD) or isoprene (IP) were conducted by complex **1a**-**1c** activated by

MMAO as a cocatalyst. The effects of ligand, reaction conditions on NB/CDN copolymerization were investigated and the physical and mechanical properties of the obtained copolymers were measured.

In Chapter VI, the results obtained in the present study were summarized.

References

1. M. Yamazaki, *J. Mol. Catal A: Chem.* **2004**, *213*, 81-87.
2. V. T. Widyaya, H. T. Vo, R. D. D. Putra, W. S. Hwang, B. S. Ahn, H. Lee, *European Polymer Journal* **2013**, *49*, 2680–2688.
3. T. Kohara, *Macromol. Symp.* **1996**, *101*, 571-579.
4. S. Sutthasupa, M. Shiotsuki, F. Sanda, *Polym. J.* **2010,** *42*, 905–915.
5. K. J. Ivin, J. C. Mol, Academic Press, San Diego, CA **1997**, 407–410.
6. Y. Takashima, Y. Nakayama, A. Harada, *Chem. Lett.* **2001**. *30*, 488-489.
7. A. Lehtonen, R. Sillanpää, *Inorg. Chem. Commun.* **2002**, *5*, 267-268.
8. K. Nomura, S. Takahashi, Y. Imanishi, *Macromolecules* **2001**, *34*, 4712-4723.
9. K. Hiya, Y. Nakayama, H. Yasuda, *Macromolecules* **2003**, *36*, 7916-7922.
10. D. M. Haigh, A. M. Kenwright, E. Khosravi, *Tetrahedron* **2004**, *60*, 7217-7224.
11. M. Bernechea, N. Lugan, B. Gil, E. lalinde, G. Lavigne, *Organometallics* **2006**, *25*, 684-692.
12. L. R. Gilliom, R. H. Grubbs, *J. Am. Chem. Soc.* **1986**, *108*, 733-742.
13. J. J. Eisch, A. A. Adeosun, *Eur. J. Org. Chem.* **2005**, 6, 993-997.
14. K. Nomura, A. Sagara, Y. Imanishi, *Macromolecules* **2002**, *35*, 1583.
15. Y. Nakayama, M. Tanimoto, T. Shiono, *Macromol. Rapid Commun.* **2007**, *28*, 646-650.

16. K. C. Wallace, A. H. Liu, J. C. Dewan, R. R. Schrock, *J. Am. Chem. Soc.* **1988**, *110*, 4964-4977.

17. J. L. Burmaghim, G. S. *Organometallics* **1999**, *18*, 1923-1929.

18. C. M. Frech Dr., O. Blacque Dr., H. W. Schmalle Dr., H. Berke Prof. Dr., C. Adlhart Dr., P. Chen Prof. Dr., *Chem. Eur. J.* **2006**, *12*, 3325-3338.

19. T. Steinhäusler, W. J. Koros, *J. Polym. Sci., Part B: Polym. Phys.* **1997**, *35*, 91-99.

20. J. P. Kennedy, H. S. Makowski, *J. Macromol. Sci. Chem.* **1967**, *A1*, 345-370.

21. N. G. Gaylord, B. M. Mandal, M. Martan, *J. Polym. Sci. Polym. Lett. Ed.* **1976**, *14*, 555-559.

22. N. G. Gaylord, A. B. Deshpande, B. M. Mandal, M. Martan, *J. Macromol. Sci. Chem.* **1977**, *A 11*, 1053-1070.

23. N. G. Gaylord, A. B. Deshpande, *J. Polym. Sci. Polym. Lett. Ed.* **1976**, *14*, 613-617.

24. S. Rush, A. Reinmuth, W. Risse, *Macromolecules* **1997**, *30*, 7375–7385.

25. B. L. Goodall, L. H. McIntosh III, L. F. Rhodes, *Makromol. Chem. Macromol. Symp.* **1995**, *89*, 421–432.

26. N. Seehof, C. Mehler, S. Breunig, W. Risse, *J. Mol. Catal.* **1992**, *76*, 219–228.

27. N. R. Grove, P. A. Kohl, S. A. B. Allen, S. Jayaraman, R. Shick, *J. Polym. Sci., Part B: Polym. Phys.* **1999**, *37*, 3003-3010.

28. T. F. A. Haselwander, W. Heitz, S. A. Krugel, J. H. Wendorff, *Macromol. Chem. Phys.* **1996**, *197*, 3435-3453.

29. K. H. Park, R. J. Twieg, R. Ravikiran, L. F. Rhodes, R. A. Shick, D. Yankelevich, A. Knoesen, *Macromolecules* **2004**, *37*, 5163-5178.

30. T. Hoskins, W. J. Chung, A. Agrawal, P. J. Ludovice, C. L. Henderson, L. D. Seger, L. F. Rhodes, R. A. Shick, *Macromolecules* **2004**, *37*, 4512-4518.

31. (i) W. Kaminsky, M. Miri, H. Sinn, R. Woldt, *Makromol. Chem. Rapid Commun.* **1983**, *4*, 417-421. (ii) I. Tritto, C. Mkalares, M. C. Sacchi, P. Locatelli, *Macromol. Chem. Phys.* **1997**, *198*, 3963-3977.

32. (i) S. Pasynkiewicz, *Polyhedron* **1990**, *9*, 429-453. (ii) K. Peng, S. Xiao, *J. Mol. Cata.* **1994**, *90*, 201-211. (iii) S. S. Reddy, K. Radhakrishnan, S. Sivaram, *Polym. Bull.* **1996**, *36*, 165-171.

33. L. Resconi, S. Bossi, L. Abis, *Macromolecules* **1990**, *23*, 4489-4491.

34. D. E. Babushkin, H. H. Brintzinger, *J. Am. Chem. Soc.* **2002**, *124*, 12869-12873.

35. L. Jia, X. Yang, C. L. Stern, T. J. Marks, *Organometallics* **1997**, *16*, 842-857.

36. W. L. Truett, D. R. Johnson, J. M. Robinson, B. A. Montague, *J. Am. Chem. Soc.* **1960**, *82*, 2337–2340.

37. X. Mi, D. Xu, W. Yan, C. Guo, Y. Ke, Y. Hu, *Polym. Bull.* **2002**, *47*, 521-527.

38. (a)T. Hasan, K. Nishii, T. Shiono, T. Ikeda, *Macromolecules* **2002**, *35*, 8933-8935. (b) T. Hasan, T. Ikeda, T. Shiono, *Macromolecules* **2004**, *37*, 7432-7436.

39. Q. Wu, Y. Lu, *J. Polymer Sci., Part A: Polym. Chem.* **2002**, *40*, 1421-1425.

40. M. Arndt, M. Gosmann, *Polym. Bull.* **1998**, *41*, 433–440.

41. (a) JP 2001059004 A2 (2001), Mitsubishi Chemical Corp. (Japan): Kenji, T.; Manbu, K. *Chem. Abstr.* 2001, 134, 193886k. (b) JP 2000302820 A2 (2000), Mitsubishi Chemical Corp. (Japan): Nishizawa, S.; Kenji, T.; Mitsutoshi, A. *Chem. Abstr.* 2000, 133, 322304z. (c) JP 08165309 A2 (1996), Mitsubishi Chemical Corp. (Japan): Osamu, N.; Kenji, T.; Mitsutoshi, A. *Chem. Abstr.* 1996, 125, 196683s. (d) JP 07041521 A2 (1995), Mitsui Toatsu Chemicals (Japan): Tadashi, A.; Tadahiro, S. *Chem. Abstr.* 1995, 123, 144895b. (e) JP 02180910 A2 (1990), Daicel Chemical Industries Ltd. (Japan): Soga, K.; Takahashi, I.; *Chem. Abstr.* 1990, 133, 192141t.

42. J. Chen, Y. Huang, Z. Li, Z. Zhang, C. Wie, T. Lan, W. Zhang, *J. Mol. Catal. A: Chem.* **2006**, *259,* 133-141.

43. U. Peucker, W. Heitz, *Macromol. Chem. Phys.* **2001**, *202*, 1289-1297.

44. P. -G. Lassahn, V. Lozan, G. A. Timco, P. Christian, C. Janiak, R. E. P. Winpenny, *J. Catal.* **2004**, *222,* 260-267.

45. L. M. Tang, J. Q. Wu, Y. Q. Duan, L. Pan, Y. G. Li, Y. S. Li, *J. Polym. Sci., Part A: Polym. Chem.* **2008**, *46*, 2038–2048.

46. Y. Sato, Y. Nakayama, H. Yasuda, *J. Organomet. Chem.* **2004**, *689*, 744-750.

47. F. Pelascini, F. Peruch, P. J. Lutz, M. Wesolek, J. Kress, *Macromol. Rapid Commun.* **2003**, *24*, 768-771.

48. F. Pelascini, F. Peruch, P. J. Lutz, M. Wesolek, J. Kress, *Macromol. Symp.* **2004**, *213*, 265.

49. F. Bao, X. Lu, Y. Qiao, G. Gui, H. Gao, Q. Wu, *Appl. Organomet. Chem.* **2005**, *19*, 957-963.

50. F. Bao, X. -Q. Lu, H. Gao, G. Gui, Q. Wu, *J. Polym. Sci., Part A: Polym. Chem.* **2005**, *43*, 5535.

51. R. G. Schultz, *J. Polym. Sci., Part B: Polym. Lett.* **1966**, *4*, 541-546.

52. (a) A. Sen. T. -W. Lai, *Organometallics* **1982**, *1*, 415-417. (b) A. Sen, T-W. Lai, R. R. Thomas, *J. Organomet. Chem.* **1988**, *358*, 567-588.

53. B. Berchtold, V. Lozan, P. -G. Lassahn, C. Janiak, *J. Polym. Sci., Part A: Polym. Chem.* **2002**, *40*, 3604-3614.

54. (a) H. Y. Cho, D. S. Hong, D. W. Jeong, Y. -D. Gong, S. I. Woo, *Macromol. Rapid Commun.* **2004**, *25*, 302-306. (b) H. Liang, J. Liu, X. Li, Y. Li, *Polyhedron* **2004**, *23*, 1619-1627.

55. M. Li, H. Song, B. Wang, *J. Organomet. Chem.* **2016**, *804*, 118-122.

56. M. Li, X. Shu, Z. Cai, M. S. Eisen, *Organometallics* **2018**, *37*, 1172−1180.

57. T. Hu, Y. -G. Li, Y. S. Li, N. -H. Hu, *J. Mol. Catal. A: Chem.* **2006**, *253*, 155-164.

58. T. J. Deming, B. M. Novak, *Macromolecules,* **1993**, *26*, 7089–7091.

59. M. Arndt, M. Gossmann, *Polym. Bull*. **1998**, *41*, 433–440.

60. E. Nelkenbaum, M. Kapon, M. S. Eisen, *Organometallics* **2005**, *24*, 2645.

61. H. Gao, W. Guo, F. Bao, G. Gui, J. Zhang, F. Zhu, Q. Wu, *Organometallics* **2004**, *23*, 6273-6280.

62. D. Zhang, G. -X. Jin, L. -H. Weng, F. Wang, *Organometallics* **2004**, *23*, 3270-3275.

63. Y. -S. Li, Y. -R. Li, X. -F. Li, *J. Organomet. Chem.* **2003**, *667*, 185-191.

64. S. A. Lee, K. Y. Shin, B. J. Park, M. K. Choi, I. -M. Lee, *Bull. Korean Chem. Soc.* 2006, 27, 475.

65. N. H. Tarte, H. Y. Cho, S. I. Woo, *Macromolecules* **2007**, *40*, 8162-8167.

66. X. -F. Li, Y. -S. Li, *J. Polym. Sci., Part A: Polym. Chem.* **2002**, *40*, 2680-2685.

67. W. -H. Sun, H. Yang, Z. Li, Y. Li, *Organometallics* **2003**, *22*, 3678-3683.

68. M. Li, Z. Cai, M. S. Eisen, *Organometallics* **2018**, *37*, 4753−4762.

69. F. Blank, C. Janiak, *Coord. Chem. Rev.* **2009**, *253*, 827–861.

70. W. S. R. Lago, C. A. -Chodur, A. P. Ahoussou, N. Yagoubi, *J. Mater. Sci.* **2017**, *52*, 6879-6904.

71. R. Lamonte, D. M. Nally, *Plast. Eng.* **2000**, *56*, 51–55.

72. R. Lamonte, D. M. Nally, *Adv. Mater. Process.* **2001**, *159*, 33–36.

73. G. Khanarian, *Opt. Eng.* **2001**, *40*, 1024–1029.

74. MN. Eakins, *Bio. Process Int.* **2005**, *3*, 52–58.

75. (a) M. Limam, L. Tighzert, F. Fricoteaux, G. Bureau, *Polym. Test* **2005**, *24*, 395–402. (b) MN. Eakins, *Am. Pharm. Rev.* **2010**, *13*, 12–16. (c) S. S. Qadry, T. H. Roshdy, H. Char, S. D. Terzo, R. Tarantino, J. Moschera, *Int. J. Pharm.* **2003**, *252*, 207–212.

76. (a) S. Roy, C. Y. Yue, Y. C. Lam, Z. Y. Wang, H. Hu, *Sens Actuators B Chem* **2010**, *150*, 537–549. (b) W. L. Hawkins, MRS. M. A. Worthington, W. Matreyek, *J. Appl. Polym. Sci.* **1960**, *3*, 277–281. (c) E. O. Dillingham, N. Webb, W. H. Lawrence, *J. Biomed. Mater. Res.* **1975**, *9*, 569–596. (d) J. Kameoka, H. G. Craighead, H. Zhang, J. Henion, *Anal. Chem.* **2001**, *73*, 1935–1941. (e) C. K. Fredrickson, Z. Xia, C. Das, R. Ferguson, F. T. Tavares, Z. H. Fan, *J. Microelectromech. Syst.* **2006**, *15*, 1060–1068. (f) J. Zhang, C. Das, Z. H, Fan. *Microfluid Nanofluid* **2008**, *5*, 327–335. (g) W. D. Niles, P. J. Coassin, *Assay Drug Dev. Technol.* **2008**, *6*, 577–590. (h) L. Yi, W. Xiaodong, Y. Fan, *J. Mater. Process. Technol.* **2008**, *208*, 63–69. (i) P. S. Nunes, P. D. Ohlsson, O. Ordeig, J.

P. Kutter, *Microfluid Nanofluid* **2010**, *9*, 145–161. (j) S. Roy, C. Y. Yue, Y. C. Lam, *Vacuum* **2011**, *85*, 1102–1104. (k) R. K. Jena, C. Y. Yue, Y. C. Lam, P. S. Tang, A. Gupta, *Sens. Actuators B Chem.* **2012**, *163*, 233–241. (l) P. Leech, X. Zhang, Y. Zhu, *J. Mater. Sci.* **2010**, *45*, 5364–5369.

77. (a) D. Sung, DH. Shin, S. Jon, *Biosens. Bioelectron.* **2011**, *26*, 3967–3972. (b) J. Raj, G. Herzog, M. Manning, C. Volcke, B. D. MacCraith, S. Ballantyne, M. Thompson, D.W. M. Arrigan, *Biosens. Bioelectron.* **2009**, *24*, 2654–2658.

78. (a) G. Emiliyanov, P. Høiby, L. Pedersen, O. Bang, *Sensors* **2013**, *13*, 3242. (b) G. Emiliyanov, J. B. Jensen, O. Bang, P. E. Hoiby, L. H. Pedersen, E. M. Kjaer, L. Lindvold, *Opt. Lett.* **2007**, *32*, 460–462. (c) K. Liu, Z. H. Fan, *The Analyst* **2011**, 136, 1288–1297. (d) G. A. D. -Quijada, R. Peytavi, A. Nantel, E. Roy, M. G. Bergeron, M. M. Dumoulin, T. Veres, *Lab. Chip. Miniat. Chem. Biol.* **2007**, *7*, 856–862. (e) A. Bhattacharyya, C. M. Klapperich, *Biomed. Microdevices* **2007**, *9*, 245–251. (f) C. Jonsson, M. Aronsson, G. Rundstrom, C. Pettersson, I. M. -Hartvig, J. Bakker, E. Martinsson, B. Liedberg, B. MacCraith, O. Ohman, J. Melin, *Lab. Chip. Miniat. Chem. Biol.* **2008**, *8*, 1191–1197. (g) Y. Liu, N. C. Cady, C. A. Batt, *Biomed. Microdevices* **2007**, *9*, 769–776. (h) S. Laib, B. D. MacCraith, *Anal Chem.* **2007**, *79*, 6264–6270.

79. M. Petrtyl, Z. Bastl, Z. Krulis, H. Hulejova, M. Polanska, J. Lisal, J. Danesova, P. Cerny, *Macromol. Symp.* **2010**, *294*, 120–132.

80. (a) S. -C. Chang, M. -J. Lee, H. -M. Lin, *J. Supercrit. Fluids.* **2007**, *40*, 420–432. (b) A. Pegoretti, A. Dorigato, A. Biani, M. Slouf, *J. Mater. Sci.* **2016**, *51*, 3907–3916. (c) S. -P. Rwei, Y. -T. Lin, Y. -Y. Su, *Text Res. J.* **2012**, *82*, 315–323.

81. J. Saade, N. Declas, P. Marote, C. Bordes, K. Faure, *J. Mater. Sci.* **2017**, *52*, 4509–4520.

82. (a) E. Brauer, H. Wiegleb, M. Helmstedt, *Polym. Bull.* **1986**, *15*, 551–557. (b) E. Brauer, C. Wild, H. Wiegleb, *Polym. Bull.* **1987**, *18*, 73–80.

83. (a) D. Ruchatz, G. Fink, *Macromolecules* **1998**, *31*, 4669–4673. (b) D. Ruchatz, G. Fink, *Macromolecules* **1998**, *31*, 4674–4680. (c) D. Ruchatz, G. Fink, *Macromolecules* **1998**, *31*, 4681–4683. (d) I. Tritto, L. Boggioni, D. R. Ferro, *Macromolecules* **2004**, *37*, 9681–9693. (e) Z. Yao, F. Lv, S. -J. Liu, K. Cao, *J. Appl. Polym. Sci.* **2008**, *107*, 286–291. (f) D. Ruchatz, G. Fink, *Macromolecules* **1998**, *31*, 4684–4686. (g) K. Thorshaug, R. Mendichi, L. Boggioni, I. Tritto, S. Trinkle, C. Friedrich, R. Malhaupt, *Macromolecules* **2002**, *35*, 2903–2911. (h) I. Tritto, C. Marestin, L. Boggioni, M. C. Sacchi, H. -H. Brintzinger, D. R. Ferro, *Macromolecules* **2001**, *34*, 5770–5777. (i) R. Benavente, T. Scrivani, M. L. Cerrada, G. Zamfirova, E. Perez, J. M. Perena, *J Appl. Polym. Sci.* **2003**, *89*, 3666–3671.

84. (a) M. Arndt, I. Beulich, *Macromol. Chem. Phys*. **1998**, *199*, 1221–1232. (b) S. Y. Park, K. Y. Choi, K. H. Song, B. G. Jeong, *Macromolecules*

2003, *36*, 4216–4225. (c) W. Kaminsky, P. -D. Tran, R. Werner, *Macromol. Symp.* **2004**, *213*, 101–108.

85. M. C. Sacchi, M. Sonzogni, S. Losio, F. Forlini, P. Locatelli, I. Tritto, M. Licchelli, *Macromol. Chem. Phys.* **2001**, *202*, 2052–2058.

86. J. Forsyth, J. M. Perena, R. Benavente, E. Perez, I. Tritto, L. Boggioni, H. -H. Brintzinger, *Macromol. Chem. Phys.* **2001**, *202*, 614–620.

87. (a) T. Hasan, T. Ikeda, T. Shiono, *Macromolecules* **2005**, *38,* 1071-1074. (b) Z. Cai, Y. Nakayama, T. Shiono, *Macromolecules* **2006**, *39,* 2031-2033.

88. L. Boggioni, F. Bertini, G. Zannoni, I. Tritto, P. Carbone, M. Ragazzi, D. R. Ferro, *Macromolecules* **2003**, *36*, 882-890.

89. (a) T. Shiono, M. Sugimoto, T. Hasan, Z. Cai, T. Ikeda, *Macromolecules* **2008**, *41*, 8292-8294. (b) Z. Cai, Y. Nakayama, T. Shiono, *Macromolecules* **2010**, *43*, 4527–4531. (c) R. Tanaka, M. Goda, Z. Cai, Y. Nakayama, T. Shiono, *Polymer* **2015**, *70*, 252-256. (d) J. -W. Lee, S. Jantasee, B. Jongsomsjit, R. Tanaka, Y. Nakayama, T. Shiono, *J. Polym. Sci., Part A: Polym. Chem.* **2013**, *51*, 5085–5090. (d) R. Tanaka, T. Ikeda, Y. Nakayama, T. Shiono, *Polymer* **2015**, *56*, 218-222. (e) X. Song, L. Yu, T. Shiono, T. Hasan, Z. Cai, *Macromol. Rapid. Commun.* **2017***, 38,* 1600815.

90. (a) Y. Xing, Y. Chen, X. He, H. Nie, *J. App. Polym. Sci.* **2012**, 124, 1323–1332. (b) P. Huo, W. Liu, X. He, G. Mei, *J. Polym. Res.* **2015**, *22*,

194. (c) M. Li, H. Zhang, Z. Cai, M. S. Eisen. *Polym. Chem.* **2019**, *10*, 2741–2748. (d) D. Yang, J. Donga, B. Wang, *Dalton Trans.* **2018**, *47*, 180–189. (e) X. He, G. Tu, F. Zhang, S. Huang, C. Cheng, C. Zhu, Y. Duan, S. Wanga, D. Chenb, *RSC Adv.* **2018**, *8*, 36298–36312.

91. X. He, S. Wang, Y. Yang, G. Tu, F. Zhang, S. Huang, Y. Duan, C. Zhu, C. Cheng, D. Chen, *Appl. Organometal. Chem.* **2019**, *33*, e4694.

92. (a) X. He, Y. Deng, X. Jiang, Z. Wang, Y. Yang, Z. Hana, D. Chenb, *Polym. Chem.* **2017**, *8*, 2390–2396. (b) M. Li, H. Zhang, Z. Cai, M. S. Eisen. *Organometallics* **2018**, *37*, 4753−4762. (c) Y. -P. Zhang, W. -W. Li, B. -X. Li, H. -L. Mu, Y. -S. Li, *Dalton Trans.* **2015**, *44*, 7382–7394. (d) S. M. -Arranz, A. C. Albeniz, P. Espinet, *Macromolecules* **2010**, *43*, 7482–7487.

Chapter II

Copolymerization of Norbornene with Styrene using Anilinonaphthoquinone-Ligated Nickel Complexes

2-1. Introduction

Polymerization of cycloolefins such as norbornene (NB) has been one of the key developments in the area of polymer chemistry because of its extensive applications.[1-3] There are three types of mechanism for polymerization of NB, that is, ring-opening metathesis polymerization (ROMP),[4,5] cationic or radical polymerization,[6-9] and coordination–insertion polymerization.[10-12] Each route of the polymerization leads to the polymers with different structures and properties. Polynorbornenes (PNBs) produced by coordination–insertion polymerization shows excellent physical properties, such as good heat and chemical resistance, high decomposition temperature, high optical transparency, and low dielectric constant.[13,14] However, it exhibits some negative properties such as brittleness and glass transition temperature (T_g) close to the decomposition temperature due to the presence of rigid rings in the polymer chain.

The inferior properties of PNBs can be improved in cyclic olefin copolymers (COCs). The most demonstrative COC is a copolymer of NB and ethylene (E).[15] The properties of COCs can be easily controlled by a kind of

comonomer, comonomer content, and sequence distribution. Copolymerization of NB with 1-alkene was also reported to modify the physical properties.[16-24] The introduction of styrene (St) unit in NB sequences should decrease the birefringence of COCs[25] because PNB and polystyrene possess positive and negative birefringence, respectively. Several examples of the copolymerization of NB with St have been reported using late and early transition catalysts. The first NB/St copolymerization was carried out by Ni-based catalysts using methylaluminoxane (MAO) as a cocatalyst.[26] Afterwards, some nickel and copper catalysts were used to synthesize NB/St copolymers.[27-33] The St incorporation was enhanced by β-diketiminato nickel complexes.[34] The highest St incorporation was 52.4% with the highest St feed ratio of 83%, but the M_w value was around 10^3. Bis(β-ketoamino) copper complexes were used for copolymerization of NB and St, whereas the results were almost the same as those of β-diketiminato nickel complexes.[35]

Shiono and his coworkers reported NB/St copolymerization by an *ansa*-fluorenylamidodimethyltitanium-based catalyst which showed the potentiality of the copolymer as a plastic substrate for flexible display materials.[25] However, the maximum St incorporation in the NB/St copolymer with a sufficient molecular weight was approximately 5 mol %. They also synthesized NB/E/St terpolymer by using the same catalyst and obtained a zero-birefringence terpolymer with the St content of 12%, but the introduction of E unit (58 mol %) caused a significant drop of the T_g to 86 °C.[36]

Therefore, the author was interested in the copolymerization of NB with St to obtain high molecular weight copolymers with controlled St content. Shiono and his coworkers have previously reported that nickel complexes activated with $B(C_6F_5)_3$ as a cocatalyst exhibit high activity for NB polymerization to give high molecular weight polymer soluble in cyclohexane.[37]

In this chapter NB/St copolymerization was conducted using anilinonaphthoquinone-ligated nickel complexes [$Ni(C_{10}H_5O_2NAr)(Ph)(PPh_3)$: **1a**, Ar = C_6H_3-2,6-^{i}Pr; **1b**, Ar = C_6H_2-2,4,6-Me; **1c,** Ar = C_6H_5], where the least bulky complex **1c** was newly synthesized in this work, in the presence of modified MAO (MMAO) or $B(C_6F_5)_3$ (**Figure 2-1**).

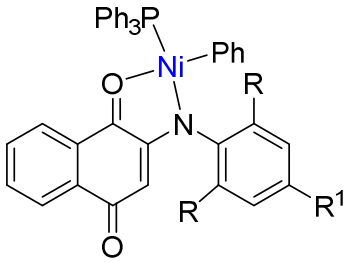

1a, R = $CH(CH_3)_2$, R^1 = H.
1b, R = R^1 = CH_3.
1c, R = R^1 = H.

Figure 2-1. Anilinonaphthoquinone-ligated nickel complexes used in this study.

2-2. Materials and Methods

Materials

All manipulations were carried out under a nitrogen atmosphere using standard Schlenk techniques. All solvents were refluxed and distilled over sodium/benzophenone or calcium hydride. NB was purified by stirring it over calcium hydride at 60 °C for one day, and then distilled. The stock solution of NB (5.5 M) was prepared in toluene. St (Wako Chemical Co. Ltd., Odawara, Japan) was dried over CaH_2, and then freshly distilled under vacuum prior to use. Modified methylaluminoxane (MMAO) solution (6.6 wt % in toluene) and toluene solution of $B(C_6F_5)_3$ were donated from Tosoh Finechem. Co. (Tokyo, Japan) and used as received. The nickel complexes **1a, 1b** were synthesized according to the literature and the references therein.[38,39] The complex **1c** was synthesized using a similar procedure to that for **1a** and **1b**.

Analytical Procedures

Molecular weights and molecular weight distributions of polymers were determined by gel permeation chromatography (GPC) with a Viscotec HT-350 GPC (Malvern, Great Malvern, UK) with three CLM6210 mixed-bed columns. This system was equipped with a triple-detection array consisting of a differential refractive index (DRI) detector, a two-angle (7, 90) light scattering (LS) detector, and a four-bridge capillary viscosity detector. Polymer characterization was carried out at 150 °C using *o*-dichlorobenzene as an eluent

and calibrated with polystyrene standards. The ^{1}H and ^{13}C NMR spectra of polymers were measured at room temperature on a Bruker 500M Hz instrument (Bruker, Rheinstetten, Germany) operated by the pulse Fourier-transform mode. The measurement for ^{1}H NMR and ^{13}C NMR, sample solution was prepared in $CDCl_3$ up to 10 wt%. The pulse angle for ^{13}C NMR was 45° and about 8000-10,000 scans were accumulated in pulse repetition of 5.0 s. The central peak of $CDCl_3$ (77.13 ppm for ^{13}C NMR) and peak of $CHCl_3$ (7.25 ppm for ^{1}H NMR) was used as an internal reference. Differential scanning calorimetry (DSC) was performed on a SII EXSTER 600 system (Seiko Instruments Inc., Chiba, Japan) under nitrogen atmosphere. Thermal history difference in the polymers was eliminated by first heating the specimen to 380 °C, cooling from 10 to 20 °C/min, and then recording the second DSC scan at a heating rate of 10 °C/min.

Synthesis of Anilinonaphthoquinone ligand 1c

The ligand was synthesized by applying the literature procedure.[38,39] First, aniline (8.6 mmol) was added drop wisely into a solution of 2-hydroxy-1,4-naphthoquione (1.50 g, 8.6 mmol) in *m*-cresol (30 mL) in the presence of trifluoroacetic acid (0.20 mL, 2.69 mmol) as a catalyst. The mixture was heated with stirring at 100 °C for 4 h and then poured into 900 mL of 5 wt.-% aqueous sodium hydroxide. The precipitate formed was filtered, washed with water and dried under a vacuum at 80 °C for 6 h. The ligand powder was purified by recrystallization using acetic acid. The yield was 1.37 g (5.43 mmol, 63%).

^{1}H NMR ($CDCl_3$, 500 MHz): δ = 8.13 (dt, 2H), 7.78 (dt, 1H), 7.69(dt, 1H), 7.58(br, 1H), 7.44(dt, 2H), 7.30 (d, 2H), 7.23 (d, 1H), 6.44 (s, 1H),

^{13}C NMR ($CDCl_3$, 500 MHz): δ = 184.1, 181.7, 144.9, 137.1, 134.9, 133.2, 132.3, 130.4, 129.7, 126.5, 125.9, 125.5, 122.6, 103.3.

Synthesis of Complex 1c

The nickel complex was synthesized by applying the literature procedure.[39] The ligand (1.01 g, 3.03 mmol) in THF (20 mL) was slowly added through a dropping funnel into a reactor containing a slurry of NaH (0.08 g, 3.31 mmol) in THF (10 mL) cooled using an ice-water bath at 0 °C, and the resultant slurry was stirred for 3 h at room temperature. The slurry thus obtained was filtered off under a nitrogen atmosphere. The residue was washed with THF and dried under a vacuum at room temperature for 6 h. The sodium salt of the ligand contained 1 eq. of THF. The sodium salt of the ligand (0.72 g, 1.68 mmol) and *trans*-[$Ni(PPh_3)_2PhCl$] (1.18 g, 1.68 mmol), which was prepared according to the literature,[39] were mixed in a Schlenk tube with THF (10 mL) at room temperature and stirred for one day. The reaction mixture was filtered off under a nitrogen atmosphere, and the filtrate was evaporated to dryness under a vacuum. The solid thus obtained was purified with a mixture of THF/hexane in a 1/5 volume ratio. The powder was identified to be the expected product by ^{1}H and ^{31}P NMR. The yield was 0.37 g (0.57 mmol, 33%).

^{1}H NMR (C_6D_6, 500 MHz): δ = 8.15 (d, 1H), 7.65 (br, 2H), 7.35(m, 7H), 6.99(m, 19H), 6.4 (s, 1H), 3.5 (THF).

^{31}P NMR (C_6D_6, 202 MHz): δ = 28.96.

Elemental analysis calculated: C, 74.33; H, 4.68, N, 2.17. Found: C, 74.19; H, 5.01; N, 2.23.

Copolymerization of NB and St

In a typical procedure, prescribed amounts of NB and St in toluene solution were introduced into a 100 mL round-bottomed glass flask. Then, the cocatalyst 0.24 mL of MMAO toluene solution (500 μmol) or 1 mL of $B(C_6F_5)_3$ toluene solution (20 μmol) and 1 mL of the nickel complex (5 μmol) solution in toluene were syringed into the well-stirred monomer solution in this order, and the total solution volume was made up to 25 mL by adding toluene. The copolymerization was conducted under continuous stirring for a required time under a certain temperature controlled by an external oil or ice bath. The copolymerization was terminated by adding 300 mL of acidic methanol (methanol/concentrated hydrochloric acid, 95/5 in volume). The resulting precipitated polymer was collected by filtration, adequately washed with methanol, and dried in vacuum at 60 °C for 6 h.

Preparation of Copolymer Film

NB/St copolymer (approximately 300 mg) was dissolved into 3 mL of toluene at room temperature and filtered through 0.20 μm PTFE membrane. The filtered solution was placed on a glass plate and stood for 3 days under ambient temperature and pressure. After almost all the solvent was vaporized, the film was placed at 60 °C under vacuum condition for 3 h.

2-3. Results and Discussion

2-3-1. Homopolymerization of NB and St

Homopolymerizations of NB and St were performed using **1**-MMAO at 70 °C in toluene. The results are shown in **Table 2-1**. In the NB polymerization, complex **1a** displayed the highest activity, and gave the polymer with the highest molecular weight among the complexes used. The opposite trends were observed in St polymerization, but the differences were not so significant.

2-3-2. Copolymerization of NB and St

Copolymerizations of NB with St were then conducted under the same conditions by changing St ratio in feed from 10 to 40 mmol with 40 mmol of NB (**Scheme 2-1**). The results are summarized in **Table 2-1**. The nickel

complexes showed moderate activity for NB/St copolymerization. The NB/St feed ratio did not significantly affect the catalytic activity, and all the complexes showed lower activity in the copolymerization than in the homopolymerization.

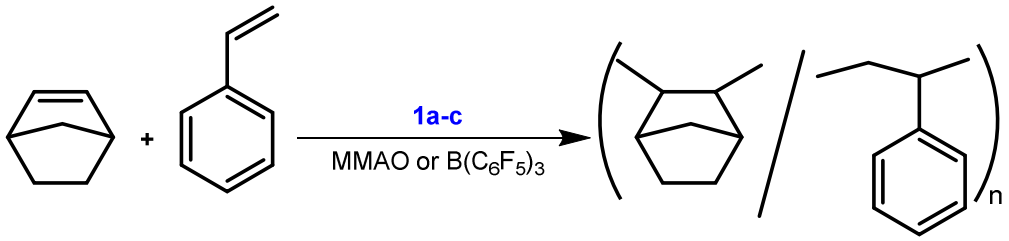

Scheme 2-1. NB/St copolymerization using Ni catalyst.

The low activity in the copolymerization could be ascribed to slow cross-propagation because of the steric hindrance between these comonomers. Complex **1a** showed the highest activity in NB polymerization and also showed the highest activity in NB/St copolymerization among the complexes used (**Table 2-1**, Run 3).

The NB/St copolymers were not only soluble in chloroform, but also in cyclohexane, similar to the PNB obtained by the same catalytic system. The incorporation of St in the produced copolymers was investigated by ^{1}H NMR in $CDCl_3$. A typical ^{1}H NMR spectrum of the copolymer (Run 15) is illustrated in **Figure 2-2**.

Table 2-1. Effects of monomer ratio of NB/St copolymerization by **1**-MMAO.

Run	(NB/St) [a] (mmol/mmol)	Com.	Y (g)	A[b]	f_{St} [c] (mol%)	M_n [d] (10^3)	M_w/M_n [d]	N [e] (μmol)
1	40/00	1a	1.10	220	0	470	1.9	2.3
2	40/10	1a	0.36	72	4	19	2.4	18.9
3	40/40	1a	0.65	130	16	6	2.5	108.3
4	00/40	1a	0.52	104	100	11	1.5	47.2
5	40/00	1b	0.54	107	0	266	2.2	2.0
6	40/10	1b	0.37	74	4	19	2.7	19.5
7	40/20	1b	0.31	62	8	12	1.7	25.8
8	40/30	1b	0.30	60	12	9	3.0	33.3
9	40/40	1b	0.44	88	19	8	2.9	55.0
10	00/40	1b	0.65	130	100	12	1.6	54.2
11	40/00	1c	0.58	115	0	309	1.6	1.9
12	40/10	1c	0.36	72	10	13	2.0	27.7
13	40/20	1c	0.32	64	16	10	1.5	32.0
14	40/30	1c	0.31	62	19	8	1.9	38.6
15	40/40	1c	0.40	80	36	7	3.0	57.1
16	00/40	1c	0.65	130	100	14	1.7	46.4

Copolymerization conditions: Ni = 5 μmol, temperature = 70 °C, time = 1h, Al/Ni = 100 (molar ratio), toluene (total volume 25 mL). [a] Norbornene and styrene in feed. [b] Activity = $kg_{(polymer)}\, mol_{(Ni)}^{-1}\, h^{-1}$. [c] f_{St} are the content of St in the NB/St copolymer determining by ^1H NMR spectrum. [d] Determined by GPC. [e] Number of polymer chains determined from yield and M_n.

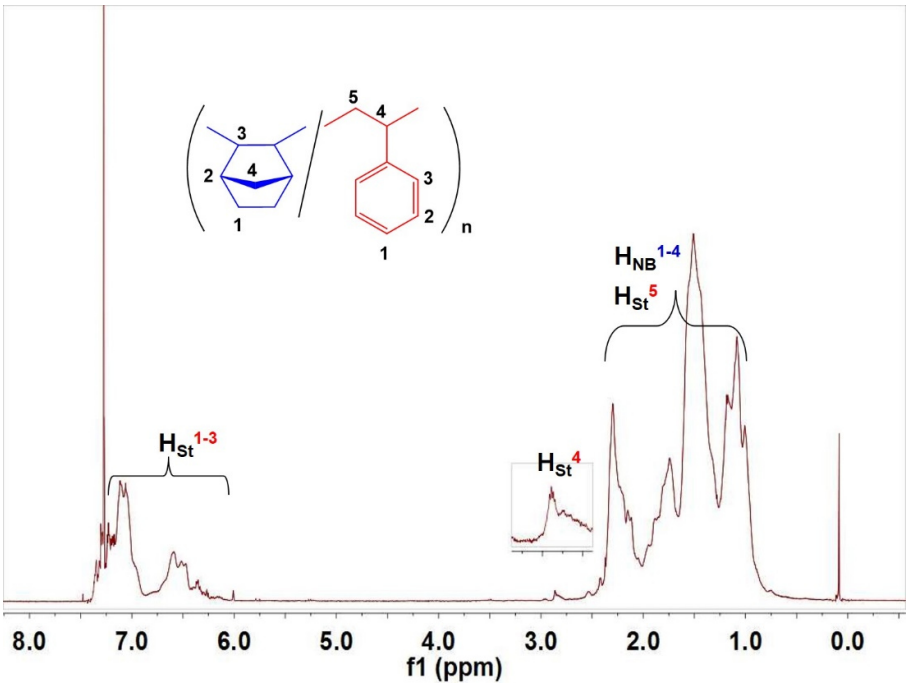

Figure 2-2. ^{1}H NMR spectrum of NB/St copolymer obtained by Run 15 ($CDCl_3$, 25 °C, 500 MHz).

No resonances are observed from 5.0 to 6.0 ppm, which is assigned to the vinylene protons of the polymer obtained via ring-opening metathesis polymerization (ROMP).[40] The signals assignable to the aliphatic protons of the NB and St units ($H_{NB}^{1–4}$ and H_{St}^{5}) are observed in the range of 0.8–2.4 ppm. The signals attributed to the aromatic protons of the St units ($H_{St}^{1–3}$) are observed in the range of 6.5–7.1 ppm. Particularly, the signal of the methine proton of the St unit (H_{St}^{4}) adjacent to the NB unit can be observed at 2.85 ppm. The copolymer with the highest incorporation of St was obtained under the highest St concentration (**Table 2-1**, Run 3, 9 and 15).

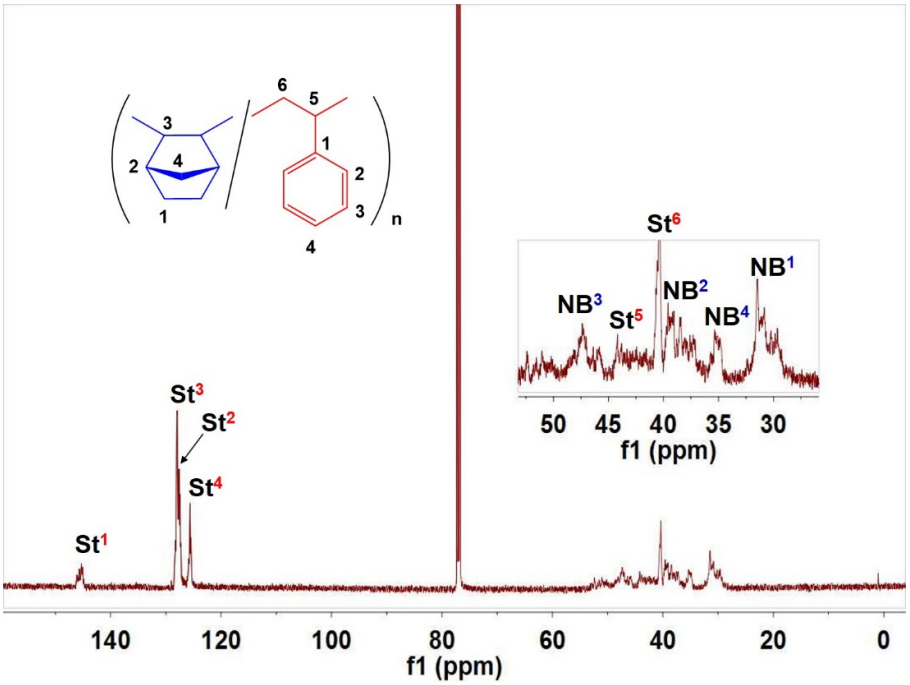

Figure 2-3. ^{13}C NMR (**b**) spectrum of NB/St copolymer obtained by Run 15 ($CDCl_3$, 25 °C, 125 MHz).

A typical ^{13}C NMR spectrum of the copolymer (Run 15) is shown in **Figure 2-3**. According to the reported assignment of the NB/St copolymer,[34] each signal was assigned as follows: 145.7 ppm for C^1, 127.3 ppm for C^2, 127.9 ppm for C^3, 125.6 for C^4, 41.5–44.2, and 40.5 ppm for C^5 and C^6 of the St segment, 47.1–52.5 ppm for C^3, 38–39.7 ppm for C^2, 34.5–37 ppm for C^4, and 29.4–31.9 ppm for C^1 of the NB unit. A clear observation of the phenyl-carbons of the St units in the regions of 125–145 ppm also indicates the presence of the St units in the NB/St copolymer. These results are similar to those obtained in the previously reported nickel–MAO catalytic system and confirm the random distribution of St unit in the obtained NB/St copolymer.[34]

The incorporation of St increased with increasing St concentration in the monomer feed ratio. The highest St content in the NB/St copolymer was achieved to be 36% at 1:1 feed ratio by complex **1c** probably because of less interaction between the ligand substituent and the aromatic ring of St.

The molecular weight of NB/St copolymer was measured by GPC. The increase of St concentration in feed caused the decrease in the molecular weights of the produced polymers accompanied by the increase in the number of polymer chains, which is ascribed to β-hydrogen elimination of the increased styryl propagation end.[41] Unimodal distribution ($M_w/M_n \approx 2$) indicates that the copolymerization should take place at a single active site.

2-3-3. Effect of Polymerization Temperature on NB/St Copolymerization

The influence of reaction temperature on NB/St copolymerization was studied using **1**-MMAO at the fixed feeding ratio (NB/St = 4/1 in molar ratio), because the low St feed ratio gave high molecular weight NB/St copolymer. The results are summarized in **Table 2-2**.

The copolymerization activity decreased with lowering the temperature from 70 to 0 °C. The highest activity around 70 $kg_{polymer}$ mol_{Ni}^{-1} h^{-1} for the copolymerization was achieved at 70 °C in each system. On the other hand, the St content and the M_n value monotonously increased with lowering of the polymerization temperature (Run 19, 22 and 25), and the NB/St copolymer with 32 mol % of St and 61,000 of M_n was obtained at 0 °C by **1c**-MMAO (**Table 2-**

2, Run 25). This M_n value would be the highest among the NB/St copolymers reported so far.[25,34,35] The molecular weight distribution became narrow with decreasing the polymerization temperature. A decreased M_n value of the copolymers obtained with an increase in the reaction temperature is ascribed to the chain transfer at high temperature.[32]

Table 2-2. Effects of temperature of NB/St copolymerization by **1**-MMAO

Run	Com.	Temp. (°C)	Yield (g)	Act. [a]	f_{St} [b] (mol%)	M_n [c] (10^3)	M_w/M_n [c]	T_g [d]
2	1a	70	0.36	72	4	19	2.4	321
17	1a	50	0.27	54	7	26	2.2	289
18	1a	30	0.14	28	9	27	2.0	267
19	1a	0	0.13	26	20	55	2.1	219
6	1b	70	0.37	74	4	19	2.7	329
20	1b	50	0.27	54	9	24	2.2	263
21	1b	30	0.20	40	12	27	2.3	252
22	1b	0	0.11	22	30	57	1.5	175
12	1c	70	0.36	72	10	13	2.0	251
23	1c	50	0.29	58	16	18	2.2	227
24	1c	30	0.24	48	21	54	1.5	212
25	1c	0	0.14	27	32	61	1.5	172

Copolymerization conditions: Ni = 5 μmol, Al/Ni = 100 (molar ratio), NB:St = 4:1 (molar ratio), toluene (total volume 25 mL) time = 1 h. [a] Activity = $kg_{(polymer)}\ mol_{(Ni)}^{-1}\ h^{-1}$. [b] f_{St} are the content of St in the NB/St copolymer determining by ^1H NMR spectrum. [c] Determined by GPC. [d] Determined by DSC.

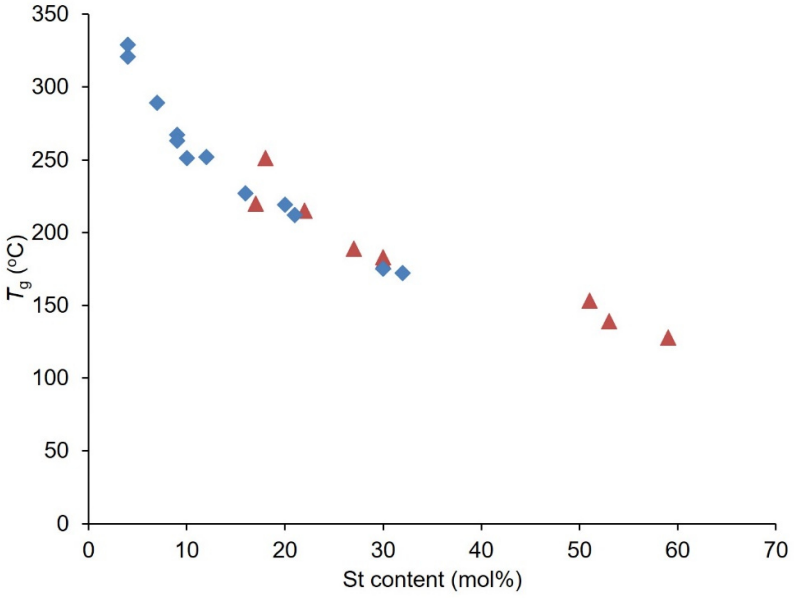

Figure 2-4. T_g vs St content plot obtained by Ni complexes: ♦, MMAO; ▲, $B(C_6F_5)_3$.

The thermal properties of NB/St copolymers were analyzed by DSC. The T_g value declined with an increase of St content as shown in **Figure 2-4**. The highest value of 329 °C and the lowest value of 172 °C were detected (**Figure 2-5**) for the copolymers with 4 and 32 mol % of St, respectively (**Table 2-2**, Run 6 and 25). The previous study has shown that the T_g value of the PNBs obtained with this catalyst was over 400 °C.[37] The T_g value of polystyrene is 100 °C. The single T_g value in the DSC curves reveal that NB and St were uniformly distributed in the NB/St copolymers obtained by the present catalysts.

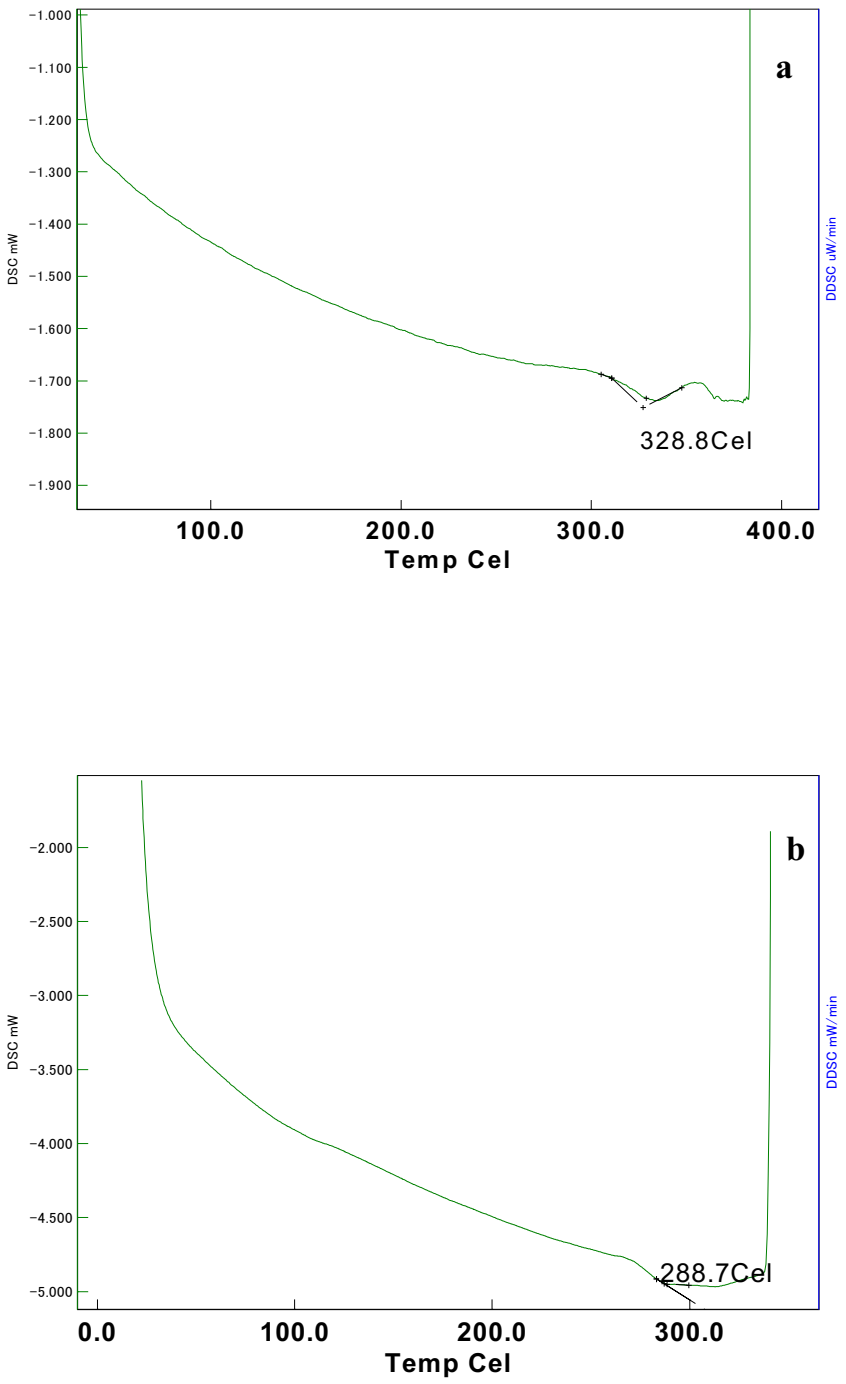

Figure 2-5. DSC curves of NB/St copolymers obtained by (**a**) Run 6 and (**b**) Run 17.

2-3-4. NB/St Copolymerization by 1-$B(C_6F_5)_3$

The author found the considerable effects of temperature on NB/St copolymerization using the **1**-MMAO system. Shiono and coworkers observed significant effects of $B(C_6F_5)_3$ in E polymerization[38] and NB polymerization[37] with **1a**, which were ascribed to the formation of zwitterionic nickel species.[39]

Thus, the NB/St copolymerization (NB/St = 4/1 in molar ratio) by the **1**-$B(C_6F_5)_3$ system was conducted at different temperatures (30, 50, and 70 °C) to investigate the cocatalyst effects.

The activity of the $B(C_6F_5)_3$ system was lower than that of the MMAO system. The incorporation of St increased with lowering the temperature, as was observed in the **1**-MMAO system. The St incorporation was almost four times higher than those of the copolymers produced by the **1**-MMAO system. The highest St incorporation of 51~59% was observed at 30 °C with the M_n values (**Figure 2-6**) of 43,000~78,000 (**Table 2-3**, Run 28, 33, and 36).

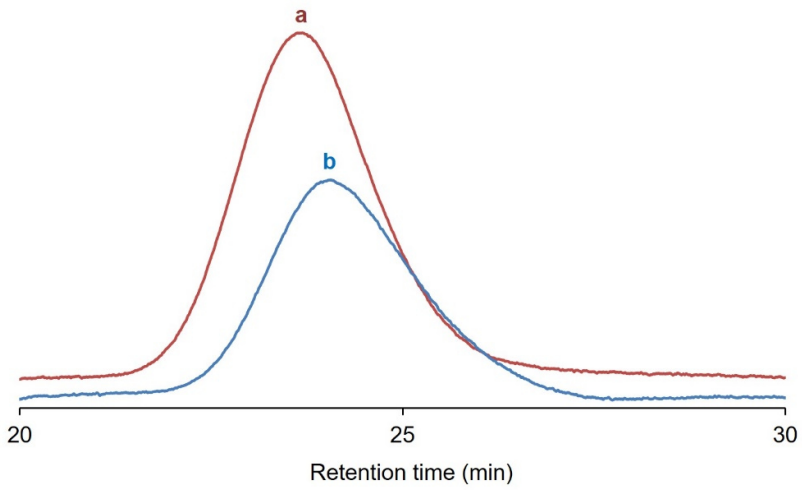

Figure 2-6. GPC traces NB/St copolymers: **a**, Run 32; **b**, Run 35.

Table 2-3. Effects of temperature of NB/St copolymers by **1**-$B(C_6F_5)_3$

Run	Com.	Ratio	Temp. (°C)	Yield (g)	Act. [a]	f_{St} [b] (mol%)	M_n [c] (10^3)	M_w/M_n [c]	T_g [d]
26	1a	4/1	70	0.126	26	17	36	1.9	220
27	1a	4/1	50	0.072	15	22	40	1.7	215
28	1a	4/1	30	0.053	11	51	43	1.9	153
29	1b	4/1	70	0.088	18	18	38	2.0	251
30	1b	4/2	70	0.110	22	27	33	1.7	197
31	1b	4/3	70	0.133	27	33	30	1.7	175
32	1b	4/1	50	0.067	14	30	55	1.6	183
33	1b	4/1	30	0.033	7	59	78	1.9	128
34	1c	4/1	70	0.082	17	27	38	2.5	189
35	1c	4/1	50	0.034	7	30	39	2.1	180
36	1c	4/1	30	0.030	6	53	46	2.0	139
37[e]	1a	4/1	70	0.330	66	17	103	1.4	232

Copolymerization conditions: Ni = 5 μmol, $B(C_6F_5)_3$/Ni = 4 (molar ratio), NB:St = 4:1 (molar ratio), toluene (total volume 25 mL), time = 1 h. [a] Activity = $kg_{(polymer)}\ mol_{(Ni)}^{-1}\ h^{-1}$. [b] f_{St} are the content of St in the NB/St copolymer determining by ^1H NMR spectrum. [c] Determined by GPC. [d] Determined by DSC. [e] $B(C_6F_5)_3$: $^iBu_3Al$: BHT = 1 : 10 : 20.

In order to evaluate the effects of the cocatalysts on NB/St copolymerization, the monomer reactivity ratios of **1b** were determined at 70 °C (**Table 2-3**). The Fineman-Ross plots of **1b**-MMAO and **1b**-$B(C_6F_5)_3$ for NB/St copolymerization are shown in **Figure 2-7**. The monomer reactivity ratios were

determined to be r_{NB} = 6.34, r_{St} = 0.39 for **1b**-MMAO and r_{NB} = 0.93, r_{St} = 0.13 for **1b**-$B(C_6F_5)_3$, indicating the better copolymerization ability of $B(C_6F_5)_3$ cocatalyst. The reactivity ratios of **1c**-MMAO were also determined to evaluate the effects of the complexes. The values, r_{NB} = 2.16, r_{St} = 0.26, indicates the better copolymerization ability of **1c** than **1b**.

The T_g values determined by DSC are shown in **Table 2-3** and are plotted against St content in Figure **2-4**. The plot is in good accordance with that of the MMAO system but extends to the higher St content as indicated by the monomer reactivity ratios. The lowest T_g value of 128 °C was obtained by the copolymer with St content of 59 mol % and M_n of 78,000 (**Table 2-3**, Run 33).

The **1**-$B(C_6F_5)_3$ system gave the copolymers with high molecular weights and high St contents compared with the **1**-MMAO system, although the activity was low. The lower activity would be due to the deactivation by impurities in the absence of scavenging reagents. Therefore, we conducted NB/St copolymerization with **1a**-$B(C_6F_5)_3$ in the presence of the reaction mixture of $^{i}Bu_3Al$ and 2,6-$^{t}Bu_2$-*p*-cresol. The addition of the scavenger increased the activity keeping the same St content and the M_n value reached 103,000 (**Table 2-3**, Run 37). The results indicate the potentiality of **1**-$B(C_6F_5)_3$ for NB/St copolymerization.

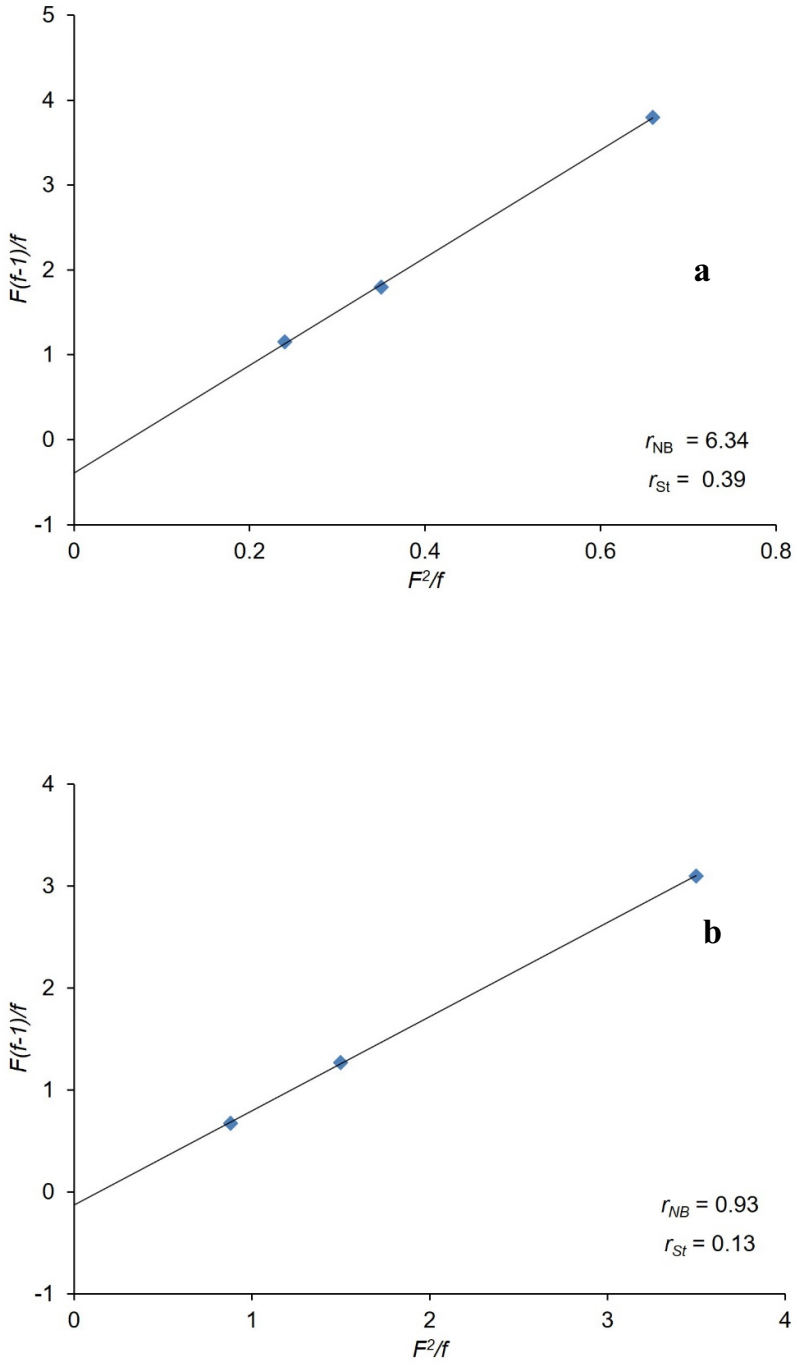

Figure 2-7. Fineman–Ross plots for copolymerization of NB/St by **1b** with (**a**) MMAO and (**b**) $B(C_6F_5)_3$.

2-3-5. Optical Property of NB/St Copolymer

The light transmittance of the NB/St copolymer (**Table 2-3**, Run 37) film with the thickness about 100 μm is displayed in **Figure 2-8**. The copolymer showed the transmittance above 85% in the visible light region (300–800 nm).

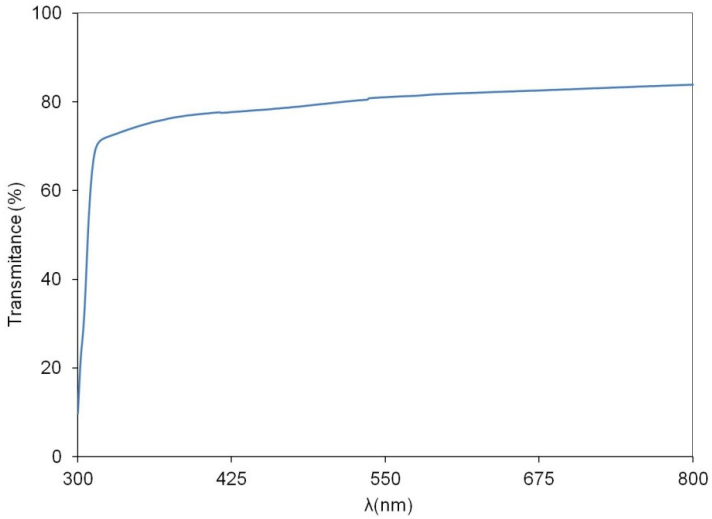

Figure 2-8. Transmittance of NB/St copolymer thin film obtained by Run 37.

2-4. Conclusions

Copolymerizations of NB and St were achieved by anilinonaphthoquinone-ligated nickel-complexes using MMAO or $B(C_6F_5)_3$ as cocatalyst. The **1**-MMAO system showed higher activity than the **1**-$B(C_6F_5)_3$ system, whereas the latter system produced the copolymers with higher molecular weight and higher St incorporation. The molecular weights of NB/St copolymers obtained by **1**-$B(C_6F_5)_3$ were the highest among those of the copolymers reported previously using nickel-, copper-, and titanium-based catalytic systems.

References

1. M. Chen, W. Zou, Z. Cai, C. Chen, *Polym. Chem.* **2015**, *6*, 2669–2676.
2. L. Pei, Y. Tang, H. Gao, *Polymers* **2016**, *8*, 69.
3. J. -F. Meng, X. Li, X. -F. Ni, Z. -Q. Shen, *RSC Adv.* **2016**, *6*, 19351–19356.
4. L. R. Gilliom, R. H. Grubbs, *J. Am. Chem. Soc.* **1986**, *108*, 733–742.
5. S. T. Nguyen, L. K. Johnson, R. H. Grubbs, J. W. Ziller, *J. Am. Chem. Soc.* **1992**, *114*, 3974–3975.
6. J. P. Kennedy, H. S. Makowski, *J. Macromol. Sci. Chem.* **1967**, *A1*, 345–370.
7. N. G. Gaylord, B. M. Mandal, M. Martan, *J. Polym. Sci. Polym. Lett. Ed.* **1976**, *14*, 555–559.
8. N. G. Gaylord, A. B. Deshpande, *J. Polym. Sci. Polym. Lett. Ed.* **1976**, *14*, 613–617.
9. N. G. Gaylord, A. B. Deshpande, B. M. Mandal, *J. Macromol. Sci. Chem.* **1977**, *A11*, 1053–1070.
10. S. Rush, A. Reinmuth, W. Risse, *Macromolecules* **1997**, *30*, 7375–7385.
11. L. Goodall, L. H. McIntosh III, L. F. Rhodes, *Macromol. Symp.* **1995**, *89*, 421–432.
12. N. Seehof, C. Mehler, S. Breunig, W. Risse, *J. Mol. Catal.* **1992**, *76*, 219–228.

13. N. R. Grove, P. A. Kohl, S. A. B. Allen, S. Jayaraman, R. Shick, *J. Polym. Sci., Part. B: Polym. Phys.* **1999**, *37*, 3003–3010.
14. C. P. Janiak, G. Lassahn, *Macromol. Rapid Commun.* **2001**, *22*, 479–492.
15. L. Boggioni, I. Tritto, *MRS Bull.* **2013**, *38*, 245–251.
16. X. He, Y. Deng, X. Jiang, Z. Wang, Y. Yang, Z. Han, D. Chen, *Polym. Chem.* **2017**, *8*, 2390–2396.
17. T. Shiono, M. Sugimoto, T. Hasan, Z. Cai, T. Ikeda, *Macromolecules* **2008**, *41*, 8292–8294.
18. Z. Cai, R. Harada, Y. Nakayama, T. Shiono, *Macromolecules* **2010**, *43*, 4527–4531.
19. Y. Xing, Y. Chen, X. He, H. Nie, *J. Appl. Polym. Sci.* **2012**, *124*, 1323–1332.
20. Y. M. Liu, M. Ouyang, X. H. He, Y. W. Chen, K. T. Wang, *J. Appl. Polym. Sci.* **2013**, *128*, 216–223.
21. W. Zhao, K. Nomura, *Macromolecules* **2016**, *49*, 59–70.
22. W. Zhao, K. Nomura, *Catalysts* **2016**, *6*, 175.
23. X. He, Y. Deng, Z. Han, Y. Yang, D. Chen, *J. Polym. Sci., Part. A: Polym. Chem.* **2016**, *54*, 3495–3505.
24. T. Hasan, T. Ikeda, T. Shiono, *Macromolecules* **2004**, *37*, 8503–8509.
25. H. Ban, H. Hagihara, Y. Tsunogae, Z. Cai, T. Shiono, *J. Polym. Sci., Part A: Polym. Chem.* **2011**, *49*, 65–71.

26. F. Peruch, H. Cramail, A. Deffieux, *Macromol. Chem. Phys.* **1998**, *199*, 2221–2227.

27. C. T. Zhao, M. D. R. Ribeiro, M. F. Portela, S. Pereira, T. Nunes, *Eur. Polym. J.* **2001**, *37*, 45–54.

28. X. Mi, Z. Ma, L. Wang, Y. Ke, Y. Hu, *Macromol. Chem. Phys.* **2003**, *204*, 868–876.

29. H. Suzuki, S. Matsumura, Y. Satoh, K. Sogoh, H. Yasuda, *React. Funct. Polym.* **2004**, *58*, 77–91.

30. H. Gao, Y. Chen, F. Zhu, Q. Wu, *J. Polym. Sci., Part A: Polym. Chem.* **2006**, *44*, 5237–5246.

31. F. Bao, R. Ma, Y. Jiao, *Appl. Organomet. Chem.* **2006**, *20*, 368–374.

32. F. Bao, X. Lu, Y. Chen, *Polym. Bull.* **2007**, *58*, 495–502.

33. K. Ogata, N. Nishimura, T. Yunokuchi, A. Toyota, *J. Appl. Polym. Sci.* **2008**, *108*, 1562–1565.

34. Y. Li, Q. Wu, M. Shan, M. Gao, *Appl. Organomet. Chem.* **2012**, *26*, 225–229.

35. Q. Feng, D. Chen, D. Feng, L. Jiao, Z. Peng, L. Pei, *J. Polym. Res.* **2014**, *21*, 497.

36. H. T. Ban, K. Nishii, Y. Tsunogae, T. Shiono, *J. Polym. Sci., Part A: Polym. Chem.* **2007**, *45*, 2765–2773.

37. M. Okada, Y. Nakayama, T. Shiono, *J. Organomet. Chem.* **2015**, 384–387.

38. M. Okada, Y. Nakayama, T. Ikeda, T. Shiono, *Rapid Commun.* **2006**, *27*, 1418–1423.

39. M. Okada, Y. Nakayama, T. Shiono, *J. Organomet. Chem.* **2007**, *692*, 5183–5189.

40. K. J. Ivin, J. C. Mol, Academic Press: San Diego, CA, USA, 1997; p. 407.

41. G. M. Benedikt, E. Elce, B. L. Goodall, H. A. Kalamarides, L. H. McIntosh, L. F. Rhodes, K. T. Selvy, C. Andes, K. Oyler, A. Sen, *Macromolecules* **2002**, *35*, 8978–8988.

Chapter III

Copolymerization of Norbornene with *p*-Substituted Styrenes using Anilinonaphthoquinone-ligated Nickel Complexes

3-1. Introduction

The introduction of functional groups in polynorbornene (PNB) or norbornene (NB)-based copolymer could improve their various properties such as toughness, solubility, and surface properties and expand their applications.[1-6]

Compared to post-functionalization, copolymerization with functionalized monomer is preferable because functional groups can be installed with exact compositions by a simple process. Ring-substituted styrene (St) derivatives provide wide application, in which the substituents can be varied from electron-withdrawing to electron-donating groups.[7-9]

Anilinonaphthoquinone-ligated nickel complexes [Ni($C_{10}H_5O_2NAr$)(Ph)(PPh_3): **1a**, Ar = C_6H_3-2,6-^{i}Pr; **1b**, Ar = C_6H_2-2,4,6-Me; **1c,** Ar = C_6H_5] were found to give high molecular weight (M_n) NB/St copolymer with controllable St content, although the activity was not sufficient.[10] Therefore, In this chapter copolymerization of NB and a series of *p*-substituted styrene (XSt) was conducted using **1** combined with modified

methylaluminoxane (MMAO) to investigate the effect of the substituent on the copolymerization and the properties of the produced polymers.

3-2. Materials and Methods

General Considerations

All manipulations were carried out under a nitrogen atmosphere using standard Schlenk techniques. All solvents were refluxed and distilled over sodium/benzophenone or calcium hydride. NB was purified by stirring it over calcium hydride at 60 °C for one day and then distilled. The stock solution of NB (5.5 M) was prepared in toluene. *p*-Substituted styrene (XSt; X- = MeO-, Me- F-, Cl- and Br-) (from FUJIFILM Wako Pure Chemical Corporation, Japan) was dried over CaH_2, and then freshly distilled under vacuum prior to use. Modified methylaluminoxane (MMAO) solution (6.6 wt % in toluene) was donated from Tosoh Finechem. Co. (Tokyo, Japan) and used as received. The nickel complexes **1a-c** were synthesized as described in Chapter II.

Analytical Procedures

Molecular weights and molecular weight distributions of polymers were determined by gel permeation chromatography (GPC) with a Viscotec HT-350 GPC (Malvern, UK) with three CLM6210 mixed-bed columns. This system was equipped with a triple-detection array consisting of a differential refractive

index detector, a two-angle (7, 90) light scattering detector and a four-bridge capillary viscosity detector. Polymer characterization was carried out at 150 °C using *o*-dichlorobenzene as an eluent and calibrated with polystyrene standards. The ^{1}H and ^{13}C NMR spectra of polymers were measured at room temperature on a Bruker 500MHz instrument (Bruker, Germany) operated by the pulse Fourier-transform mode. The measurement for ^{1}H NMR and ^{13}C NMR, sample solution was prepared in $CDCl_3$ up to 10 wt%. The pulse angle for ^{13}C NMR was 45° and about 8000-10,000 scans were accumulated in pulse repetition of 5.0 s. The central peak of $CDCl_3$ (77.13 ppm for ^{13}C NMR) and the peak of $CHCl_3$ (7.25 ppm for ^{1}H NMR) was used as an internal reference. Differential scanning calorimetry (DSC) was performed on a SII EXSTER 600 (Seiko Instruments Inc., Japan) system under nitrogen atmosphere. Thermal history difference in the polymers was eliminated by first heating the specimen to 380 °C, cooling at 10 °C/min to 20 °C, and then recording the second DSC scan at a heating rate of 10 °C/min.

Copolymerization of NB and XSt

In a typical procedure, prescribe amounts of NB and XSt in toluene solution were introduced into a 100-mL round-bottomed glass flask and then 0.24 mL of MMAO toluene solution (500 μmol) and 1 mL of the nickel complex (5 μmol) solution in toluene were syringed into the well-stirred monomer solution in this order, and the total solution volume was made to 25

mL by adding toluene. The copolymerization was conducted under continuous stirring for a required time under a certain temperature controlled with an external oil or ice bath. The copolymerization was terminated by adding 300 mL of acidic methanol (methanol/concentrated hydrochloric acid, 95/5 in volume). The resulting precipitated polymer was collected by filtration, adequately washed with methanol, and dried in vacuum at 60 °C for 6 h.

Preparation of Copolymer Films

NB/XSt copolymer (approximately 300 mg) was dissolved into 3 mL of toluene at room temperature and filtered through 0.20 μm PTFE membrane. The filtered solution was placed on a glass plate and stood for 3 days under ambient temperature and pressure. After almost all the solvent was vaporized, the film was placed at 60 °C under vacuum condition for 3 h.

3-3. Results and Discussion

3-3-1. NB/XSt Copolymerization

Copolymerizations of NB/MeOSt, NB/MeSt and NB/ClSt were carried out using the nickel complexes [Ni($C_{10}H_5O_2NAr$)(Ph)(PPh_3); Ar = C_6H_3-2,6-^{i}Pr (**1a**); Ar = C_6H_2-2,4,6-Me (**1b**); Ar = C_6H_5 (**1c**)] activated by MMAO in toluene (**Scheme 3-1**). In the previous chapter, NB/St copolymers with high molecular weight were obtained at the NB/St feed ratio of 4/1 by the same catalytic

system.[23] Therefore, the author conducted NB/XSt copolymerization with the NB/XSt feed ratio of 4/1 at the copolymerization temperature from 0 to 70 °C. The results are summarized in **Table 3-1.**

In all the copolymerizations, the activities increased with increasing the polymerization temperature. Thus, the substituent effects of the Ni complex and XSt were compared by the results obtained at 70 ºC. In the case of the NB/MeOSt and NB/MeSt copolymerizations, the yield decreased in the following order: **1a** > **1b** ≥ **1c**. Whereas, the opposite trend was observed in the NB/ClSt copolymerization: **1c** > **1b** > **1a**.

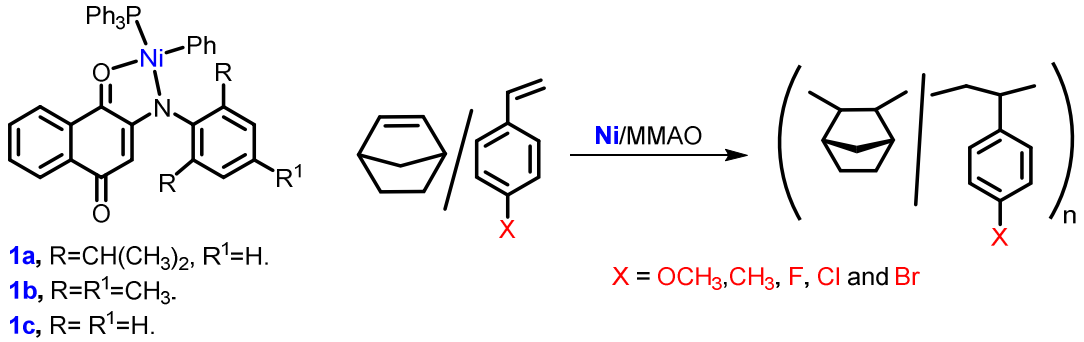

Scheme 3-1 NB/XSt copolymerization using Ni catalyst.

The effect of the ligand on the yield was not so significant in the case of the NB/St copolymerization. The yield also depended on the comonomer XSt and decreased as follows irrespective of the Ni complex, ClSt > St ≥ MeSt > MeOSt.

Table 3-1 Copolymerization of NB with XSt by **1**-MMAO[a]

Run	Cat.	Mono.	T (°C)	Yield (g)	f_{XSt} [b] (mol %)	TOF [c] (10^3 h^{-1})	M_n [d] (10^3)	M_w/M_n [d]	T_g [e]
1	1a	MeOSt	0	0.07	69	0.12	103	1.3	-[f]
2	1a	"	30	0.10	30	0.19	98	1.4	195
3	1a	"	70	0.23	18	0.45	79	1.5	261
4	1b	"	70	0.11	17	0.22	72	1.3	271
5	1c	"	0	0.07	73	0.11	107	1.3	-[f]
6	1c	"	30	0.08	33	0.13	103	1.4	-[f]
7	1c	"	70	0.10	19	0.20	65	1.4	255
8	1a	MeSt	0	0.07	70	0.13	117	1.6	125
9	1a	"	30	0.29	25	0.58	109	1.4	274
10	1a	"	70	0.37	10	0.75	74	1.8	321
11	1b	"	0	0.07	70	0.13	120	1.3	-[f]
12	1b	"	30	0.27	29	0.53	109	1.4	237
13	1b	"	70	0.37	13	0.75	98	1.5	293
14	1c	"	0	0.07	73	0.13	132	1.3	120
15	1c	"	30	0.21	29	0.43	126	1.3	239
16	1c	"	70	0.35	11	0.72	120	1.3	308
17	1a	ClSt	0	0.80	13	1.60	225	1.4	346
18	1a	"	30	1.30	9	2.67	110	1.5	350
19	1a	"	70	1.50	5	3.12	63	1.4	354
20	1b	"	0	0.90	19	1.76	504	1.4	304
21	1b	"	30	1.13	10	2.35	169	1.4	345
22	1b	"	70	1.55	4	3.24	87	1.8	362
23	1c	"	0	0.95	19	1.85	517	1.3	309
24	1c	"	30	1.43	11	2.89	218	1.5	344
25	1c	"	70	1.74	4	3.63	87	1.7	358

[a] Polymerization conditions: Ni = 5 μmol; norbornene = 40 mmol; XSt = 10 mmol; Al/Ni = 100; time = 1 h; solvent = toluene (total volume 20 mL). [b] f_{XSt} are the content of XSt in the NB/XSt copolymer determined by ^{1}H NMR. [c] TOF = $W_{yield}/ [M_{XSt} \times f_{XSt} + M_{NB} \times (1-f_{XSt})]$. $mol_{Ni.}$ h (M_{XSt} molecular weight of XSt, M_{NB} molecular weight of NB). [d] Determined by GPC. [e] T_g was determined by DSC. [f] Not determined.

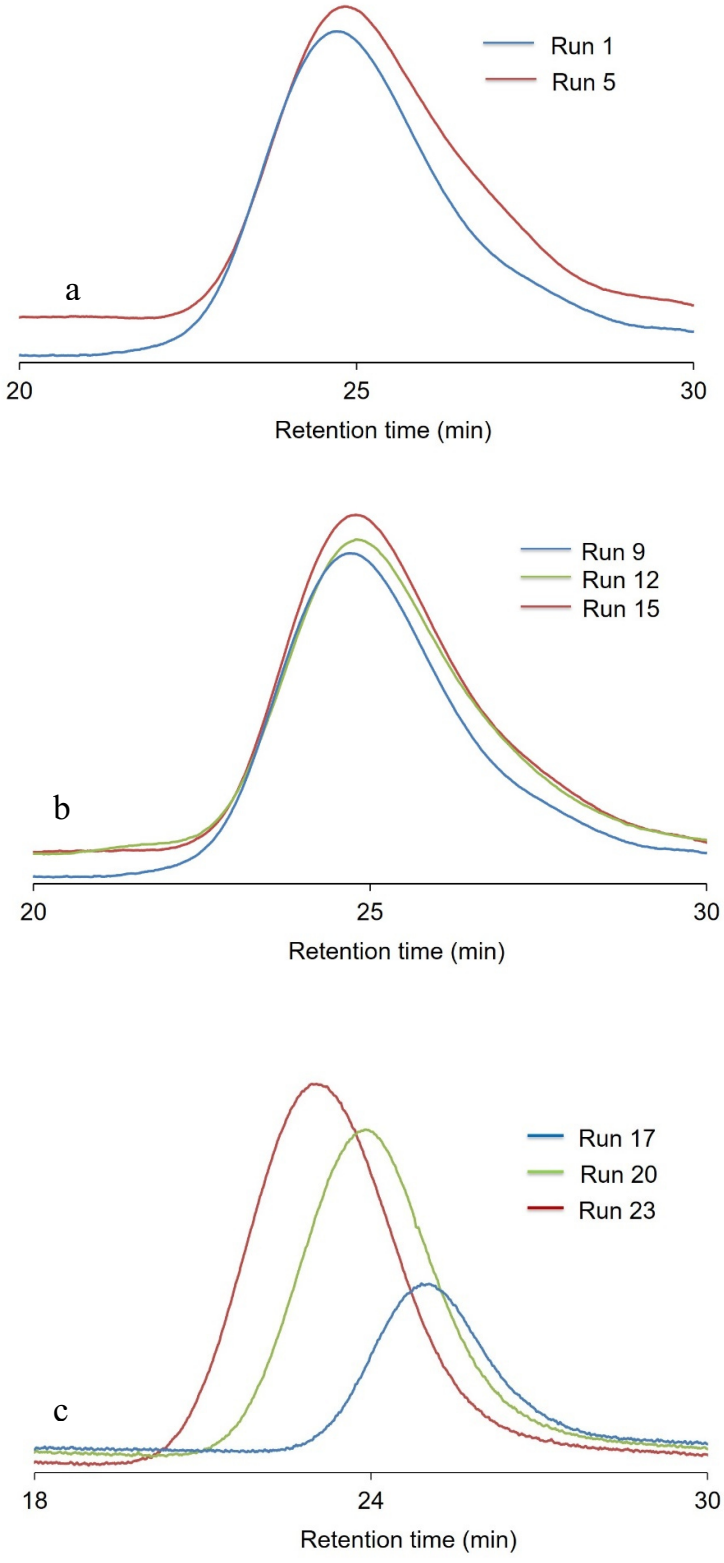

Figure 3-1. GPC traces of copolymers: (a) NB/MeOSt (b) NB/MeSt (c) NB/ClSt.

The molecular weights of the copolymers were measured by GPC. In comparison to the yield, the number-average molecular weight (M_n) was not clearly depended on the complex and/or the comonomer at 70 ºC. The decrease of the polymerization temperature increased the M_n value irrespective of the comonomer and the complex.

The M_n values of NB/XSt copolymers showed the following tendency at 0 °C, ClSt > MeSt > MeOSt and **1c** > **1b** > **1a**. Catalyst **1c** showed the highest M_n of 517000 for NB/ClSt copolymer at 0 °C. Unimodal distribution ($M_w/M_n \approx 1.3 \sim 2.0$) indicates that the copolymerization should take place at a single active site (**Figure 3-1**).

3-3-2. Structures of NB/XSt Copolymers

The copolymers were not only soluble in chloroform but also in cyclohexane similar to the PNB obtained by the same catalytic system. The incorporation of XSt in the produced copolymers was investigated by ^{1}H NMR in $CDCl_3$. Typical ^{1}H NMR spectra of the NB/MeOSt, NB/MeSt and NB/ClSt copolymers (Run 2, 9 and 18) are illustrated in **Figure 3-2a**, **3-3a** and **3-4a**.

The signals assignable to the aliphatic protons of the NB and XSt units (H^{4-9}) are observed in the range of 0.8–2.4 ppm. Strong methyl peaks (H^3) of NB/MeOSt and NB/MeSt copolymers are observed at 3.7 and 2.4 ppm, respectively (**Figure 3-2a** and **3-3a**). The signals attributed to the aromatic protons of the St units ($H^{1,2}$) are observed in the range of 6.5–7.2 ppm.

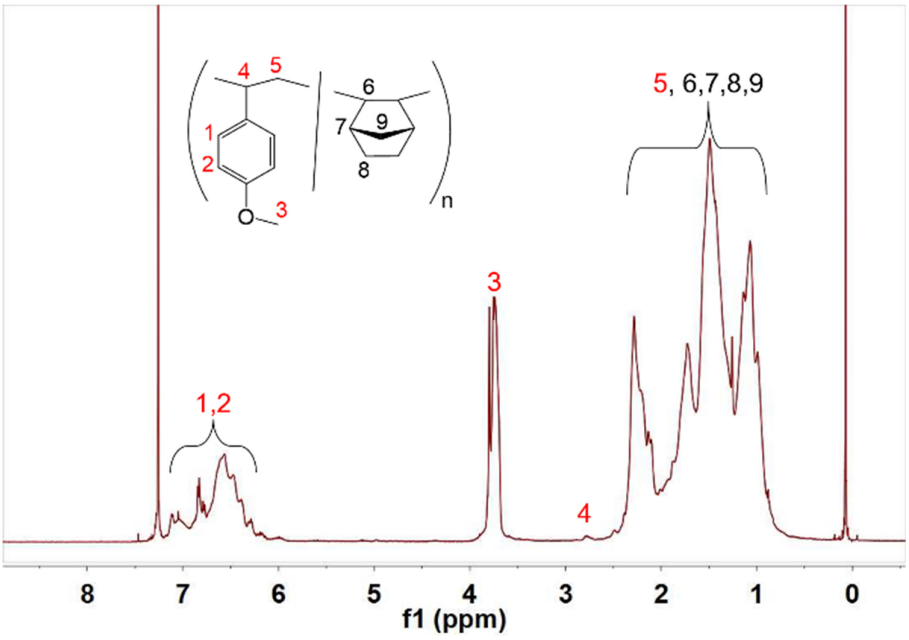

Figure 3-2a. [1]H NMR spectrum of NB/MeOSt copolymer obtained by Run 2.

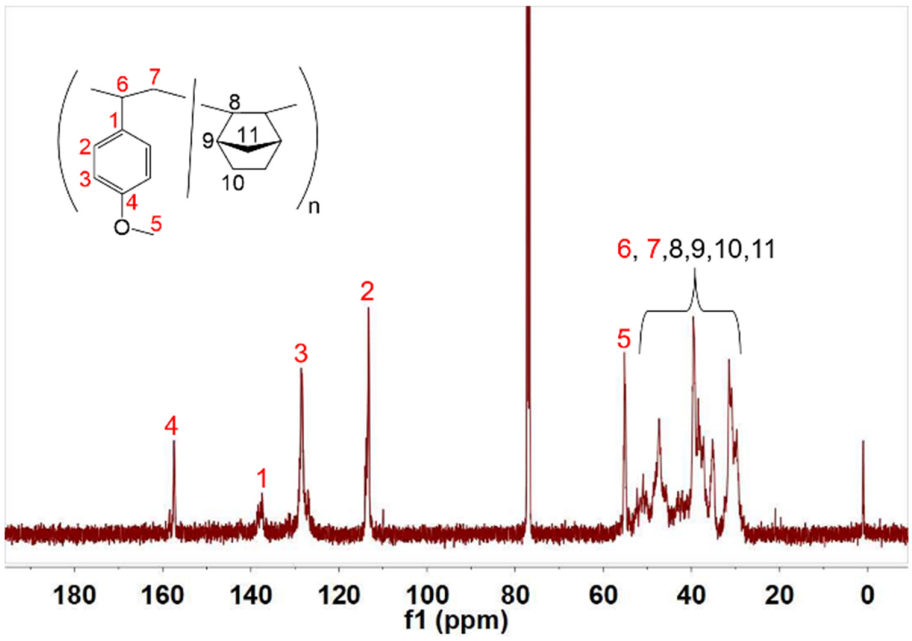

Figure 3-2b. [13]C NMR spectrum of NB/MeOSt copolymer obtained by Run 2.

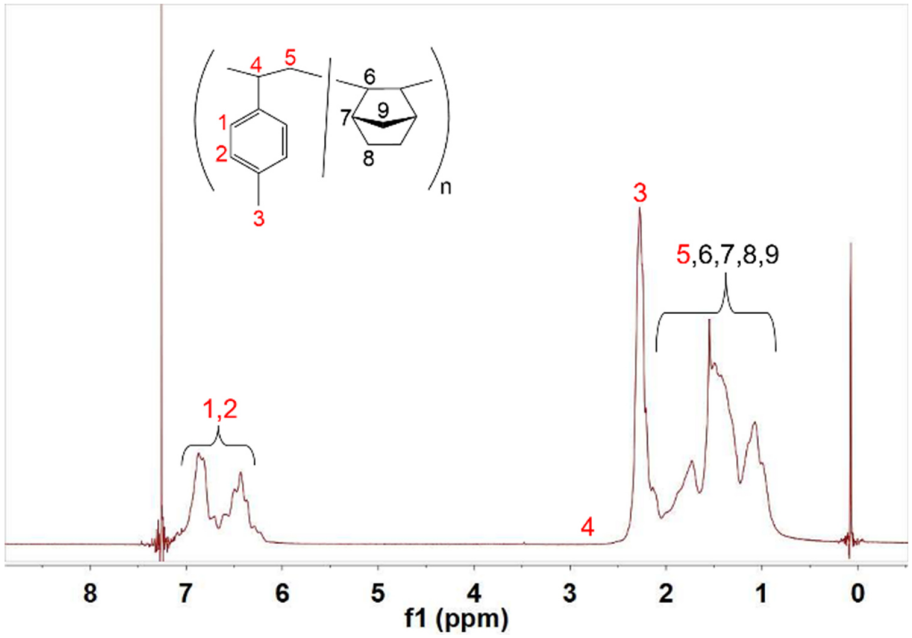

Figure 3-3a. [1]H NMR spectrum of NB/MeSt copolymer obtained by Run 9.

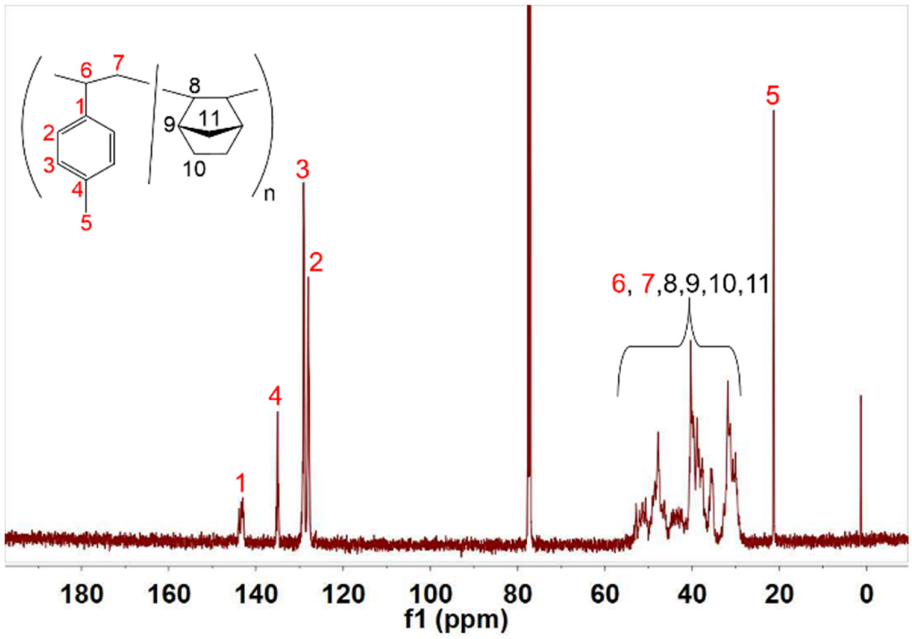

Figure 3-3b. [13]C NMR spectrum of NB/MeSt copolymer obtained by Run 9.

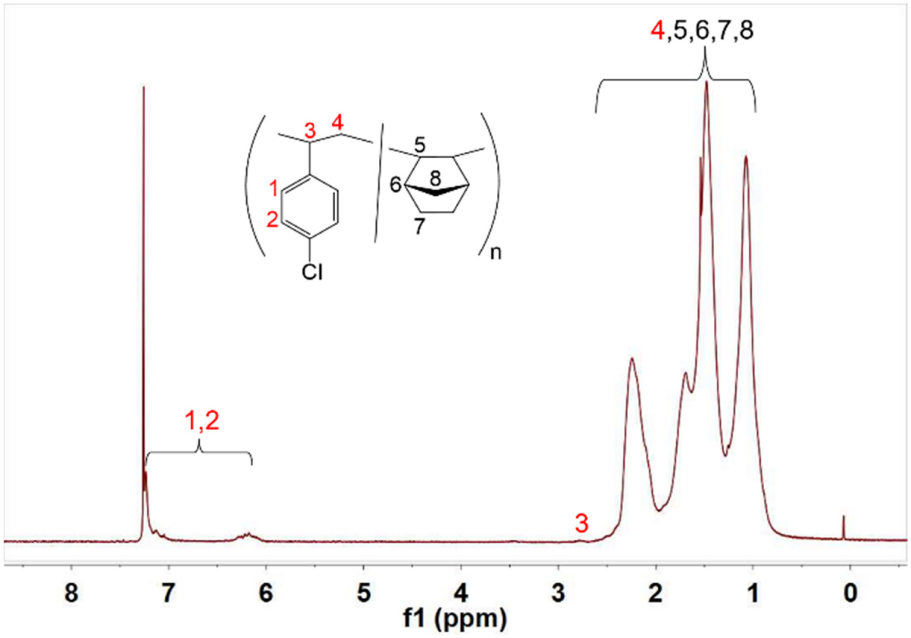

Figure 3-4a. ^{1}H NMR spectrum of NB/ClSt copolymer obtained by Run 18.

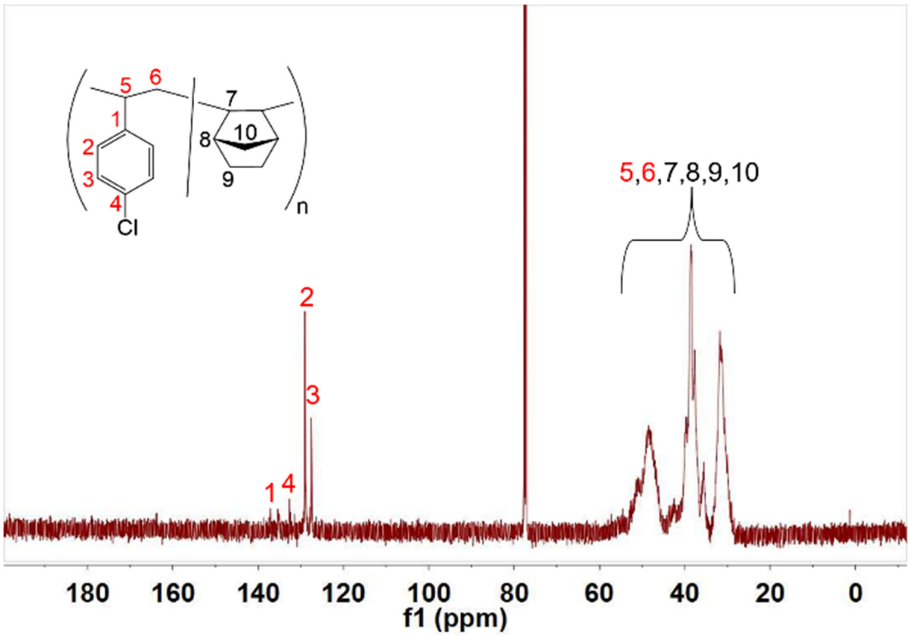

Figure 3-4b. ^{13}C NMR spectrum of NB/ClSt copolymer obtained by Run 18.

Particularly, the signal of the methine proton of the St unit (H^4) adjacent to the NB unit can be observed at 2.85 ppm.

Typical ^{13}C NMR spectra of the NB/MeOSt, NB/MeSt and NB/ClSt copolymers (Run 2, 9 and 18) are shown in **Figure 3-2b**, **3-3b** and **3-4b**. Each signal of the NB/MeOSt copolymer was assigned as follows in reference to those of NB/St copolymer obtained by the same catalyst[10] and St/MeOSt copolymer obtained by an yttrium-based catalyst:[11, 12] 137.0 ppm for C^1, 112.9 ppm for C^2, 128.1 ppm for C^3, 157.5 for C^4, 54.9 for C^5, 47.0 and 39.3 ppm for C^6 and C^7 of the MeOSt segment; 49-52.7 ppm for C^8, 36.5–38.8 ppm for C^9, 33.8–36 ppm for C^{10} and 28.0–31.9 ppm for C^{11} of the NB unit. The phenyl-carbons of the MeOSt units in the regions of 113–157 ppm and methoxy-carbon in the regions of 55 ppm indicates the presence of the MeOSt units in the NB/MeOSt copolymer (**Figure 3-2b**).

Each signal of the NB/MeSt copolymer was assigned as follows in reference to those of the NB/St copolymer[10] and St/MeSt copolymer obtained by a titanium-based catalyst:[13] 142.7 ppm for C^1, 127.3 ppm for C^2, 128.5 ppm for C^3, 134.1 for C^4, 21.0 for C^5, 41.4-45.1 and 39.8 ppm for C^6 and C^7 of the MeSt segment; 47.0-52.9 ppm for C^8, 36.1–38.7 ppm for C^9, 33.8–36 ppm for C^{10} and 27.8–33.8 ppm for C^{11} of the NB unit. The phenyl-carbons of the MeSt units in the regions of 134–143 ppm and methyl-carbon in the regions of 21 ppm indicates the presence of the MeSt units in the NB/MeSt copolymer (**Figure 3-3b**).

Each signal of NB/ClSt copolymer was assigned as follows in reference to those of the NB/St copolymer[10] and St/ClSt copolymer obtained by a scandium-based catalyst:[14] 136.7 ppm and 135 ppm for C^1, 128.4 ppm for C^2, 126.7 ppm for C^3, 131.9 for C^4, 40.7–44.5 and 38.0 ppm for C^5 and C^6 of the ClSt segment; 46.5-52.7 ppm for C^7, 35.8–37.7 ppm for C^8, 33.4–36.2 ppm for C^9 and 27.5–32.4 ppm for C^{10} of the NB unit. The phenyl-carbons of the ClSt units in the regions of 127–137 ppm indicates the presence of the ClSt units in the NB/ClSt copolymer (**Figure 3-4b**).

The incorporation of XSt did not significantly depend on the Ni complex and decreased in the following order, MeOSt ≥ MeSt > St ≥ ClSt. The incorporation of XSt increased with lowering the polymerization temperature. As a result, the highest XSt incorporation in each copolymer was achieved at 0 °C: MeOSt, 73 mol%; MeSt, 73 mol%; St, 32 mol%;[23] ClSt,19 mol% (Run 5, 12, 20). The comonomer with electron-donating substituent was found to incorporate more in NB/XSt copolymerization.

3-3-3. Activity of NB/XSt Copolymerization

Since the molecular weights of the comonomers are different, the activity should be evaluated by turn over frequency (TOF) calculated from the yield, the comonomer content and the molecular weights of NB and XSt. The TOF values thus obtained are shown in **Table 3-1**. The TOF value of the NB/ClSt copolymerization decreased in the following order both at 0 and 70 °C, **1c** > **1b**

> **1a**, depending on the complex used. In the case of the NB/MeSt and NB/MeOSt copolymerizations, the opposite tendency was observed at 70 °C but it was not clear at 0 °C due to the low polymer yields. The TOF value was decreased according to XSt as follows, ClSt > MeSt > MeOSt, even though it depended on the complex and the temperature.

The effects of the substituent X on the activity as well as the M_n value and the XSt content of the NB/XSt copolymer can be interpreted as follows. The active species of the NB/XSt copolymerization is a coordinatively-unsaturated cationic Ni-alkyl species and the propagation proceeds via coordination of monomer followed by the insertion to Ni-alkyl bond. The electron-donating substituent of XSt increases the electron density of the vinyl group and enhances the coordination of XSt to the cationic Ni species, which results in higher incorporation of XSt in the copolymer. However, the XSt-inserted propagation chain with electron-donating X is less reactive to next monomer coordination and/or insertion due to the decrease of the electrophilicity of the cationic Ni species, which causes low activity and the low molecular weight of the produced polymer. The effects of the ligand on TOF were depended on the comonomer, which could be interpreted by the compensation of the electrophilicity of the cationic Ni species and the nucleophilicity of XSt.

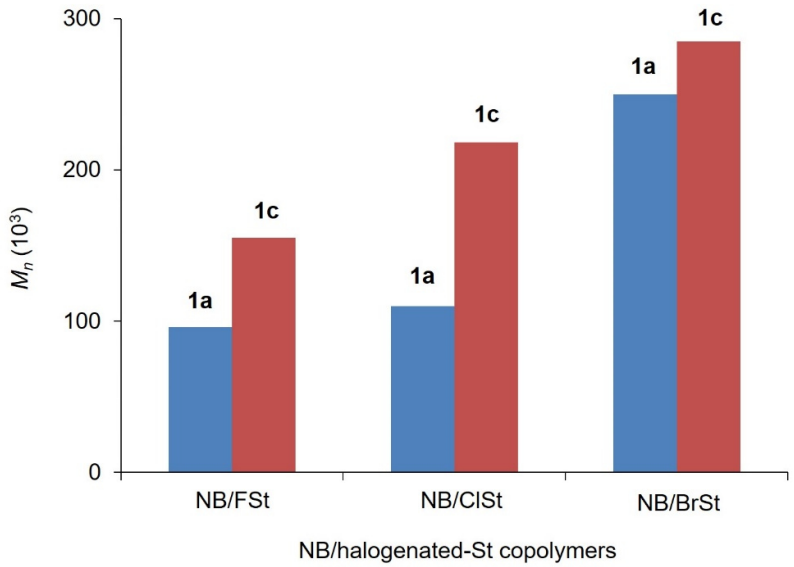

Figure 3-5. Comparison of M_n values of NB/halogenated-St copolymers.

3-3-4. Copolymerization of NB with Halogenated St

The NB/ClSt copolymerization showed the highest activity and gave the highest M_n copolymers. Thus, the author tried to copolymerize NB with FSt and BrSt under the same conditions with those for the NB/ClSt copolymerization at 30 °C using **1a** and **1c**. Complex **1c** also gave higher yields for NB/FSt and NB/BrSt copolymerization than complex **1a** (**Table 3-2,** Run 27 and 29). The NB/BrSt copolymerization gave the highest yield to give the highest M_n copolymer among the halogenated St used.

The yield and the M_n value of copolymer decreased in the following order, BrSt > ClSt > FSt. The NB/BrSt copolymer with the highest M_n of

285000 was obtained by complex **1c** (**Figure 3-5**). The M_w/M_n values were in the range of 1.3 ~1.5.

Table 3-2 Copolymerization of NB with XSt by **1**-MMAO[a]

Run	Cat.	Mono.	Yield (g)	f_{XSt} [b] (mol %)	TOF [c] (10^3 h^{-1})	M_n [d] (10^3)	M_w/M_n [d]	T_g [e]
26	1a	FSt	1.10	10	2.27	96	1.4	336
27	1c	"	1.30	12	2.67	155	1.4	335
18	1a	ClSt	1.30	9	2.67	110	1.5	350
24	1c	"	1.43	11	2.89	218	1.5	345
28	1a	BrSt	2.30	5	4.67	250	1.3	363
29	1c	"	2.70	5	5.50	285	1.5	365

[a] Polymerization conditions: Ni = 5 μmol; norbornene = 40 mmol; XSt = 10 mmol; Al/Ni = 100; time = 1 h; temperature = 30 °C; solvent = toluene (total volume 20 mL). [b] f_{XSt} are the content of XSt in the NB/XSt copolymer determined by ^{1}H NMR. [c] TOF = $W_{yield}/ [M_{XSt} \times f_{XSt} + M_{NB} \times (1-f_{XSt})]$. $mol_{Ni.}$ h (M_{XSt} molecular weight of XSt, M_{NB} molecular weight of NB). [d] Determined by GPC. [e] T_g was determined by DSC.

The structures of the NB/FSt and NB/BrSt copolymers were also confirmed by the ^{13}C NMR spectra of the copolymers (**Figure 3-6**). The XSt content of the copolymer was decrease in the following order, FSt > ClSt > BrSt.

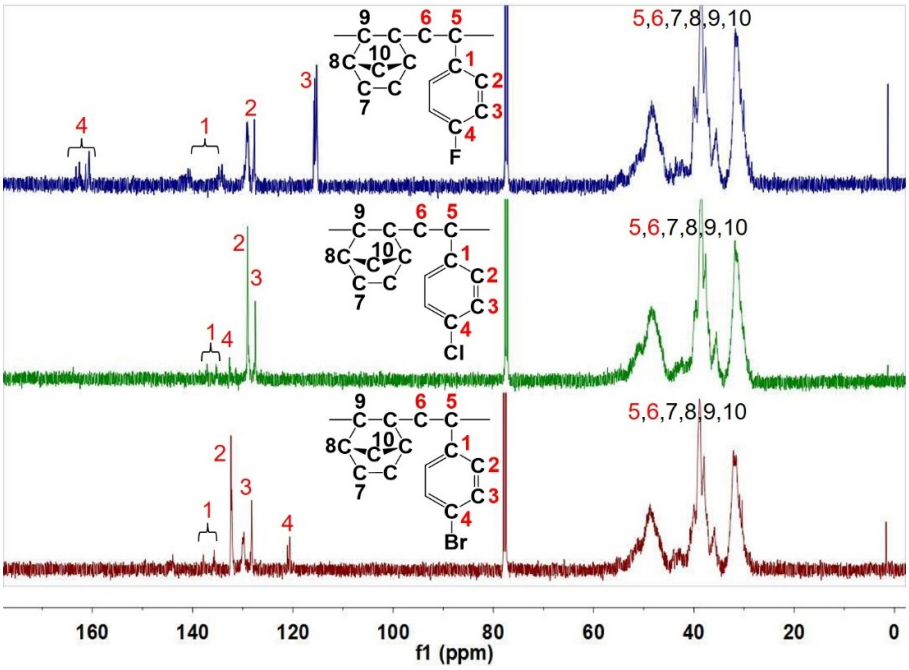

Figure 3-6. ^{13}C NMR spectra of NB/FSt, NB/ClSt and NB/BrSt copolymer obtained by Run 18, 26 and 28.

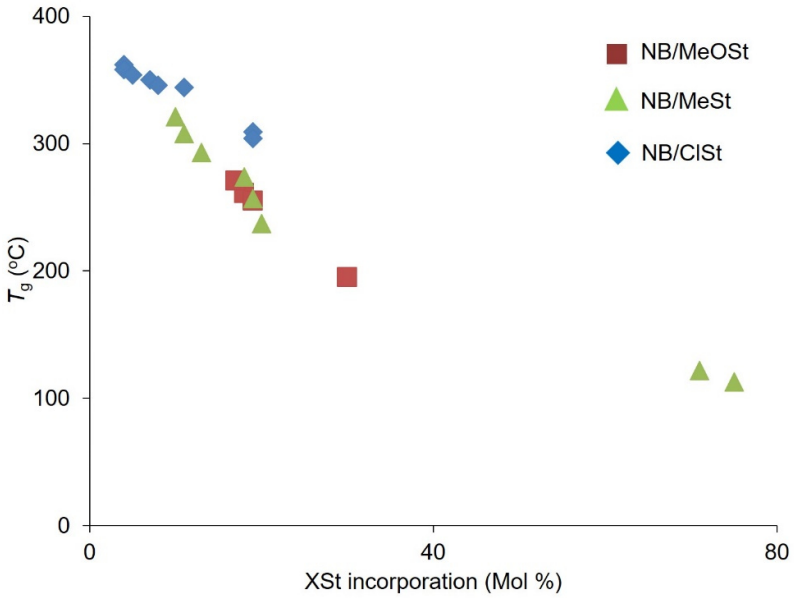

Figure 3-7. T_g vs XSt incorporation plot in NB/XSt copolymers obtained by **1**-MMAO.

The highest XSt incorporation was found to be 12% in the NB/FSt copolymerization using complex **1c** (Run 23, 27 and 29). The TOF values were calculated for the evaluation of the activity and are shown in **Table 3-2**.

The effects of halogen substituent on the activity, the molecular weight of the copolymer and the comonomer content are in good agreement with those of the other substituent and well explained by the electron-withdrawing nature of the substituent as described above.

3-3-5 Physical and Mechanical Properties of NB/XSt Copolymer

The thermal properties of the NB/XSt copolymers were analyzed by DSC. The T_g value declined with an increase of XSt content as shown in **Figure 3-7**. The lowest T_g value of 120 °C (**Figure 3-8**) and the highest value of 365 °C were detected for the copolymers with 73 mol% of MeS and 5 mol% of BrS, respectively (**Table 3-1**, Run 14 and **Table 3-2**, Run 29). Previous study has shown that the T_g value of the PNBs obtained with this catalyst was over 400 °C.[4] The T_g value of polystyrene (PS) is 100 °C.

The single T_g value in the DSC curves reveal that NB and XSt were uniformly distributed in the NB/XSt copolymer obtain by the present catalysts. The inversely proportional relation between the T_g and the XSt content in the NB/XSt copolymer also indicates that the XSt monomer is randomly incorporated into the PNB sequences (Run 12, 13 and 14).

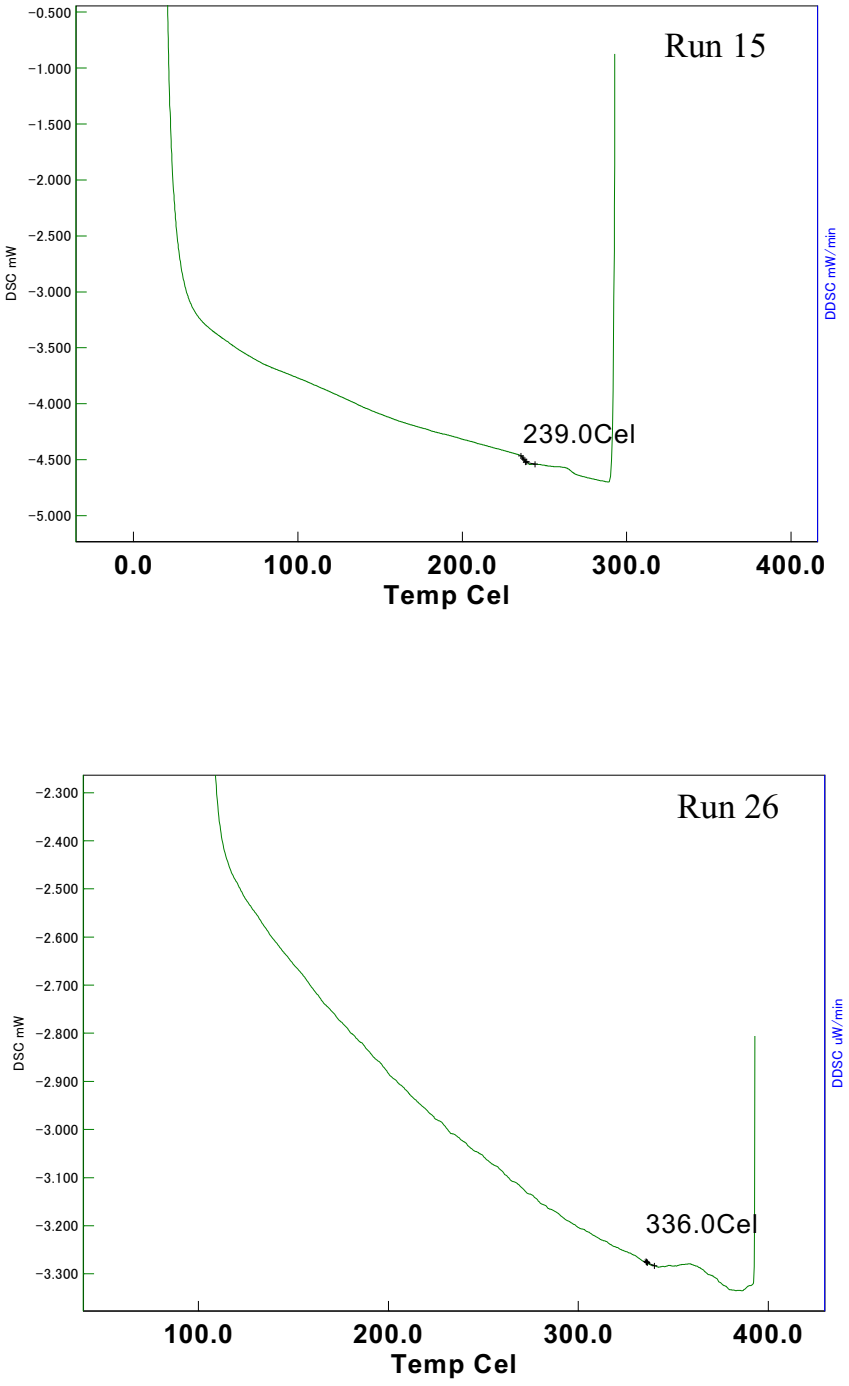

Figure 3-8 DSC curves of NB/XSt copolymer obtained by Run 15 and 26.

The light transmittance of the films prepared from the NB/MeSt, NB/FSt, NB/ClSt and NB/BrSt copolymers with the thickness of approximately 91, 101, 99 and 93 μm are displayed in **Figure 3-9** (Run 9, 24, 27 and 29). All the copolymer films show high transmittance around 90% in the visible light region (300–800 nm).

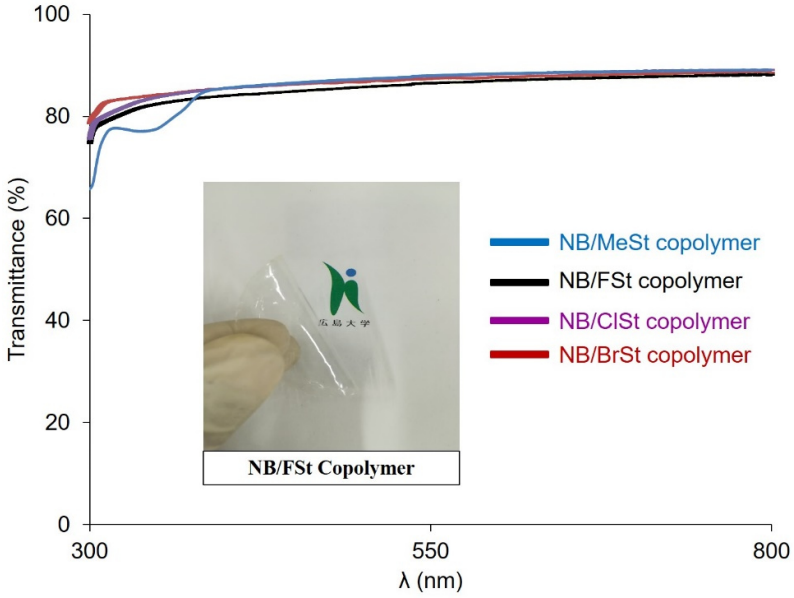

Figure 3-9 The light transmittance of the NB/XSt copolymer thin films.

Despite having a high T_g, the films of the halogenated functional copolymers displayed good flexibility at room temperature (**Figure 3-10**). The mechanical properties were investigated by a universal testing machine (**Table 3-3**). The NB/MeSt copolymer showed low elongation at break, which was improved up to four-fold by the NB/FSt copolymer.

Table 3-3 Mechanical properties of NB/XSt copolymers[a]

Sample	Copolymer	f_{XSt}	T_g	σ (MPa)	ε (%)	E (GPa)
Run 9	NB/MeSt	25	274	63.7	1.3	10.7
Run 27	NB/FSt	12	335	61.3	5.5	2.5
Run 24	NB/ClSt	11	344	62.5	4.3	3.0
Run 29	NB/BrSt	5	365	64.0	3.6	3.1

[a] Determined by tensile test, film thickness ≈ 0.1 mm. Stress at break (σ) and strain at break (ε), determined at fracture using uniaxial tensile test. Young's modulus (E), is the initial slop of the nominal stress and strain curve in the linier region.

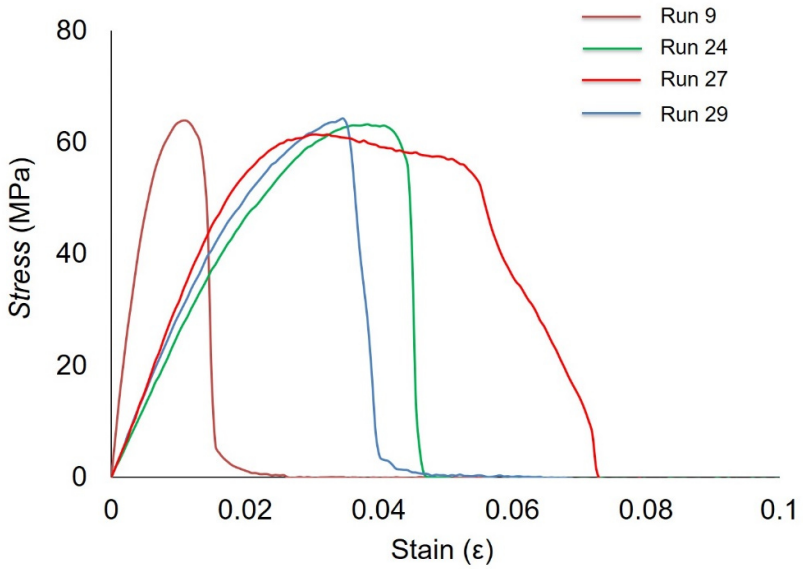

Figure 3-10. Stress−strain curves of the NB/XSt copolymers.

The elongation at break also depended on the halogenated St and decreased in the following order, FSt > ClSt > BrSt (**Figure 3-10**). The NB/XSt copolymers showed tensile strength at ranging from 61.3 to 64 MPa.

3-4. Conclusions

Copolymerization of NB and XSt (X = Br, Cl, F, Me, OMe) were conducted using anilinonapthoquinone-ligated nickel complexes **1** activated by MMAO in toluene with the NB/XSt feed ratio of 4/1. The activity and the M_n value of the produced polymer were found to decrease in the following order, BrSt > ClSt > FSt > (St) > MeSt > MeOSt, which is in a good relationship with the electron-withdrawing ability of X. The XSt content in the copolymer was decreased in the opposite order. The M_n value and the XSt content were also depended on the polymerization temperature and increased with lowering the temperature. The NB/MeOSt and NB/MeSt copolymers of 73 mol% XSt content were obtained with the M_n value of over 100000 and the M_w/M_n value of 1.3 at 0 ºC, whereas the NB/ClSt copolymer of 19 mol% XSt with the M_n value of 517000 and the M_w/M_n value of 1.3 was obtained in the same conditions. The effect of the substituent X on the T_g value of the NB/XSt copolymer was not significant and the T_g value was controlled by the content of XSt. The incorporation of halogenated St groups resulted in the improvement of the mechanical properties, and the copolymer films were transparent and flexible. These copolymers should be used for optical plastics and medical devises.

References

1. S. Liu, Z. Yao, K. Cao, B. Li, S. Zhu, *Macromol. Rapid Commun.* **2009**, *30*, 548–553.
2. S. M. Arranz, A. C. Albeniz, P. Espinet, *Macromolecules* **2010**, *43*, 7482–7487.
3. C. Ye, B. Vogt, *Soft Matter* **2015**, *11*, 8499—8507.
4. X. He, J. Liu, H. Zhu, Y. Zheng, D. Chen, *RSC Adv.* **2015**, *5*, 63215–63225.
5. S. M. Arranz, E. S. Perez, J. A. M. Torre, I. P. Ortega, A. C. Albeniz, *RSC Adv*. **2016**, *6*, 105878 –105887.
6. R. G. Loma, A. C. Albeniz, *RSC Adv*. **2015**, *5*, 70244–70254.
7. L. Sessions, B. Cohen, R. Grubbs, *Macromolecules* **2007**, *40*, 1926−1933.
8. M. Wiacek, S. Jurczyk, M. Kurcok, H. Janeczek, S. E. Balcerzak, *Polym. Eng. Sci.* **2014**, *54*, 1170−1181.
9. S. Rahmani, A. A. Entezami, *Catal. Lett.* **2011**, *141*, 1625–1634.
10. S. I. Chowdhury, R. Tanaka, Y. Nakayama, T. Shiono, *Polymers*, **2019**, *11*, 1100.
11. D. Liu, R. Wang, M. Wang, C. Wu, Z. Wang, C. Yao, B. Liu, X. Wan. D. Cui, *Chem. Commun.* **2015**, *51*, 4685-4688.
12. Dr. D. Liu, Dr. M. Wang, Z. Wang, Dr. C. Wu, Y. Pan, Prof. D. Cui, *Angew. Chem. Int. Ed.* **2017**, *56*, 2714–2719.

13. S. Rahmani, A. A. Entezami, *Catal. Lett.* **2011**, *141*, 1625–1634.

14. F. Guo, N. Jiao, L. Jiang, Y. Li, Z. Hou, *Macromolecules* **2017**, *50*, 8398−8405.

Chapter IV

Copolymerization of Norbornene with Divinylbenzene using Anilinonaphthoquinone-ligated Nickel Complexes

4-1. Introduction

The vinyl functionality into the polyolefin copolymers is attractive since the existence of –C=C– bonds in the copolymer can provide reaction sites for the synthesis of graft polymers, cross-coupling reaction, vulcanization and functionalized polyolefins.[1-3] Asymmetric dienenes in which one of the C=C bonds hardly be polymerized are generally used in order to prohibit cross-linking. However, Shiono and coworkers succeeded in the synthesis of highly soluble COC possessing pendant vinyl groups by copolymerization of norbornene (NB) and 1,5-hexadaiene using an *ansa*-fluorenylamidotitanium-based catalyst.[4] They considered that the steric circumstance of the pendant butenyl group should have prevented the cross-linking because the gel product was obtained when 1,7-octadiene was used in place of 1,5-hexadiene.

In Chapter II and Chapter III, anilinonaphthoquinone-ligated nickel complexes [Ni($C_{10}H_5O_2NAr$)(Ph)(PPh_3): **1a**, Ar = C_6H_3-2,6-^{i}Pr; **1b**, Ar = C_6H_2-2,4,6-Me; **1c,** Ar = C_6H_5] were proved to be effective for copolymerization of

NB with St or *p*-substituted St (*p*-substituted = -OMe, -Me, -F, -Cl and -Br) combined with modified methylaluminoxane (MMAO) as a cocatalyst.[5,6] The copolymerization activity depended on the substituent and decreased in the following order, Br > Cl > F > Me > OMe. The author therefore expected that divinylbenzene (DVB), i.e., vinyl substituted styrene, would copolymerize with NB by this catalyst and the styryl group in the copolymer should be less reactive than DVB.

In this chapter, the author conducted copolymerization of NB and DVB using **1** combined with modified methylaluminoxane (MMAO) and successfully obtained poly(NB-*co*-DVB) possessing the pendant styryl group. The styryl group was transformed to epoxy and di-hydroxyl group by epoxidation and the following hydrolysis. The styryl group of poly(NB-*co*-DVB) was also used for graft polymerization of methyl methacrylate (MMA) using reverse atom transfer radical polymerization (RATRP).

4-2. Materials and Methods

General Considerations

All manipulations were carried out under a nitrogen atmosphere using standard Schlenk techniques. All solvents were refluxed and distilled over sodium/benzophenone or CaH_2. NB was purified by stirring it over calcium hydride at 60 °C for one day and then distilled. The stock solution of NB (5.5

M) was prepared in toluene. DVB (from FUJIFILM Wako Pure Chemical Corporation, Japan) was dried over CaH_2, and then freshly distilled under vacuum prior to use. Modified methylaluminoxane (MMAO) solution (6.6 wt % in toluene) was donated from Tosoh Finechem. Co. (Tokyo, Japan) and used as received. $CuCl_2$, bipyridine, 2,2′-azobisisobutyronitrile (AIBN) and 3-chloroperoxybenzoic acid (*m*-CPBA) (from FUJIFILM Wako Pure Chemical Corporation, Japan) was used as received. The nickel complexes **1a-c** were synthesized as described in Chapter II.

Analytical Procedures

Molecular weights and molecular weight distributions of polymers were determined by gel permeation chromatography (GPC) with a Viscotec HT-350 GPC (Malvern, UK) with three CLM6210 mixed-bed columns. This system was equipped with a triple-detection array consisting of a differential refractive index detector, a two-angle (7, 90) light scattering detector and a four-bridge capillary viscosity detector. Polymer characterization was carried out at 150 °C using *o*-dichlorobenzene as an eluent and calibrated with polystyrene standards. The ^{1}H and ^{13}C NMR spectra of polymers were measured at room temperature on a Bruker 500MHz instrument (Bruker, Germany) operated by the pulse Fourier-transform mode. The measurement for ^{1}H NMR and ^{13}C NMR, sample solution was prepared in $CDCl_3$ up to 10 wt%. The pulse angle for ^{13}C NMR

was 45° and about 8000-10,000 scans were accumulated in pulse repetition of 5.0 s. The central peak of $CDCl_3$ (77.13 ppm for ^{13}C NMR) and peak of $CHCl_3$ (7.25 ppm for ^{1}H NMR) was used as an internal reference. Differential scanning calorimetry (DSC) was performed on a SII EXSTER 600 (Seiko Instruments Inc., Japan) system under nitrogen atmosphere. Thermal history difference in the polymers was eliminated by first heating the specimen to 380 °C, cooling at 10 °C/min to 20 °C, and then recording the second DSC scan at a heating rate of 10 °C/min.

Copolymerization of NB and DVB

In a typical procedure, prescribed amounts of NB and DVB in toluene solution were introduced into a 100-mL round-bottomed glass flask. Then, 0.24 mL of MMAO toluene solution (500 μmol) and one mL of the nickel complex (5 μmol) solution in toluene were syringed into the well-stirred monomer solution in this order, and the total solution volume was made to 25 mL by adding toluene. The copolymerization was conducted under continuous stirring for a required time under a certain temperature controlled with an external oil bath. Copolymerization was terminated by adding 300 mL of acidic methanol (methanol/concentrated hydrochloric acid, 95/5 in volume). The resulting precipitated polymer was collected by filtration, adequately washed with methanol, and dried in vacuum at 60 °C for 6 h.

Synthesis of Epoxy and Dihydroxyl Functional NB/DVB Copolymer

Vinyl group containing NB/DVB copolymers (0.25 g, obtained in Run 1) in chlorobenzene (2 mL) solution were introduced into a 10-mL Schlenk. For epoxidation, *m*-CPBA (0.17 g, 1 mmol) was added to the solution and stirred for 5 h. The product was precipitated in excess ethanol, filtered and dried in vacuum at 60 °C for 6 h. The resulting polymer was again dissolved in chlorobenzene (5 mL) and acidic water was added to the solution. The solution kept constant stirring for 6 h at 90 °C. The polymer was precipitated in methanol and dried in vacuum at 60 °C for 6 h.

Graft Polymerization of MMA from NB/DVB Copolymer

In a general procedure, NB/DVB copolymers (0.25 g, obtained in Run 1) in toluene (2 mL) solution were introduced into a 10-mL Schlenk tube. $CuCl_2$ (0.13 mg, 0.1 mmol) and bipyridine (0.31 mg, 0.2 mmol) were added to the tube. After the catalyst was dissolved, an initiator AIBN (0.13 mg, 0.1 mmol) and MMA (0.5 mL, 4.7 mmol) were added in this order. The graft polymerization was conducted under continuous stirring for 12 h at 70 °C controlled with an external oil bath. The polymerization was terminated by adding 100 mL of acidic methanol. The resulting precipitated polymer was collected by filtration, adequately washed with methanol. THF was added to the

polymer to dissolve homo PMMA present in the grafted polymer and filtered out. The grafted polymer was dried in vacuum at 60 °C for 6 h.

Preparation of Copolymer Films

Copolymer (approximately 300 mg) was dissolved into 3 mL of toluene at room temperature and filtered through a 0.20 μm PTFE membrane. The filtered solution was placed on a glass plate and stood for 3 days under ambient temperature and pressure. After almost all the solvent was vaporized, the film was placed at 60 °C under vacuum condition for 3 h.

4-3. Results and Discussion

4-3-1. NB/DVB Copolymerization

Copolymerization of NB and DVB was carried out using the nickel complexes [Ni($C_{10}H_5O_2NAr$)(Ph)(PPh_3): **1a**, Ar = C_6H_3-2,6-^{i}Pr; **1b**, Ar = C_6H_2-2,4,6-Me; **1c,** Ar = C_6H_5] activated by MMAO (**Scheme 4-1**). The results are summarized in **Table 4-1,** which indicate that the catalytic systems were active toward the NB/DVB copolymerization. First, the copolymerization was conducted with the different DVB feed ratio at 70 °C by complex **1a**. The activity increased with decreasing the DVB ratio from 20 to 5 mol% in feed (Run 1, 2 and 5).

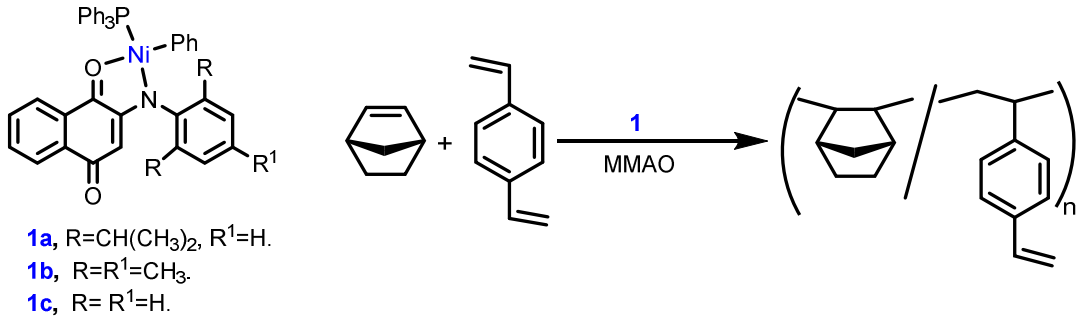

1a, R=CH(CH$_3$)$_2$, R^1=H.
1b, R=R^1=CH$_3$.
1c, R= R^1=H.

Scheme 4-1. NB/DVB copolymerization using Ni catalyst.

The activity of 220 $kg_{polymer}$ mol_{Ni}^{-1} h^{-1} was obtained for NB/DVB copolymerization using **1a** with the DVB ratio of 5 mol% at 70 °C. Then, the effects of copolymerization temperatures were investigated from 0 to 70 °C at 20 mol% of DVB by **1a**. The activity of NB/DVB copolymerization exhibited a rapid increase with increasing the polymerization temperature from 0 to 70 °C (Run 5 - 8). The influence of reaction time on NB/DVB copolymerization with the same feed ratio was also studied at 70 °C. The conversion of copolymer was gradually increased with increasing the polymerization time from 1 to 3 h (Run 2 - 4). The conversion of 35% was achieved for NB/DVB copolymerization using **1a** with the DVB ratio of 10 mol% for 3 h at 70 °C Complex **1a** gave the highest conversion for NB/DVB copolymerization among the complex used (Run 5, 9 and 11).

Table 4-1. Copolymerization of NB and DVB by **1**-MMAO[a]

Run	Cat.	Ratio (NB/DVB)	T (°C)	t (h)	Con. (%)	A[b]	M_n [c] (10^3)	M_w/M_n [c]	f_{DVB} [d] (mol %)
1	1a	95:05	70	1	23.3	220	60	1.8	5
2	1a	90:10	70	1	12.7	122	57	1.5	9
3	1a	90:10	70	2	24.0	115	62	1.5	9
4	1a	90:10	70	3	34.8	111	54	1.7	7
5	1a	80:20	70	1	7.0	70	46	1.5	15
6	1a	80:20	50	1	4.4	44	54	1.5	19
7	1a	80:20	30	1	3.0	30	62	1.6	23
8	1a	80:20	0	1	1.4	14	65	1.5	25
9	1b	80:20	70	1	5.9	58	49	1.8	20
10	1c	90:10	70	1	6.1	58	69	1.7	17
11	1c	80:20	70	1	3.0	30	40	1.7	23

[a] Polymerization conditions: Ni = 5 μmol; Al/Ni = 100; solvent = toluene (total volume 25 mL). [b] Activity = $kg_{(polymer)}mol_{(Ni)}^{-1}h^{-1}$. [c] Determined by GPC. [d] f_{DVB} are the content of DVB in NB/DVB copolymer determined by ^1H NMR.

The molecular weights of the copolymers were measured by GPC. The number-average molecular weight (M_n) was increased with decreasing the DVB ratio in feed (Run 1, 2, 5 and **Figure 4-1**) and decreasing the polymerization temperature (Run 5 - 8). The copolymers with the M_n values of 46000 – 62000 were obtained. The M_n value did not strongly depend on the complex used. The

molecular weight distribution was almost independent of feed ratio, polymerization temperature and time to be below 2.

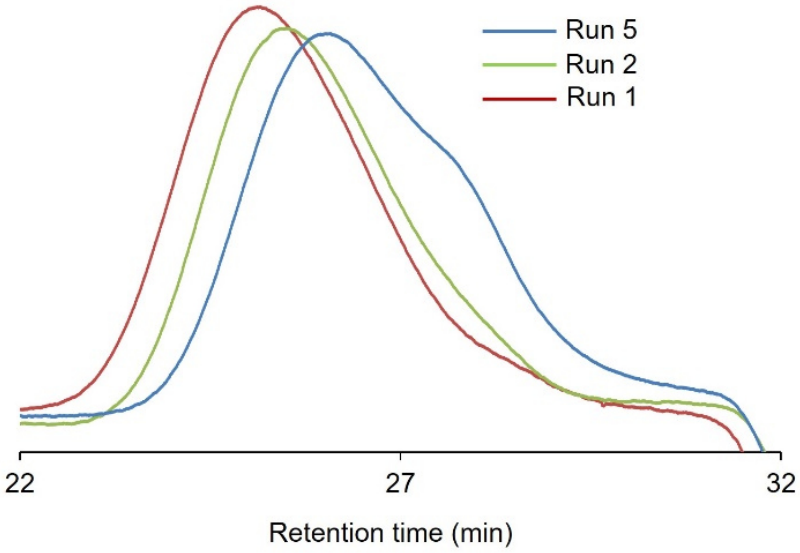

Figure 4-1. GPC traces of poly(NB-*co*-DVB).

A typical ^{1}H NMR spectrum of the NB/DVB copolymer is shown in **Figure 4-2a**. The signals assignable to the aliphatic protons of NB and DVB units are observed in the range of 0.8-2.4 ppm. The signals attributed to the aromatic protons of the DVB units are observed in the range of 6.5-7.1 ppm. The chemical shifts ($H^{1,2}$) of intact vinyl group (-CH=CH_2) of DVB are observed at 5.2 and 5.8 ppm. Particularly, the signal of the methine proton (H^{3}) of the DVB unit adjacent to the NB unit can be observed at 2.81 ppm.[14]

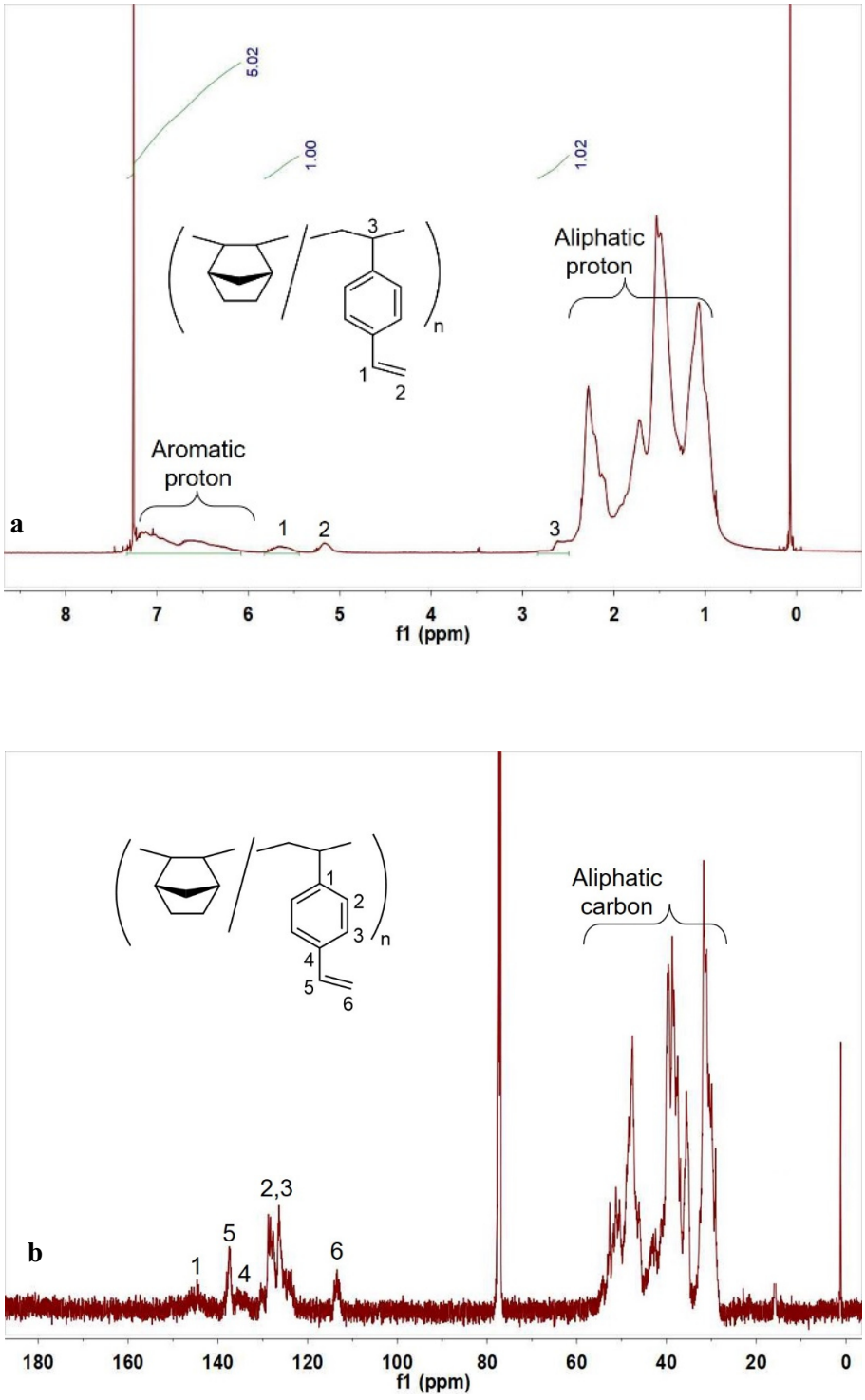

Figure 4-2. (**a**) ^{1}H NMR spectrum and (**b**) ^{13}C NMR spectrum of poly(NB-*co*-DVB) obtained by Run 5.

The integration values of methine protons (H^1 and H^3) are the same each other and also the same with those of aromatic proton of DVB (**Figure 4-2a**). This result confirms that one vinyl group was quantitatively intact in the polymer chain. The DVB contents in the copolymers determined by ^{1}H NMR are shown in **Table 4-1**. The incorporation of DVB increased with increasing DVB ratio in feed (Run 1, 2 and 5) and decreasing the polymerization temperatures (**Table 4-1**, Run 5-8). The highest incorporation of DVB was achieved to be 23% at 20 mol% of DVB in feed by complex **1c**. The same trend in the comonomer incorporation was observed in the previously reported NB/St copolymerization.[5]

In the corresponding ^{13}C NMR spectrum (**Figure 4-2b)**, the signals at 139.7, 122.1, 127.5 and 128.9 ppm ($C^{1\text{-}4}$) are attributed to the aromatic carbons, while the signals appearing in 129.8 ppm (C^5) and 117.8 ppm (C^6) are attributed to the vinyl carbons of the DVB unit in the copolymer. The signals in the range of 29.1-52.3 ppm are attributed to the carbons of NB unit. The results indicate that NB was polymerized into copolymer via vinyl addition and the DVB unit was distributed in the obtained NB/DVB copolymer.

The monomer reactivity ratios in the NB/DVB copolymerization catalyzed by **1a**-MMAO at 70 °C were determined by the Fineman-Ross method to be r_{NB} = 0.96 and r_{DVB} = 0.22 (**Figure 4-3**). The values indicate the good copolymerization ability of the catalyst.

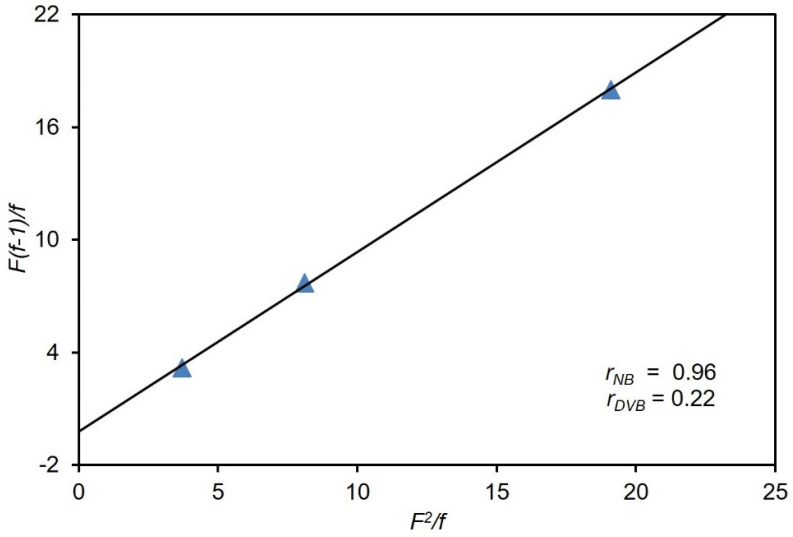

Figure 4-3. Fineman-Ross plot for copolymerization of NB/DVB by **1a**-MMAO.

4-3-2. Epoxidation and Di-hydroxylation of Poly(NB-*co*-DVB)

The vinyl group of poly(NB-*co*-DVB) can be modified very easily to epoxy and finally dihydroxy functional group. The epoxy functionalized poly(NB-*co*-DVB) was obtained by *m*-CBPA at room temperature and epoxy ring-opening reaction was conducted by hydrolysis at 90 °C (**Scheme 4-2**). The dihydroxy functionalized NB/DVB copolymer showed higher solubility (200 mg/mL in $CHCl_3$) than the NB/DVB copolymer (70 mg/mL in $CHCl_3$).

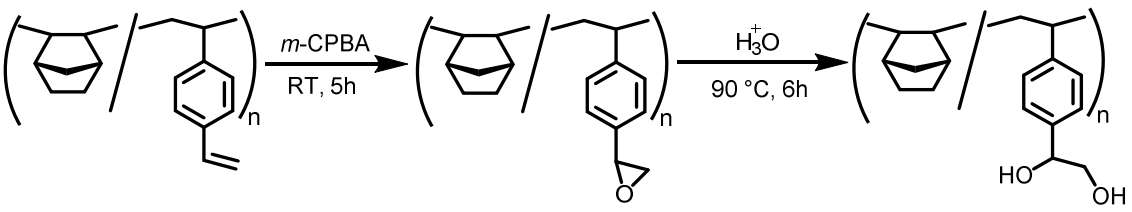

Scheme 4-2: Vinyl group modification of poly(NB-*co*-DVB).

The microstructures of the epoxy and di-hydroxy poly(NB-*co*-DVB) were determined by ^{1}H NMR analysis. **Figure 4-4a** shows the epoxy-functionalized poly(NB-*co*-DVB), where the vinyl protons at 5.2 and 5.8 ppm completely disappeared and the signals assignable to the aliphatic protons of NB and DVB units appear in the range of 0.8-2.4. The signals attributed to the aromatic protons of the DVB units are observed in the range of 6.5-7.1 ppm.

The new broad chemical shift of epoxy (-CH-CH_2-) of DVB is observed at 3.7 and 3.4 ppm.

After ring opening of epoxy group, the hydroxy peak appears at 5 ppm (**Figure 4-4b**). The NMR results cleared the transformation of vinyl group to epoxy and dihydroxy groups.

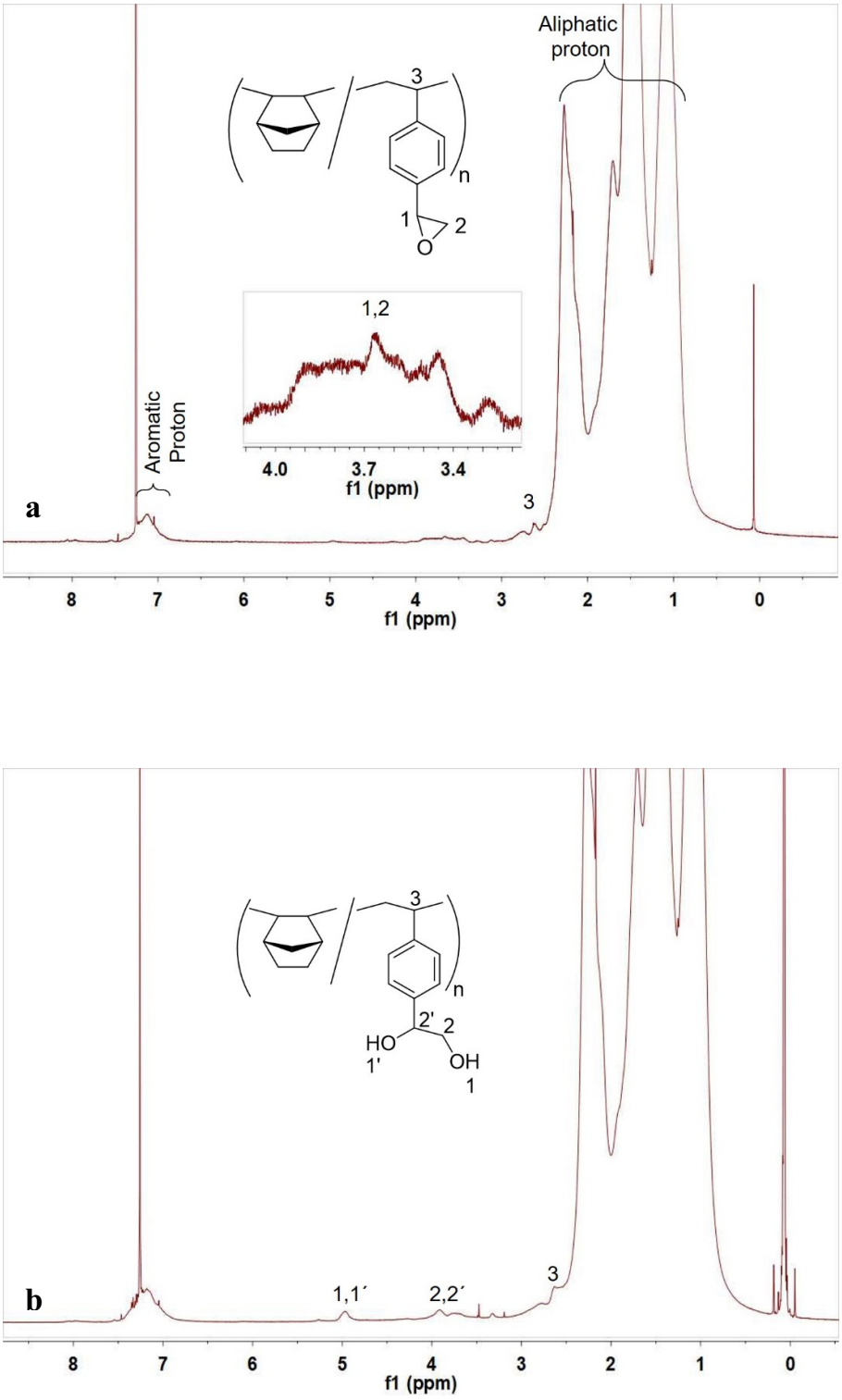

Figure 4-4 ^{1}H NMR spectra of **(a)** epoxy functional NB/DVB copolymer **(b)** dihydroxy functional NB/DVB copolymer obtained by Run 2.

4-3-3. Synthesis and Characterization of Poly(NB-*co*-DVB)-*graft*-PMMA

NB/St copolymers have several potential properties. However, its usefulness in various applications is limited by the absence of functionality. The incorporation of polar segment into non-polar chain in controlled fashion is to afford graft copolymers obtained by radical polymerization.[7,8] Reverse atom transfer radical polymerization (RATRP) is one of the easiest methods for graft polymerization. Grafting-PMMA from poly(NB-*co*-DVB) by RATRP affords polar/non-polar hybrid polymeric material. The route of graft polymerization is shown in **Scheme 4-3**.

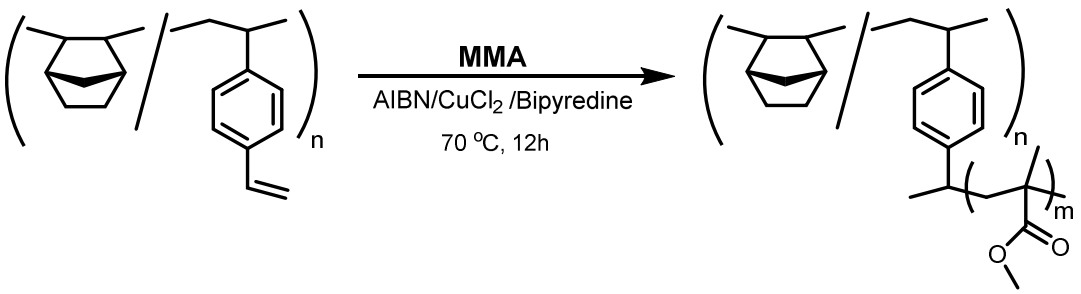

Scheme 4-3: Graft polymerization of MMA from poly(NB-*co*-DVB) using AIBN.

The graft polymerization was conducted by RATRP using AIBN in the presence of $CuCl_2$ and bipyridine. Poly(NB-*co*-DVB) with different DVB contents were used for graft polymerization of MMA. The results of the graft polymerization are shown in **Table 4-2**. The conversions of MMA in the polymerization were around 80-90%.

The M_n value was increased accompanied by narrowing the molecular weight distribution after the graft polymerization in all the samples. The results indicate that the graft copolymerization proceeds in a controlled manner (**Figure 4-5**).

Table 4-2. Graft polymerization of MMA and poly(NB-*co*-DVB) by RATRP[a]

Entry	Sample	M_n [b] (10^3)	M_w/M_n [b]	f_{DVB} [c] (mol %)	T_g [d]	Con. (%)	M_n [b] (10^3)	M_w/M_n [b]	T_g [d]
1	Run 1	60	1.8	5	318	79	71	1.5	186
2	Run 2	57	1.5	9	284	82	67	1.4	192
3	Run 9	49	1.8	20	-[e]	88	55	1.5	165

[a] Polymerization conditions: NB/DVB copolymer = 0.25 g, MMA = 0.5 ml (4.7 mmol), time = 12 h; temperature = 70 °C; solvent = toluene (3 mL). [b] Determined by GPC. [c] f_{DVB} are the content of DVB in NB/DVB copolymer determined by ^{1}H NMR. [d] Determined by DSC. [e] Not observed clearly.

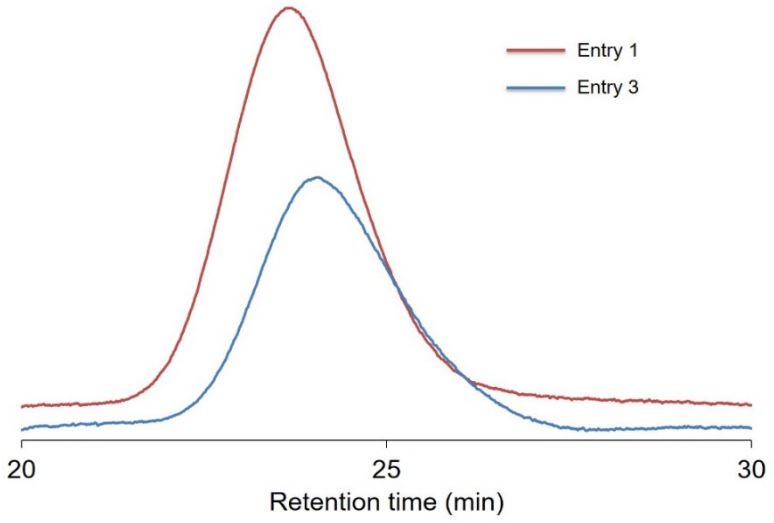

Figure 4-5. GPC traces of poly(NB-*co*-DVB)-*graft*-PMMA obtained by Entry 1 and 3.

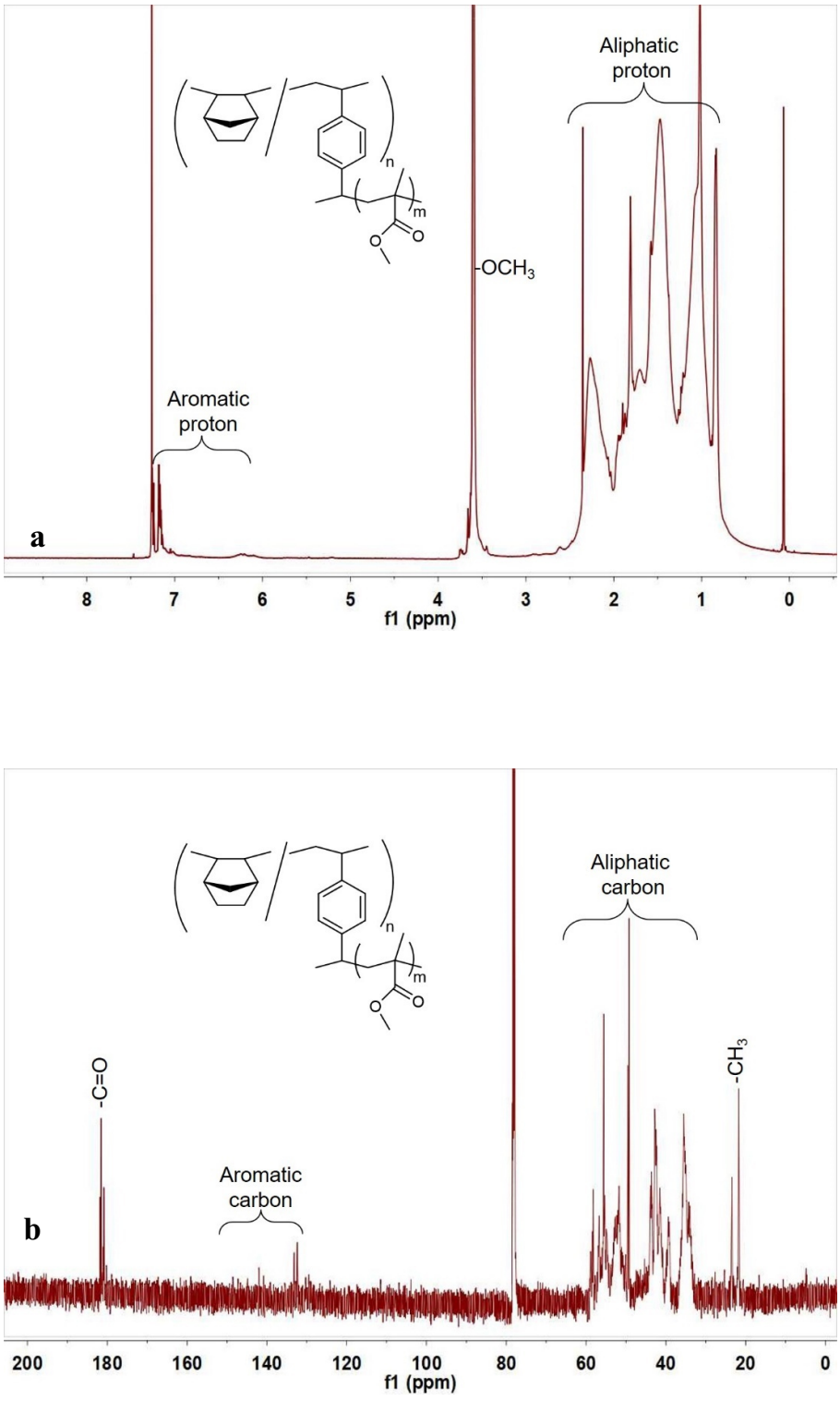

Figure 4-6 NMR spectra of NB/DVB-*g*-MMA copolymer obtained by Entry 1: **(a)** ^{1}H, **(b)** ^{13}C.

The microstructure of poly(NB-*co*-DVB)-*graft*-PMMA (Entry 1) was determined by ^{1}H and ^{13}C NMR analysis. The ^{1}H NMR spectrum is shown in **Figure 4-6a,** where the new chemical shift of -OCH_3 assignable to MMA unit is observed at 3.7 ppm in addition to those of poly(NB-*co*-DVB). The vinyl proton peak completely disappeared, which suggested that all the vinyl group of DVB should have undergone for the graft polymerization.

In the corresponding ^{13}C NMR spectrum shown in **Figure 4-6b**, the new signals appear in 181 ppm (-C=O) and 22.8 ppm (-CH_3) attributed to the carbonyl carbon and methyl carbon of the MMA segments in the copolymer. The results indicate that MMA was polymerized from poly(NB-*co*-DVB) in grafting form.

4-3-4. Thermal properties

The thermal properties of the poly(NB-*co*-DVB) and the poly(NB-*co*-DVB)-*graft*-PMMA were investigated by thermogravimetry-differential thermal analysis (TG-DTA) and differential scanning calorimetry (DSC). The degradation temperature, 5% weight loss, of the poly(NB-*co*-DVB) with 5 mol% of DVB was 365 °C while that of the poly(NB-*co*-DVB) with 19 mol% of DVB was 443 °C (**Figure 4-7**).

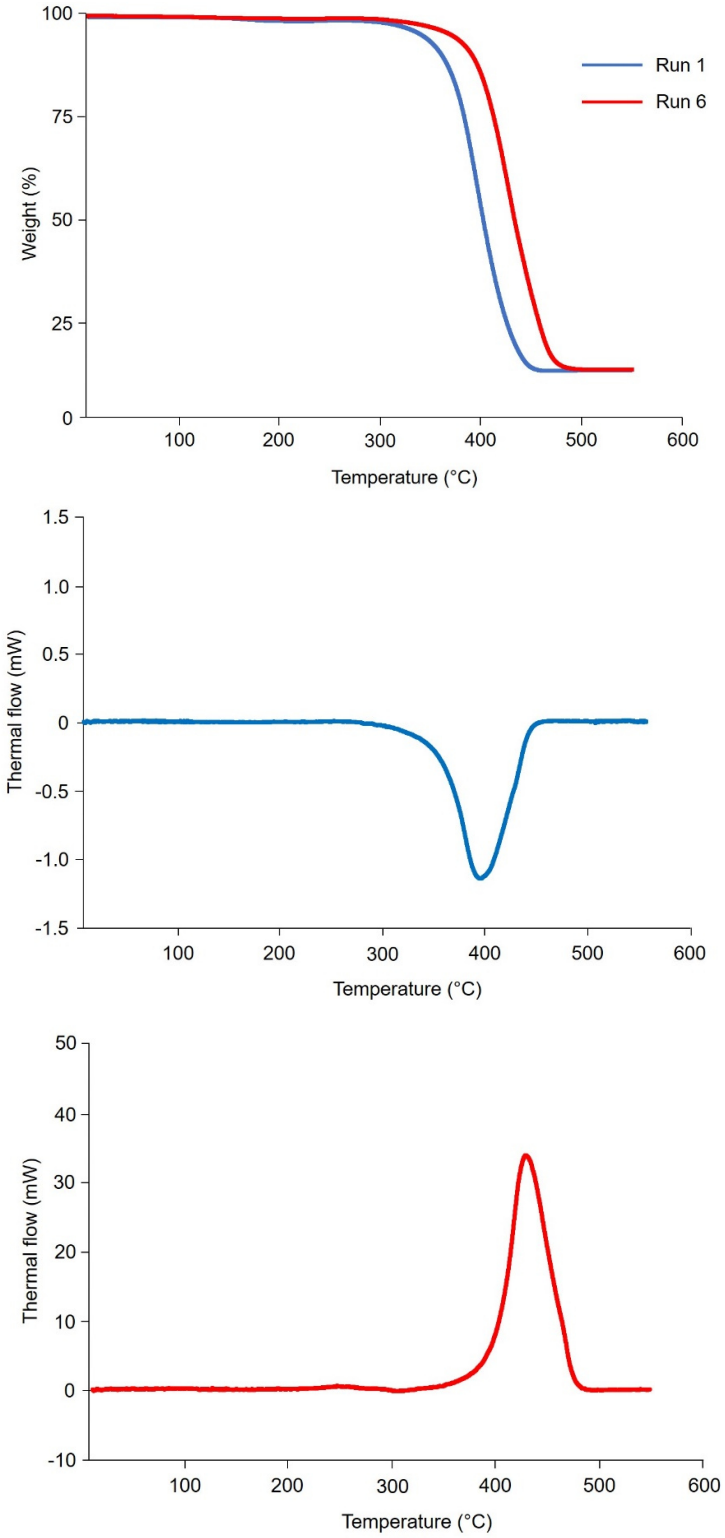

Figure 4-7 TGA and DTGA traces of poly(NB-*co*-DVB) obtained by Run 1 and 6.

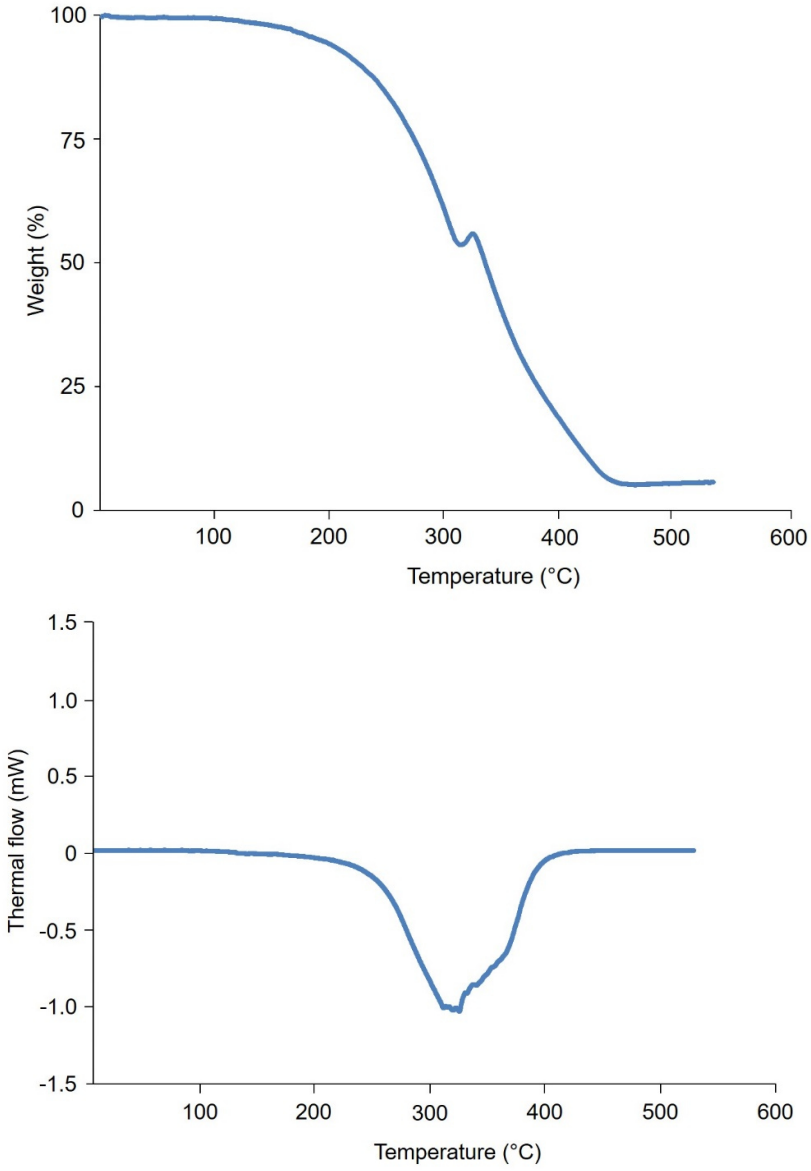

Figure 4-8 TGA and DTGA trace of poly(NB-*co*-DVB)-*graft*-PMMA obtained by Entry 1.

The corresponding TDA curves showed the endotherm and exotherm peaks, respectively, suggesting that the high thermal stability should be ascribed the thermally-induced cross-linking of the high-content styryl groups.

The poly(NB-*co*-DVB)-*graft*-PMMA showed two-stage weight loss (**Figure 4-8**). The first stage was observed from 329 °C to 340 °C which was corresponds to the thermal degradation of grafted PMMA. The T_g value was tuned according to the MMA unit present in the poly(NB-*co*-DVB)-*graft*-PMMA. For example, the T_g value reduced from 318 to 186 °C (**Table 2**, Entry 1) for the graft chain of PMMA (**Figure 4-9 and 4-10**).

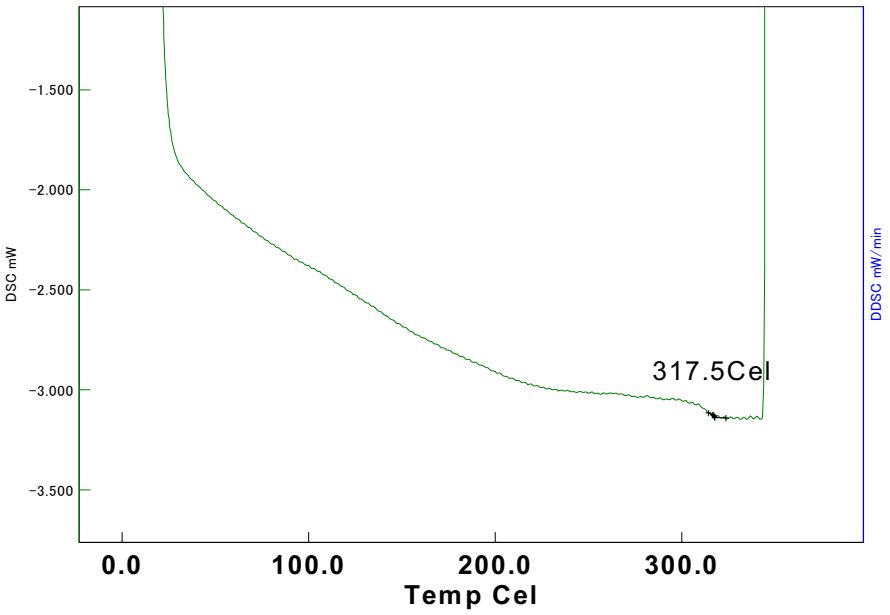

Figure 4-9 DSC trace of poly(NB-*co*-DVB) obtained by Run 1.

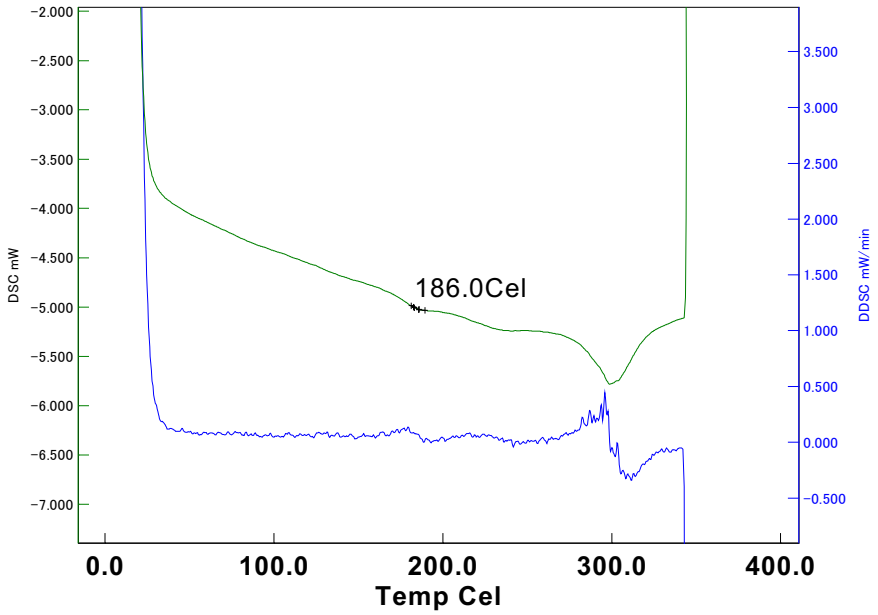

Figure 4-10 DSC trace of poly(NB-*co*-DVB)-*graft*-PMMA obtained by Entry 1.

4-3-5. Optical and Mechanical Properties

The light transmittance of the films prepared from poly(NB-*co*-DVB) (Run 10) and poly(NB-*co*-DVB)-*graft*-PMMA (Entry 3) with the thickness of approximately 120 μm are displayed in **Figure 4-11**. Poly(NB-*co*-DVB) showed an absorption of the styryl group around 300 nm,[14] which perfectly disappeared in the spectrum of the poly(NB-*co*-DVB)-*graft*-PMMA. These results also confirm that the poly(NB-*co*-DVB)-*graft*-PMMA was successfully obtained by the RATRP process. Both polymers showed the transmittance around 85% in the visible light region (400–800 nm).

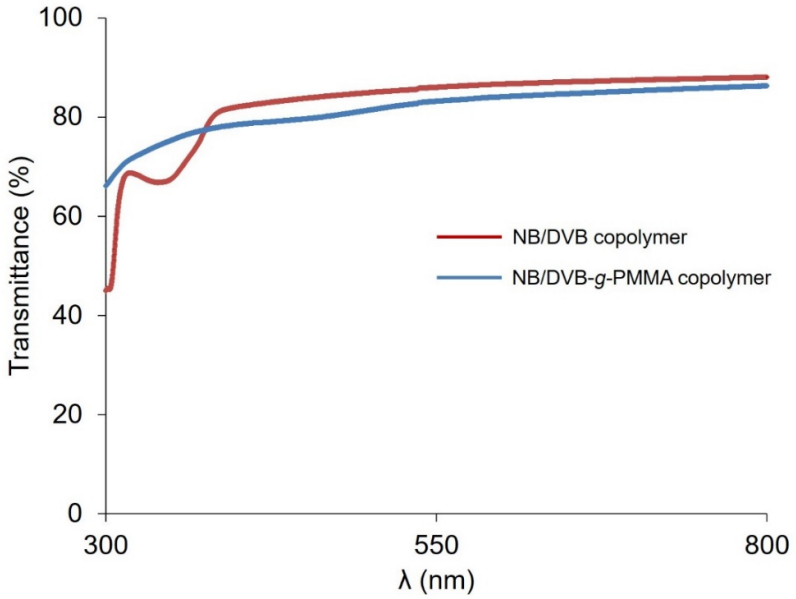

Figure 4-11. The light transmittance of poly(NB-*co*-DVB) obtained by Run 10 and poly(NB-*co*-DVB)-*graft*-PMMA obtained by Entry 3.

The mechanical properties were investigated by a universal testing machine (**Table 4-3**). Poly(NB-*co*-DVB)-*graft*-PMMA showed lower stress value and higher flexibility than poly(NB-*co*-DVB) (**Figure 4-12)**.

Table 4-3. Mechanical properties of the copolymers.

Sample	Copolymers	E (MPa)	σ (MPa)	ε (%)
Run 10	Poly(NB-*co*-DVB)	2533±43	63.1	4.5
Entry 3	Poly(NB-*co*-DVB)-*graft*-PMMA	1456 ±15	45.2	8.0

[a] Determined by tensile test, film thickness ≈ 0.12 mm. Stress at break (σ) and strain at break (ε), determined at fracture using uniaxial tensile test. Young's modulus (E), is the initial slop of the nominal stress and strain curve in the linier region.

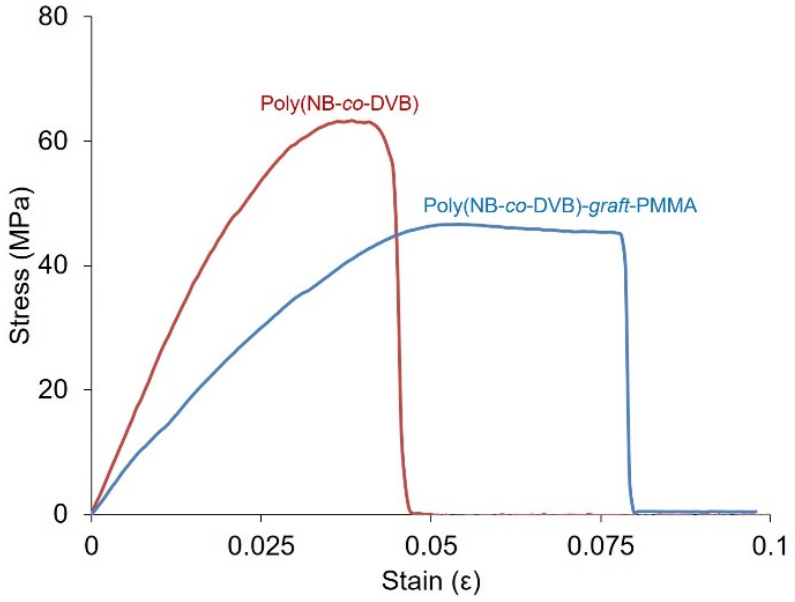

Figure 4-12. Stress-strain curves of poly(NB-*co*-DVB) and poly(NB-*co*-DVB)-*graft*-PMMA thin films: Run 10 and Entry 3.

4-4. Conclusions

Copolymerizations of NB and DVB were achieved by anilinonaphthoquinone-ligated nickel complexes using MMAO as cocatalyst. The catalysts showed good activity for long polymerization time. These copolymers afforded controllable DVB content and high molecular weight. The T_g value was controlled in a wide range differing the DVB contents. The vinyl group of poly(NB-*co*-DVB) was transformed to epoxy and di-hydroxy group as well as PMMA graft chain. The process ability of the polymers was improved by the introduction of polar groups.

References

1. H. J. Jo, C. S. Hong, *Polym. Chem*. **2017**, *8*, 3307–3316.
2. R. Abee, R. Sablong, H. Goossens, V. M. Duin, A. Spoelstra, R. Duchateau, *Macromol. Chem. Phys*. **2010**, *211*, 334–344.
3. S. Shin, K. Y. Yoon, T. L. Choi, *Macromolecules* **2015**, *48*, 1390−1397.
4. R. Tanaka, A. Sasaki, T. Takenaka, Y. Nakayama, T. Shiono, *Polymer* **2018**, *136*,109-113.
5. S. I. Chowdhury, R. Tanaka, Y. Nakayama, T. Shiono, *Polymers* **2019**, *11*, 1100.
6. S. I. Chowdhury, R. Tanaka, Y. Nakayama, T. Shiono, *Macromol. Chem. Phys.* **2020**, *221*, 1900494.
7. Y. Inoue, T. Matsugi, N. Kashiwa, K. Matyjaszewski, *Macromolecules* **2004**, *37,* 3651-3658.
8. C. S. Hong, T. Pakula, K. Matyjaszewski, *Macromol. Chem. Phys*. **2001**, *202*, 3392-3402.

Chapter V

Copolymerization of Norbornene with Conjugated Dienes Using Anilinonaphthoquinone-ligated Nickel Complexes

5-1. Introduction

The introduction of vinyl functionality into polyolefin backbone is attractive for further functionalizing the polymer. In Chapter IV, the author succeeded in the vinyl functionalization of polynorbornene (PNB) by copolymerization of norbornene (NB) and divinyl benzene (DVB) by anilinonaphthoquinone-ligand nickel complex **1** activated by modified methylaluminoxane (MMAO) and the copolymer was applied for the introduction of polar functional groups and the poly(methyl methacrylate) graft copolymer. If a simple conjugated diene (CDN) such as butadiene (BD) and isoprene (IP), of which *cis*-polymers are known to be good elastomers, can be copolymerized with NB, the copolymers should show the wide range of the glass transition temperatures (T_g) with improved brittleness.

Several papers reported copolymerization of NB with CDN. Copolymer of NB with BD or IP was obtained with good activity by a series of nickel catalysts combined with MMAO as cocatalyst. However, the number-average molecular weight ($M_n < 10^4$) was low.[1] Recently, a NB/BD copolymer with a

high BD content was obtained by (bpy)$NiBr_2$/MAO catalytic system, which also suffered from low M_n of the products.[2]

The random copolymerization of NB with IP was conducted by a cationic η^3-allyl-scandium complex/$[Ph_3C][B(C_6F_5)_4]$/Al^iBu_3 ternary system, where the M_n value was increased up to 15,000.[3] The copolymerization of NB and IP was conducted using a cationic tropidinyl dialkylscandium complex activated by $[PhNMe_2H][B(C_6F_5)_4]$ to give the copolymer with almost the same molecular weight in a similar activity.[4] A traditional Ziegler–Natta catalyst composed of $TiCl_4$ and Al^iBu_3 was applied for the copolymerization of NB with IP, and the M_n was increased up to 60,000.[5] The M_n of NB/BD copolymer was increased up to 10^5 by bis(phenoxyimine)titanium complex with Al^iBu_3 binary system in the activity of 2 $kg_{polymer}$ mol_{Ti}^{-1} h^{-1}.[6] NB/IP alternate copolymer with high transparency and relatively high M_n was also obtained by the same catalytic system in almost the same activity.[7] The previous study showed that the nickel and scandium catalysts suffered from low M_n of the copolymers and the titanium catalysts did from low activity.

The copolymerization of NB with CDN still attracts interest in academic research as well as commercial applications for the fantastic potential properties.[8] NB units in the copolymer chain improve its thermo stability and tensile strength, while CDN units would offer good elasticity, favorable solubility and T_g of the copolymer for better process ability. The existence of –

C=C– bonds in the copolymer can provide reaction sites for the synthesis of graft polymers, cross-linked polymer and functionalized polyolefins.

In the previous chapters, the author showed that anilinonaphthoquinone-ligated nickel complexes [Ni($C_{10}H_5O_2NAr$)(Ph)(PPh_3): **1a**, Ar = C_6H_3-2,6-^{i}Pr; **1b**, Ar = C_6H_2-2,4,6-Me; **1c,** Ar = C_6H_5] were effective for copolymerization of NB with styrene, a typical conjugated hydrocarbon monomer and its derivatives activated by MMAO or $B(C_6F_5)_3$ as a cocatalyst.

In this chapter, therefore, the author applied the catalytic system for the copolymerization of NB with BD or IP and investigated the properties of the obtained copolymers.

5-2. Materials and Methods

General Considerations

All manipulations were carried out under a nitrogen atmosphere using standard Schlenk techniques. All solvents were refluxed and distilled over sodium/benzophenone or calcium hydride. NB was purified by stirring it over calcium hydride at 60 °C for one day and then distilled. The stock solution of NB (5.5 M) was prepared in toluene. BD (from FUJIFILM Wako Pure Chemical Corporation, Japan) was dissolved in toluene to afford a saturated solution at room temperature (3.2 mmol/mL). IP (from FUJIFILM Wako Pure Chemical Corporation, Japan) was stirred over CaH_2 for 24 h and distilled under

nitrogen before use. MMAO solution (6.6 wt % in toluene) was donated from Tosoh Finechem. Co. (Tokyo, Japan) and used as received. The nickel complexes **1a-c** were synthesized as described in Chapter II.

Analytical Procedures

Molecular weights and molecular weight distributions of polymers were determined by gel permeation chromatography (GPC) with a Viscotec HT-350 GPC (Malvern, UK) with three CLM6210 mixed-bed columns. This system was equipped with a triple-detection array consisting of a differential refractive index detector, a two-angle (7, 90) light scattering detector and a four-bridge capillary viscosity detector. Polymer characterization was carried out at 150 °C using *o*-dichlorobenzene as an eluent and calibrated with polystyrene standards. The ^{1}H and ^{13}C NMR spectra of polymers were measured at room temperature on a Bruker 500MHz instrument (Bruker, Germany) operated by the pulse Fourier-transform mode. The measurement for ^{1}H NMR and ^{13}C NMR, sample solution was prepared in $CDCl_3$ up to 10 wt%. The pulse angle for ^{13}C NMR was 45° and about 8000-10,000 scans were accumulated in pulse repetition of 5.0 s. The central peak of $CDCl_3$ (77.13 ppm for ^{13}C NMR) and peak of $CHCl_3$ (7.25 ppm for ^{1}H NMR) was used as an internal reference. Differential scanning calorimetry (DSC) was performed on a SII EXSTER 600 (Seiko Instruments Inc., Japan) system under nitrogen atmosphere. Thermal history difference in

the polymers was eliminated by first heating the specimen to 380 °C, cooling at 10 °C/min to 20 °C, and then recording the second DSC scan at a heating rate of 10 °C/min.

Copolymerization of NB and CDN

In a typical procedure, prescribe amounts of NB and BD or IP in toluene solution were introduced into a 100-mL round-bottomed glass flask and then 0.24 mL of MMAO toluene solution (500 μmol) and one mL of the nickel complex (5 μmol) solution in toluene were syringed into the well-stirred monomer solution in this order, and the total solution volume was made to 25 mL by adding toluene. The copolymerization was conducted under continuous stirring for a required time under a certain temperature controlled with an external oil or ice bath. The copolymerization was terminated by adding 300 mL of acidic methanol (methanol/concentrated hydrochloric acid, 95/5 in volume). The resulting precipitated polymer was collected by filtration, adequately washed with methanol, and dried in vacuum at 60 °C for 6 h.

Preparation of Copolymer Films

NB/CDN copolymer (approximately 300 mg) was dissolved into 3 mL of toluene at room temperature and filtered through 0.20 μm PTFE membrane. The filtered solution was placed on a glass plate and stood for 3 days under ambient

temperature and pressure. After almost all the solvent was vaporized, the film placed further 3 h under vacuum condition at 60 °C.

5-3. Results and Discussion

5-3-1. NB/CDN Copolymerization

Copolymerizations of NB and CDN (BD or IP) were carried out using the nickel complexes [Ni($C_{10}H_5O_2NAr$)(Ph)(PPh_3): **1a**, Ar = C_6H_3-2,6-^{i}Pr; **1b**, Ar = C_6H_2-2,4,6-Me; **1c,** Ar = C_6H_5] activated by MMAO (**Scheme 5-1**). The results are summarized in **Table 5-2**, which indicate that the catalytic systems were active toward the copolymerization of NB with BD or IP.

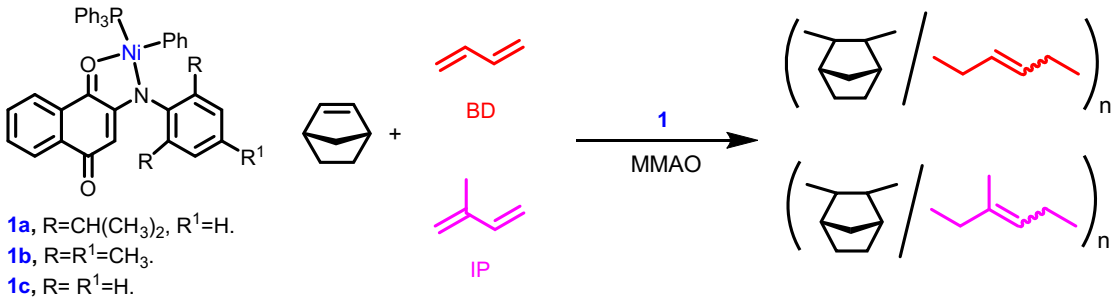

1a, R=CH(CH_3)$_2$, R^1=H.
1b, R=R^1=CH_3.
1c, R= R^1=H.

Scheme 4-1 Copolymerization of NB with BD or IP using Ni-complexes.

The effect of the Al/1**a** ratio was investigated for NB/BD (9/1) copolymerization keeping the amount of **1a** constant (**Table 5-1**). The catalytic system showed good activity even at low Al/Ni ratio of 50 (134 $kg_{polymer}$ mol_{Ni}^{-1}

h^{-1}). The activity improved gradually with increasing the Al/Ni ratio, while the number-average molecular weight (M_n) was decreased accompanied by broadening PDI (M_w/M_n) value. In the following experiments, the Al/Ni ratio was fixed to 100.

Table 5-1. Copolymerization of NB/BD by complex **1a**[a]

Run	Al/Ni (mol/mol)	Yield (g)	Act.[b]	f_{BD}[c] (mol %)	M_n[d] (10^3)	M_w/M_n[d]
1	50	0.67	134	11	63	1.4
2	100	1.15	230	11	60	1.5
3	200	1.31	262	10	36	1.9

[a] Polymerization conditions: Ni = 5 μmol; norbornene = 45 mmol; BD = 5 mmol; time = 1 h; temperature = 70 °C; solvent = toluene (total volume 25 mL). [b] Activity = $kg_{(polymer)}mol_{(Ni)}^{-1}h^{-1}$. [c] f_{BD} are the content of diene in the NB/BD copolymer determining by ^{1}H NMR spectrum. [d] Determined by GPC.

The copolymerization was conducted with the different CDN feed ratio at 70 °C by the complex **1a**. The yield increased by changing the NB:CDN ratio from 6:4 to 9:1 (**Table 5-2,** Run 1-3 and 12-14). Then, the effect of copolymerization temperatures was investigated from 0 to 70 °C at the feed ratio 8/2 by complex **1a**. The yield of NB/CDN copolymerization exhibited a rapid increase with increasing the polymerization temperature from 30 to 70 °C and the conversion of NB/BD copolymerization was higher than that of NB/IP copolymerization (Run 2, 4, 5, 13, 15, 16 and **Figure 5-2**).

Table 5-2. Copolymerization of NB and CDN by **1**-MMAO[a]

Run	Cat.	M	Ratio (NB/CDN)	T (°C)	Y (%)	A[b]	M_n [c] (10^3)	M_w/M_n[c]	f_{CDN} [d] (mol %)	T_g[e]
1	1a	BD	9:1	70	27.0	230	60	1.5	11	199
2	1a	"	8:2	70	17.5	150	33	1.3	16	178
3	1a	"	6:4	70	6.3	54	15	1.5	33	101
4	1a	"	8:2	50	14.0	118	27	1.4	17	175
5	1a	"	8:2	30	5.4	46	26	1.6	17	175
6	1a	"	8:2	0	-	-	-	-	-	-
7	1b	"	8:2	70	6.8	58	30	1.5	17	176
8	1c	"	8:2	70	6.3	54	41	1.3	15	183
9	1c	"	8:2	50	5.8	50	36	1.5	15	181
10	1c	"	8:2	30	3.3	28	25	1.3	17	174
11[f]	1a	"	8:2	70	11.2	102	56	1.3	4	-
12	1a	IP	9:1	70	18.7	166	79	2.1	15	205
13	1a	"	8:2	70	13.0	114	56	1.3	23	184
14	1a	"	6:4	70	4.5	40	34	1.5	41	97
15	1a	"	8:2	50	7.5	66	54	1.4	26	177
16	1a	"	8:2	30	4.3	38	43	1.7	29	170
17	1b	"	8:2	70	5.6	50	61	1.7	27	175
18	1c	"	8:2	70	5.6	50	83	1.5	27	176
19	1c	"	8:2	50	4.7	42	73	1.4	29	172
20	1c	"	8:2	30	3.8	34	61	1.5	30	168
21[f]	1a	"	8:2	70	7.5	60	98	1.2	7	-

[a] Polymerization conditions: Ni = 5 μmol; Al/Ni = 100; time = 1 h; solvent = toluene (total volume 25 mL). [b] Activity = $kg_{(polymer)}\ mol_{(Ni)}^{-1}\ h^{-1}$. [c] Determined by GPC. [d] f_{CDN} are the content of CDN in the NB/BD or NB/IP copolymer determining by ^1H NMR spectrum. [e] Determined by DSC. [f] $B(C_6F_5)_3$ was used in place of MMAO (B/Ni = 4).

The activity was depended on the complex and decreased in the following order: **1a** > **1b** ≥ **1c**. The order is in good agreement with that of the bulkiness

and the electron-donating ability of the ligand. The low activity of NB/CDN copolymerization should be ascribed to the strong coordination of electron-rich CDN, which causes the resting state and/or retarding next monomer insertion. Thus, the electron-donating ligand could have given higher activity.

Table 5-3. Homopolymerization of BD and IP by **1a**/MMAO[a]

Run	Mono.	Yield (g)	Conv. (%)	Act.[b]	M_n[c] (10^3)	M_w[c] (10^3)	M_w/M_n[c]
20	BD	0.59	28	120	7.3	15.7	2.1
21	IP	0.30	11	60	10.7	23.2	2.1

[a] Polymerization conditions: Ni = 5 μmol; BD = IP = 40 mmol; Al/Ni = 100; time = 1 h; Temperature = 70 °C; solvent = toluene (total volume 25 mL). [b] Activity = $kg_{(polymer)}\, mol_{(Ni)}^{-1}\, h^{-1}$. [c] Determined by GPC.

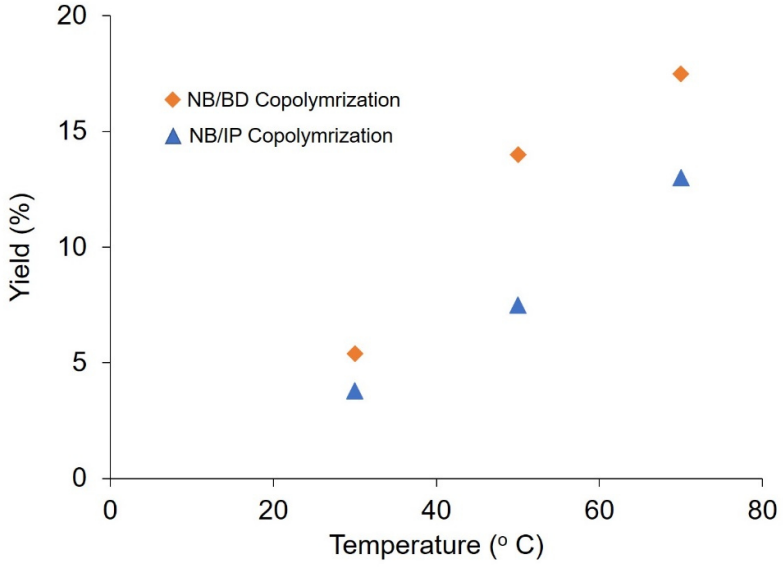

Figure 5-1. Conversion vs temperature of NB/CDN copolymerization by Ni-MMAO catalytic system.

The activity of 230 $kg_{polymer}$ mol_{Ni}^{-1} h^{-1} was obtained for NB/BD copolymerization using **1a** with the NB:BD ratio of 9:1 at 70 °C. NB/BD copolymerization showed higher activity than NB/IP copolymerization which could be ascribed to the steric and/or electron-donating Me- substituent.

The molecular weights of the copolymers were measured by GPC. The number-average molecular weight (M_n) was increased with decreasing CDN ratio in feed (Run 1-3 and 11-13, **Figure 5-2)**. The M_n value was also increased with raising the temperature keeping the narrow molecular weight distribution (Run 2, 4, 5, 13, 15 and 16). The NB/IP copolymers showed higher M_n value than the NB/BD copolymers under the same conditions.

When $B(C_6F_5)_3$ was used as a cocatalyst in place of MMAO, the BD content was decreased to 1/4 and the IP content was decreased to approximately 1/3 accompanied by the increase of the M_n value (Run 11 and 21).

The IP homopolymer also possessed higher M_n value than the BD homopolymer (**Table 4-3**). The higher M_n value was obtained by complex **1c** than complex **1a** possibly because of the steric effect of bulky ligand of complex **1a**. The highest M_n value was 83,000 for NB/IP copolymer obtained by complex **1c**.

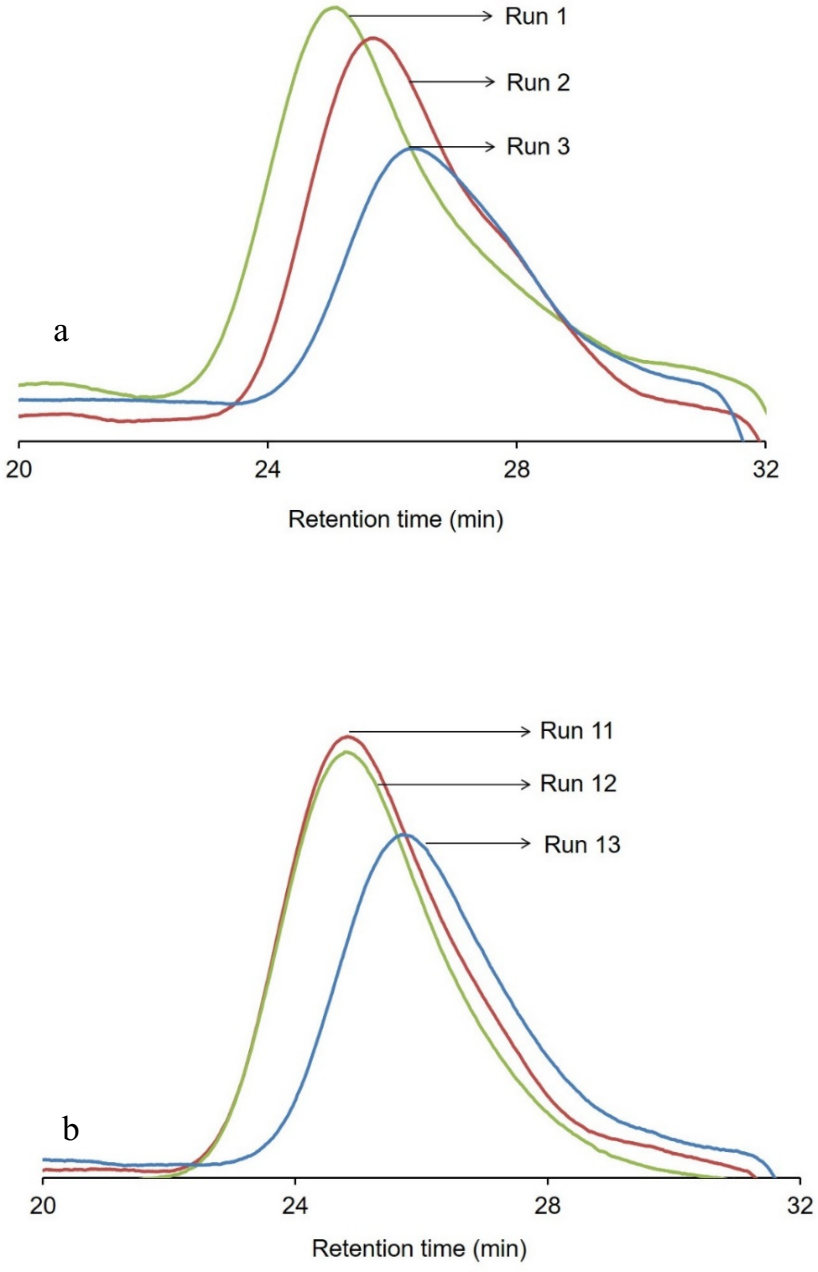

Figure 5-2. GPC traces of (a) NB/BD and (b) NB/IP copolymers.

A typical ^{1}H NMR spectrum of the NB/BD copolymer is illustrated in **Figure 5-3a**. The signals assignable to the aliphatic protons of the NB and BD units are observed in the range of 0.8-2.4 ppm. The signal at 5.4 ppm is attributed to olefin protons of 1,4-units in BD. The BD contents in the copolymers determined by ^{1}H NMR are shown in **Table 5-2**. The incorporation of BD increased with increasing BD ratio in feed (Run 1-3) to reach 33 mol% at the NB:BD ratio of 6:4. The BD incorporation did not significantly change by the temperatures from 30 to 70 °C (Run 2, 4, 5).

In the corresponding ^{13}C NMR spectrum (**Figure 5-3b)**, the signals at 130.3 and 129.9 ppm (C^{9}) are attributed to the unsaturated carbons, while the signals appearing in the range 44–54 ppm (C^{1-4}) and 27.5–40 ppm (C^{5-8}) to the saturated carbons of the NB and BD segments in the copolymer. The results indicate that NB was polymerized into copolymer via 2,3-addition, and the BD unit was inserted via 1,4-addition (**Figure 5-3a** and **5-3b**). According to the reported assignment of BD copolymer,[9] the isomer (*cis*- or *trans*-) can be calculated from the ^{13}C NMR spectra of butadiene double bond (-C=C-). Increasing the NB:BD ratio into the monomer feed from 9:1 to 6:4 causes increase of *cis*-1,4-unit from 56 to 65 % (**Figure 5-3c, 5-3d and 5-3e**).

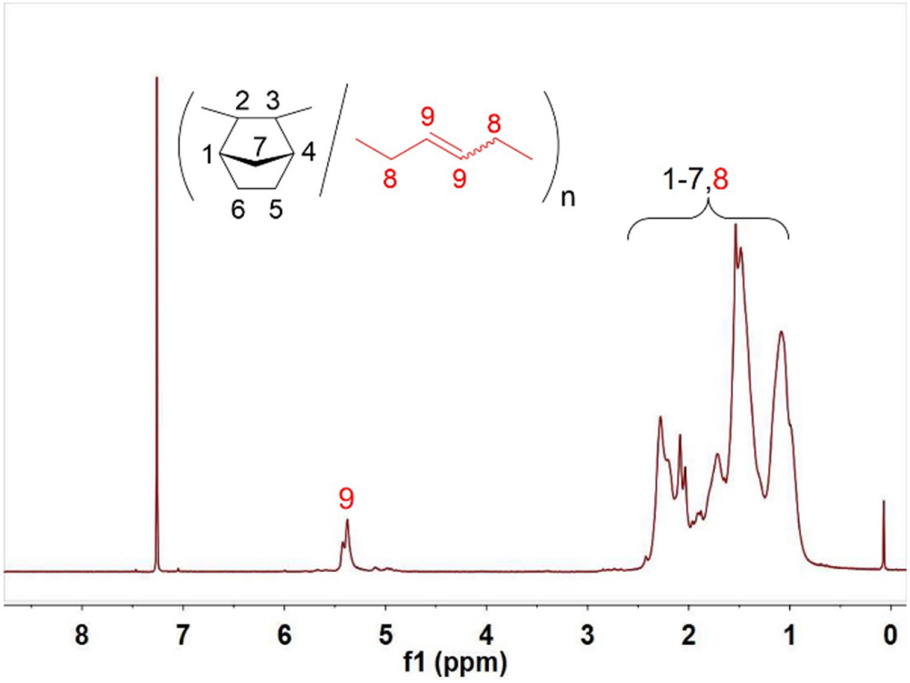

Figure 5-3a ^{1}H NMR spectrum of NB/BD copolymer obtained by Run 2.

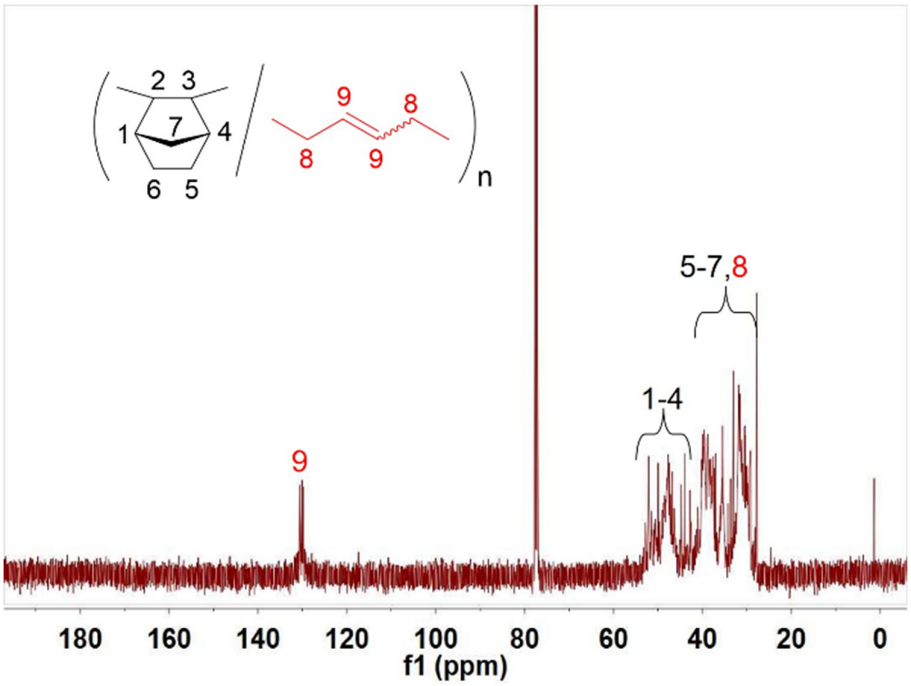

Figure 5-3b ^{13}C NMR spectrum of NB/BD copolymer obtained by Run 2.

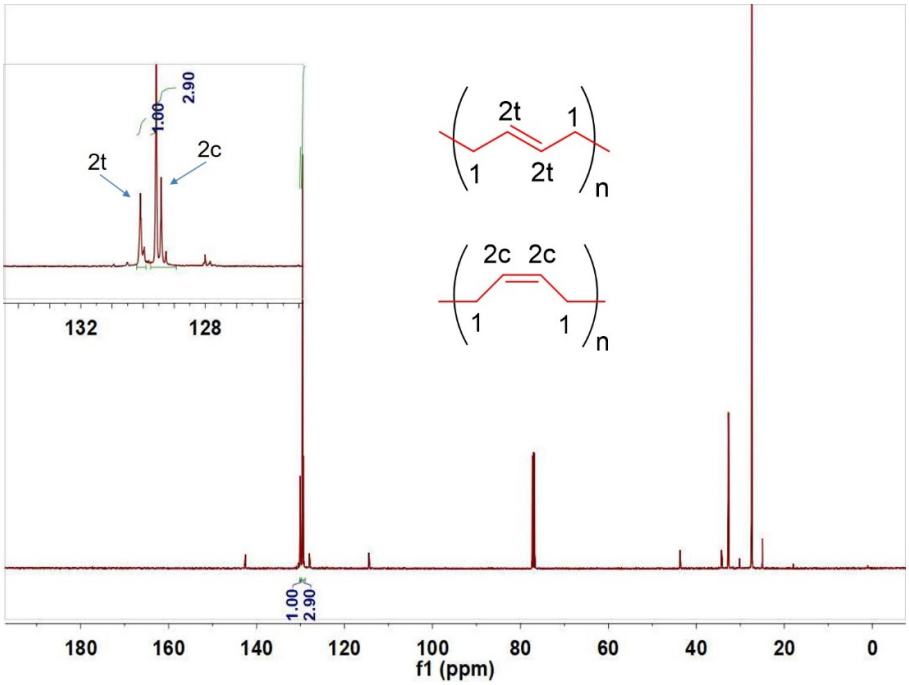

Figure 5-3c ^{13}C NMR spectrum of BD homopolymer obtained by **1a**-MMAO system.

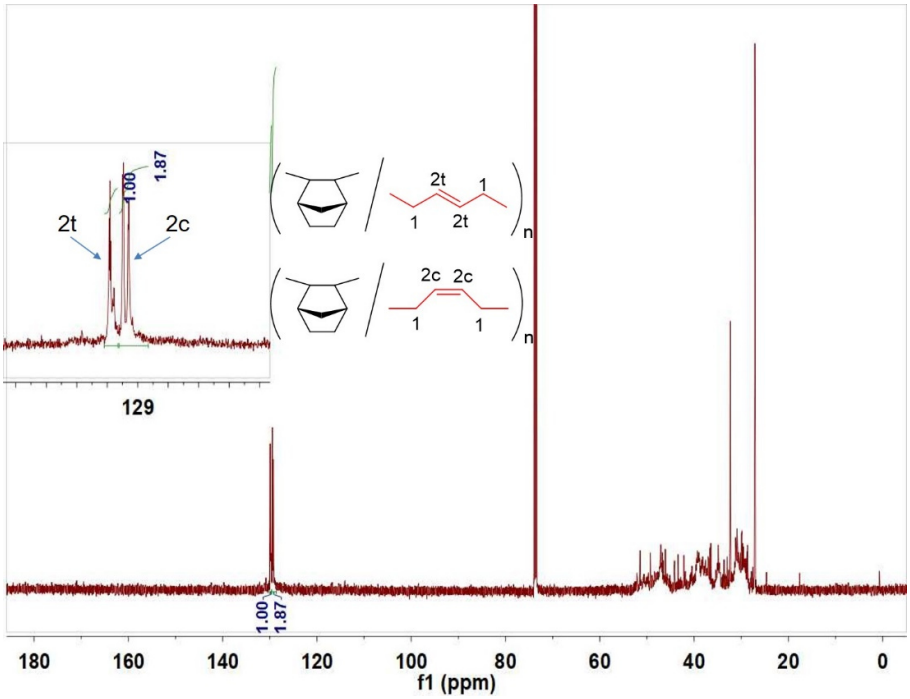

Figure 5-3d ^{13}C NMR spectrum of NB/BD copolymer obtained by Run 3.

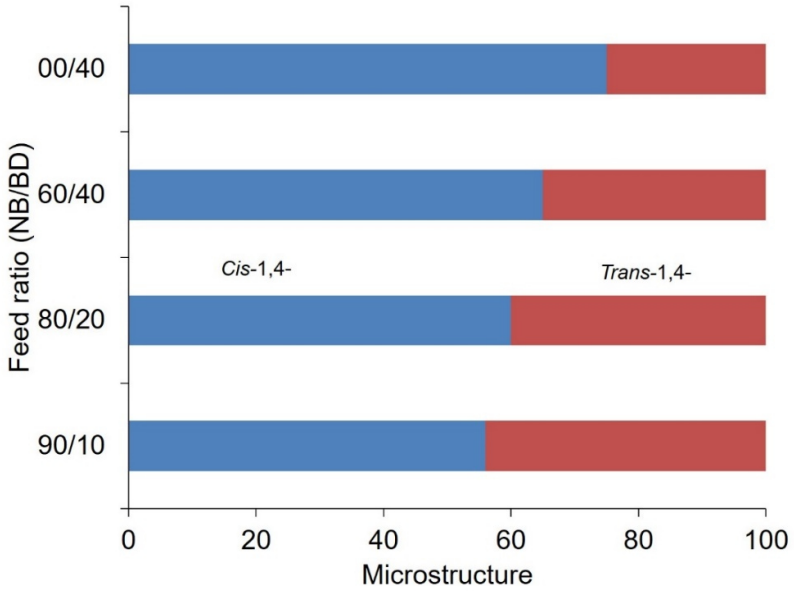

Figure 5-3e Feed ratio vs microstructure of NB/BD copolymer.

It is consistent with the result that *cis*-1,4-BD unit (75%) is dominant in the homopolymer obtained by complex **1a**

A typical ^{1}H NMR spectrum of the NB/IP copolymer is shown in **Figure 5-4a**. The signal at 5.1 ppm shows to the presence of olefin proton of 1,4-units in IP. The IP content in the produced copolymer was also determined by ^{1}H NMR. The incorporation of IP increased with increasing IP ratio in feed (Run 11-13) to reach 41 mol% at the NB:IP ratio of 6:4.

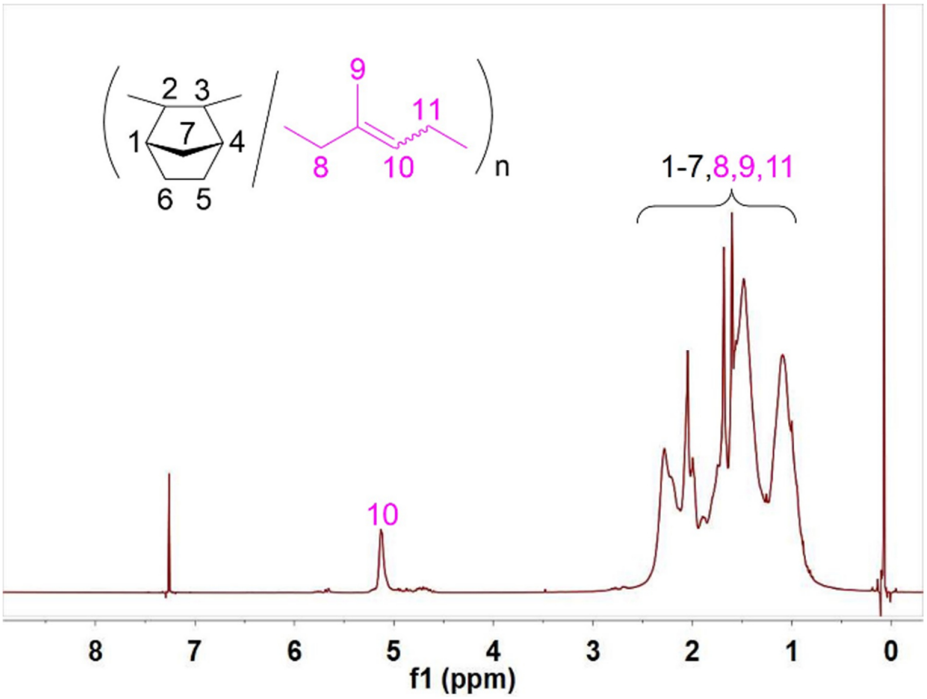

Figure 5-4a ^{1}H NMR spectrum of NB/IP copolymer obtained by Run 12.

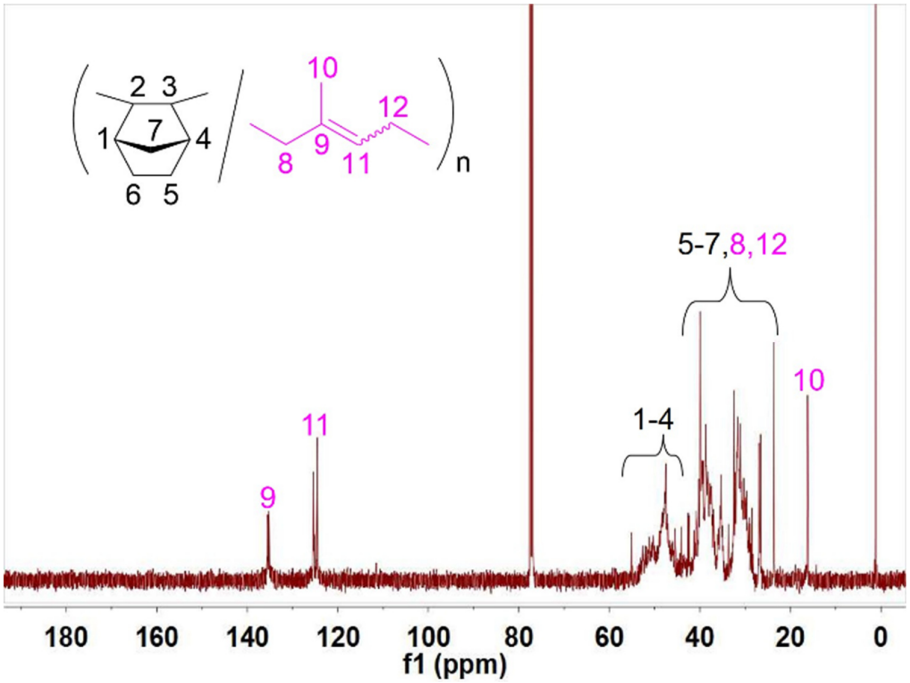

Figure 5-4b ^{13}C NMR spectrum of NB/IP copolymer obtained by Run 12.

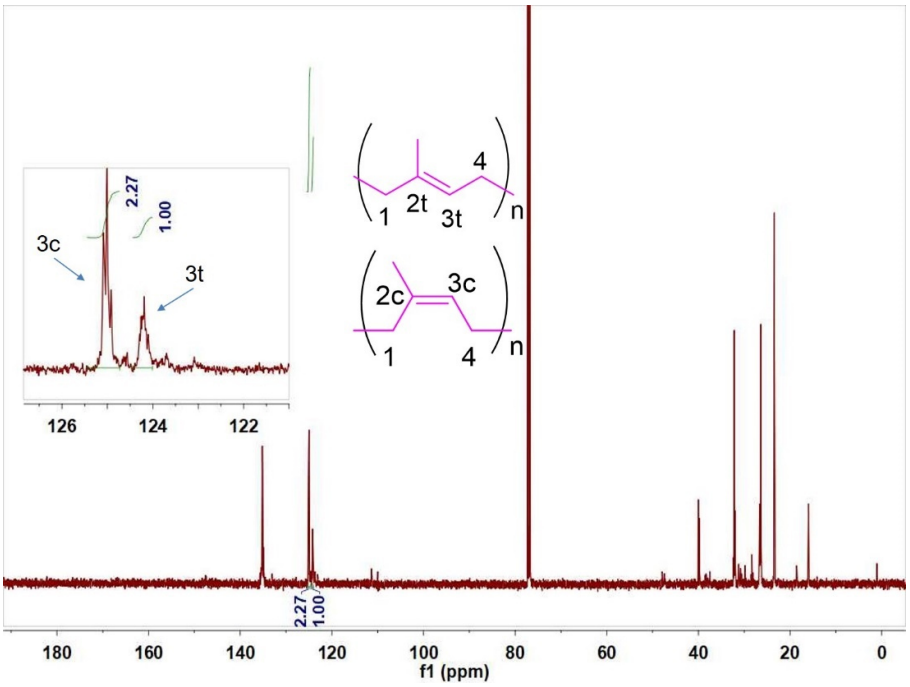

Figure 5-4c ^{13}C NMR spectrum of IP homopolymer obtained by **1a**-MMAO system.

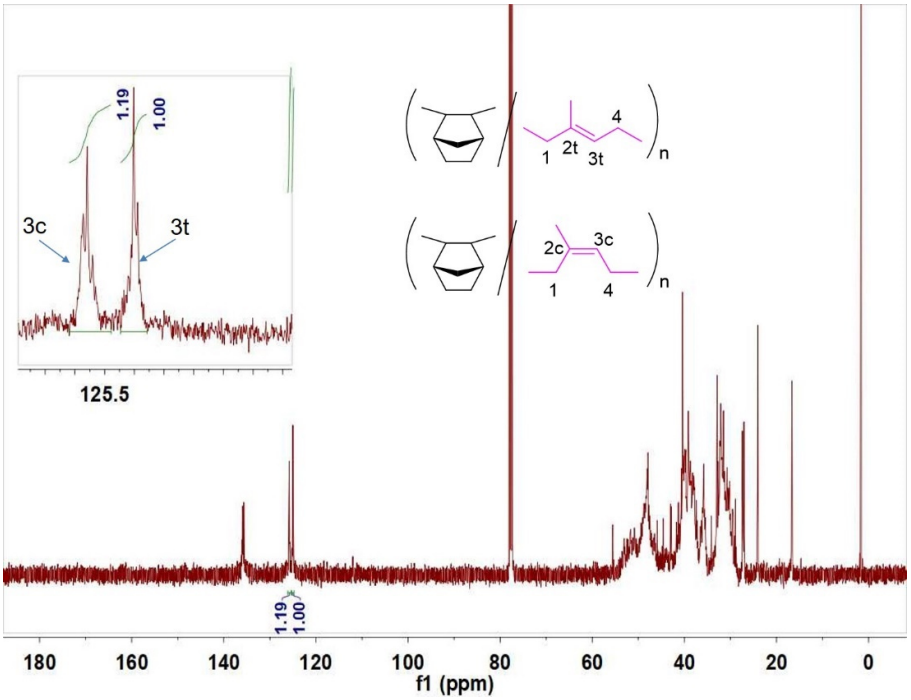

Figure 5-4d ^{13}C NMR spectrum of NB/IP copolymer obtained by Run 13.

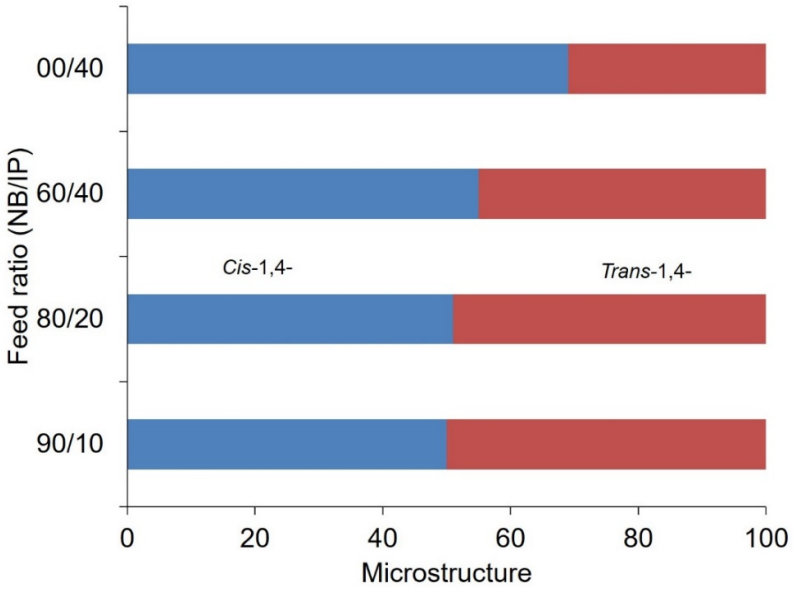

Figure 5-4e Feed ratio *vs* microstructure of NB/IP copolymer.

The NB/IP copolymer was further characterized by ^{13}C NMR (**Figure 5-4b**), and the signal appearing at 16 ppm (C^{10}), 27– 40 and 23.5 ppm ($C^{5–8,12}$), and 44–55 ppm ($C^{1–4}$) are assigned to the alkyl carbons of the NB and IP segments in the copolymer, respectively. The signals appearing in the range of 135.5 and 125 ppm ($C^{9,11}$) correspond to the olefin carbons.

The results indicate that NB was polymerized into copolymer via 2,3-addition, and the IP unit was inserted via 1,4-addition (**Figure 5-4a** and **5-4b**). According to the reported assignment of IP copolymer,[10] the isomer (*cis*- or *trans*-) can also be calculated from the ^{13}C NMR spectra of IP double bond (-C=C). Increasing the NB:IP ratio into the monomer feed from 9:1 to 6:4 causes the increase of *cis*-1,4-unit from 50 to 55 % (**Figure 5-4c, 5-4d and 5-4e**). It is

consistent with the result that *cis*-1,4-IP unit (69%) is dominant in the homopolymer obtained by complex **1a**. The NB/BD copolymers showed higher *cis*- unit then the NB/IP copolymers probably because of steric repulsion of methyl group of isoprene monomer.

The monomer reactivity ratios in the NB/BD and NB/IP copolymerizations catalyzed by **1a**-MMAO at 70 °C were determined by the Fineman-Ross method to be r_{NB} = 0.82 and r_{BD} = 0.037 for NB/BD copolymerization and r_{NB} = 0.52 and r_{IP} = 0.039 for NB/IP copolymerization, respectively (**Figure 5-5** and **5-6**). The monomer reactivity ratios indicate that NB prevailingly inserts at the diene-inserted nickel species. In some Runs, the conversions reached almost 30 %. Then, the remained comonomers and the comonomer ratios were calculated from the copolymer yield and the comonomer compositions. Which are shown in the **Table 5-4**. The results indicate that the comonomer ratios in feed were almost constant during the copolymerization. Thus, the Fineman-Ross method was applicable under these conditions.

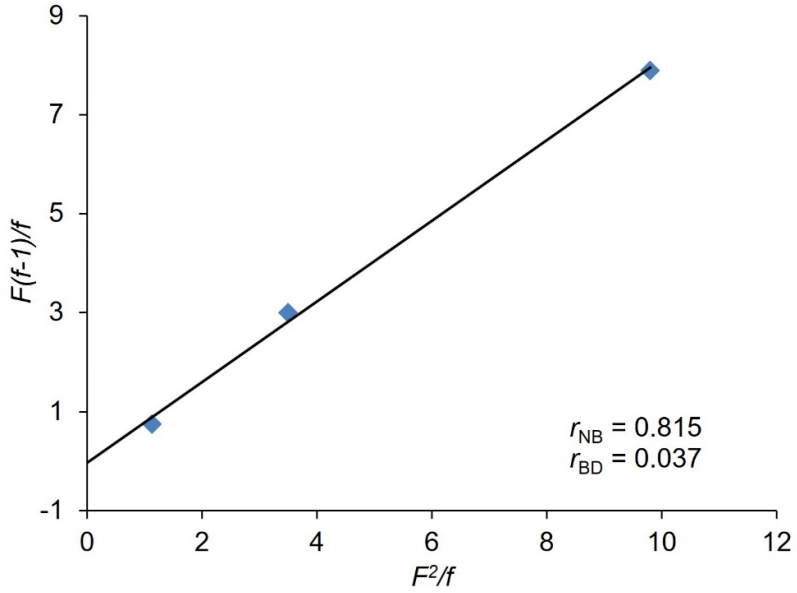

Figure 5-5. Fineman-Ross plots for NB/BD copolymerization by **1a** with MMAO.

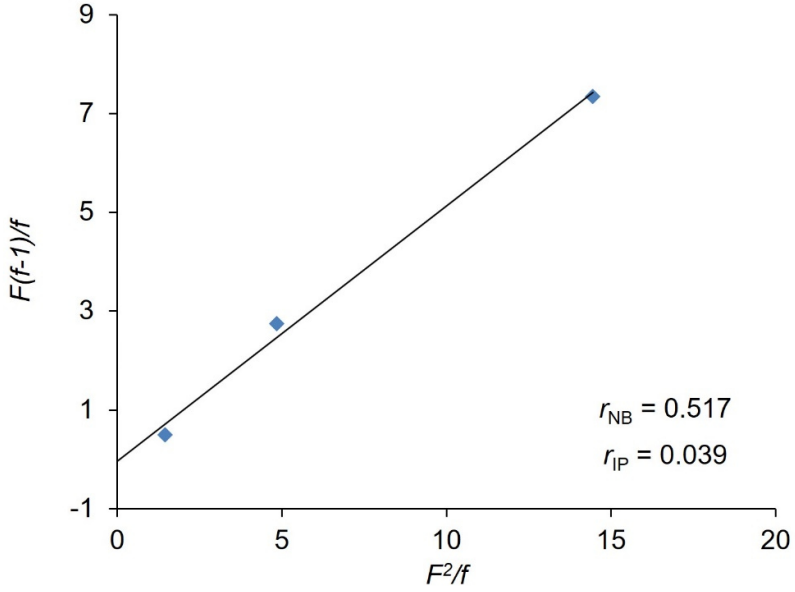

Figure 5-6. Fineman-Ross plots for NB/IP copolymerization by **1a** with MMAO.

Table 5-4. Copolymerization data of NB and CDN for Fineman-Ross plots

Run	NB	CDN	NB	CDN	NB	CDN	[NB]/[CDN] (mol/mol)	
	Polymer (mmol)				Remained (mmol)		Initial	final
1	11.3	1.4	0.25	0.28	33.7	3.6	9.0	9.3
2	7.2	1.4	0.18	0.14	32.8	8.6	4.0	3.8
3	2.1	1.0	0.07	0.05	27.9	19	1.5	1.5
11	8.1	1.4	0.18	0.27	36.9	3.6	9.0	10
12	5.2	1.3	0.13	0.15	34.8	8.7	4.0	4.0
13	1.5	1.0	0.05	0.05	28.5	19	1.5	1.5

Polymerization conditions: Ni = 5 μmol; Al/Ni = 100; time = 1 h; temperature = 70 °C, solvent = toluene (total volume 25 mL). f_{CDN} are the content of CDN in the NB/BD or NB/IP copolymer determining by ^{1}H NMR spectrum.

5-3-2. Effect of Time on NB/CDN Copolymerization

The influence of reaction time on NB/CDN copolymerization with the feed ratio 8/2 (NB/BD or NB/IP = 8/2 in molar ratio) was studied using **1a**-MMAO at 70 °C. The results are summarized in **Table 5-5**.

The yields of both copolymers were gradually increased with increasing the polymerization time from one to 3 h. The M_n values increased with increasing the copolymerization time with keeping almost the same CDN content and narrow molecular weight distribution (**Figure 5-7**).

Table 5-5. Effect of time on copolymerization of NB and CDN by **1a**-MMAO[a]

Run	Mono.	Time (h)	Yield (%)	Act. [b]	M_n [c] (10^3)	M_w/M_n [c]	f_{CDN} [d] (mol %)	T_g [e]
2	BD	1	17.5	150	33	1.3	16	178
20	"	2	32.6	140	43	1.3	17	176
21	"	3	46.6	133	51	1.2	17	177
12	IP	1	12.9	114	56	1.3	23	184
22	"	2	24.8	110	61	1.3	23	183
23	"	3	35.4	104	68	1.5	24	183

[a] Polymerization conditions: Ni = 5 μmol; norbornene = 40 mmol; BD = IP = 10 mmol; Al = 500 μmol; temperature = 70 °C; solvent = toluene (total volume 25 mL). [b] Activity = $kg_{(polymer)}\ mol_{(Ni)}^{-1}\ h^{-1}$. [c] Determined by GPC. [d] f_{CDN} are the content of CDN in the NB/BD or NB/IP copolymer determining by ^1H NMR spectrum. [e] Determined by DSC.

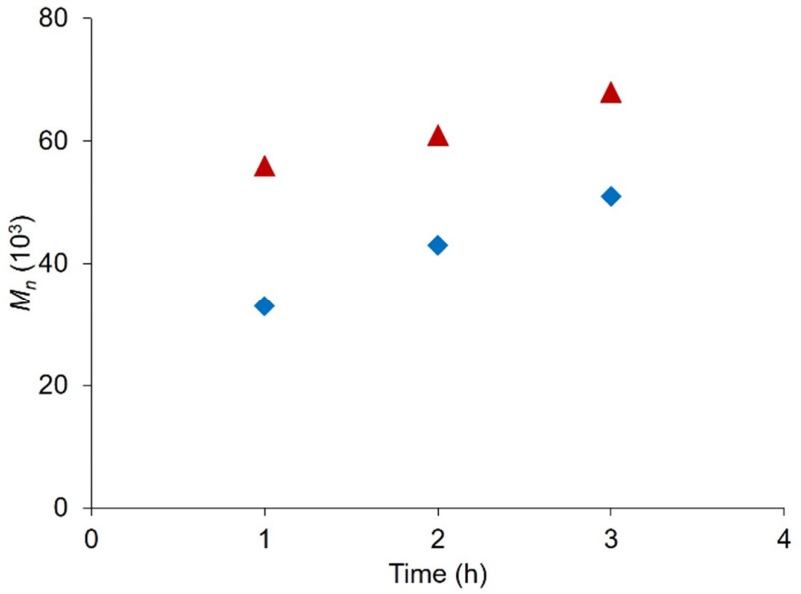

Figure 5-7. M_n vs time plot for NB/BD (◆) and NB/IP (▲) by Ni complexes.

5-3-3. Physical and Mechanical Properties of NB/CDN Copolymers

The glass transition temperature (T_g) of the copolymers were determined by DSC. The single T_g value was observed in each DSC curve in the range of 25 to 350 °C, indicating that NB and CDN were uniformly distributed in the NB/CDN copolymer obtain by the present catalysts. The T_g verses CDN content values are plotted in **Figure 5-8**, which clearly shows that the T_g value can be contorted by the diene content approximately between 100 and 200 °C (**Figure 5-9a** and **5-9b**).

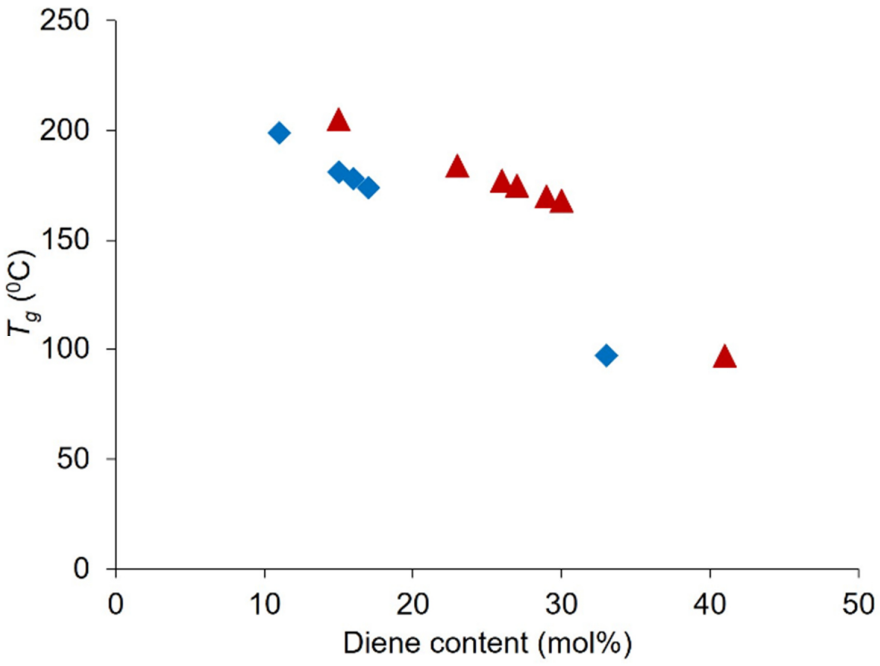

Figure 5-8. T_g vs diene content plot obtained by Ni complexes: (◆) NB/BD copolymers, (▲) NB/IP copolymers.

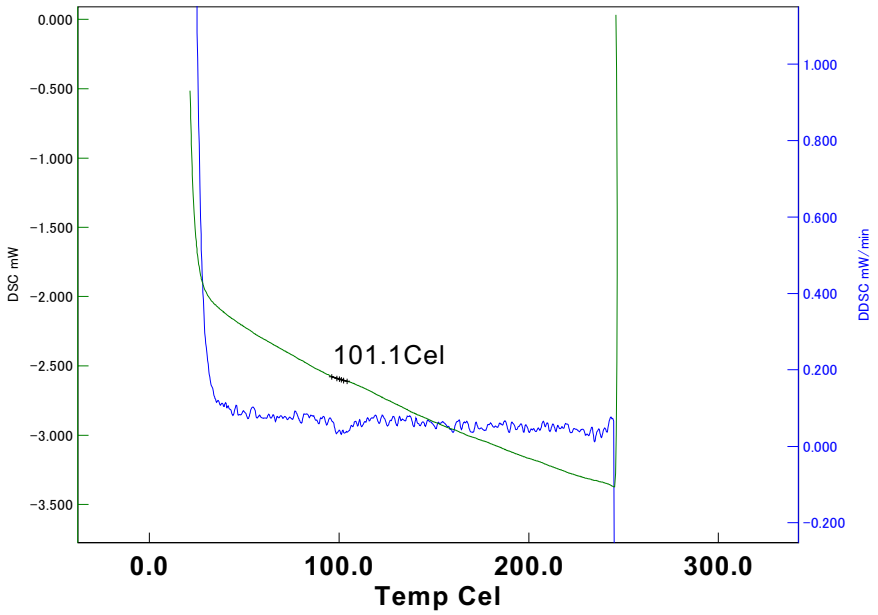

Figure 5-9a. DSC curve of NB/BD copolymer obtained in Run 3.

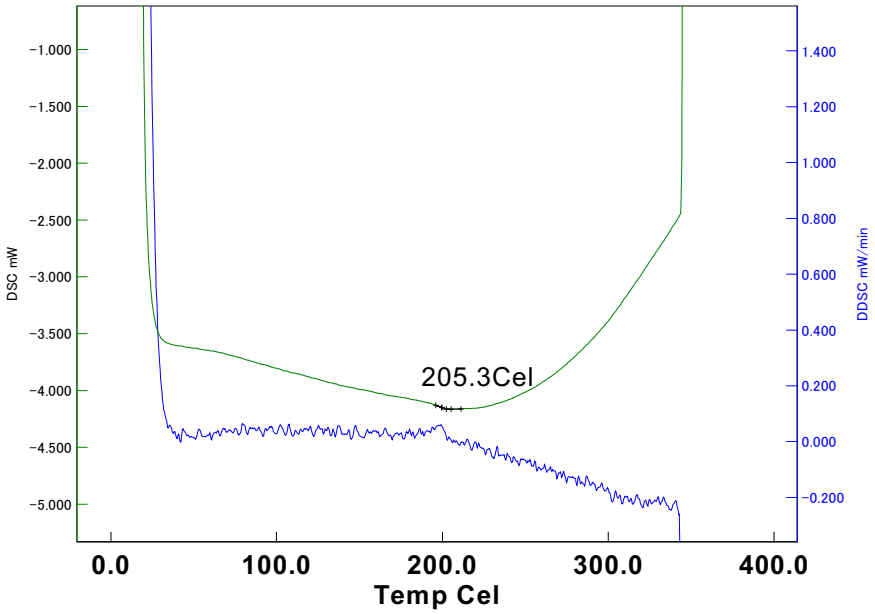

Figure 5-9b DSC curve of NB/IP copolymer obtained in Run 12.

The light transmittance of the films prepared from the NB/BD and NB/IP copolymers with the thickness of approximately 95 μm are displayed in **Figure 5-10**. Both copolymer films showed high light transmittance around 90% in the visible light region (350–800 nm).

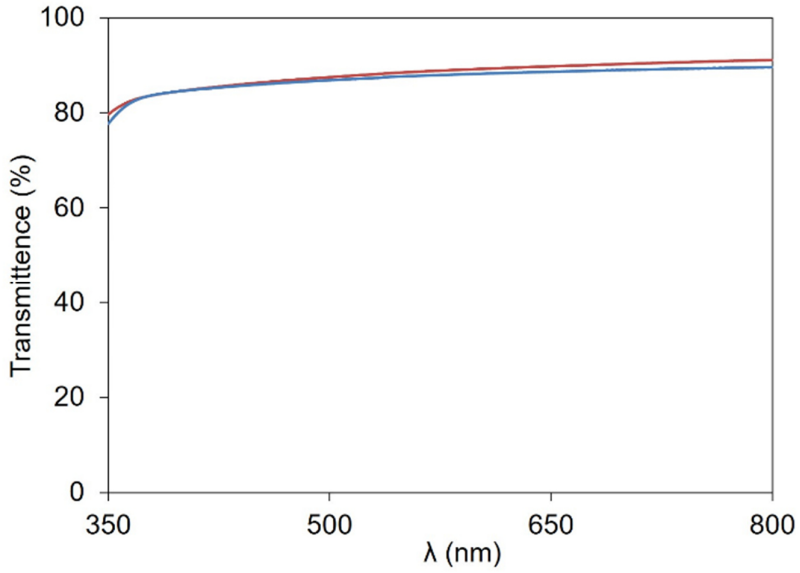

Figure 5-10. The light transmittance of the NB/BD (—) and NB/IP copolymer (—) thin films (93 and 97 μm) obtained by Run 1 and 12.

The mechanical properties were investigated by a universal testing machine (**Table 5-6**). All copolymers showed good flexibility. The highest elongation at break of NB/IP copolymer with 23 mol% of IP content was around 27% (**Figure 5-11)**.

Table 5-6 Mechanical properties of NB/CDN copolymers[a]

Sample	f_{CDN} (mol %)	T_g (°C)	σ (MPa)	ε (%)	E (GPa)
Run 1	11	199	63.6	11	2.6
Run 2	16	178	42.6	15	1.4
Run 11	15	205	46.9	13	1.6
Run 12	23	184	41.2	27	1.5

[a] Determined by tensile test, film thickness ≈ 0.1 mm. Stress at break (σ) and strain at break (ε), determined at fracture using uniaxial tensile test. Young's modulus (E), is the initial slop of the nominal stress and strain curve in the linier region.

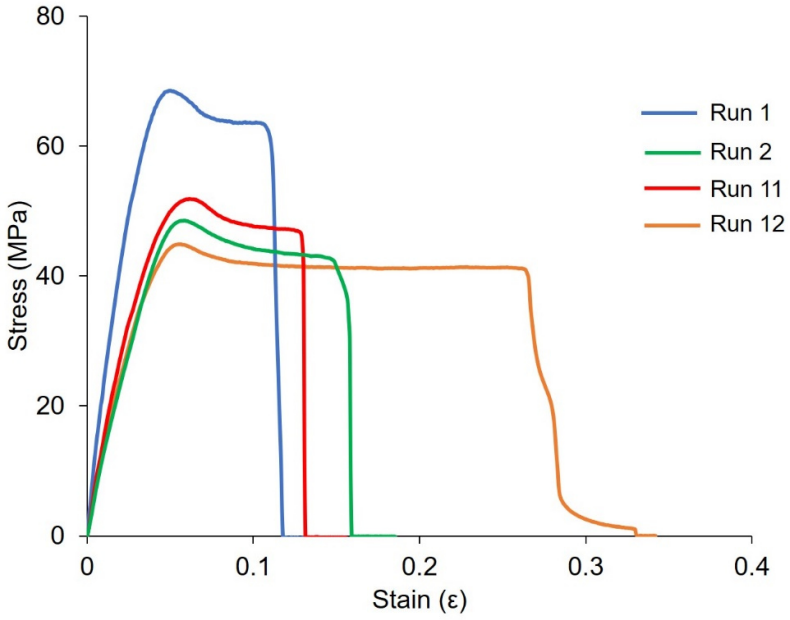

Figure 5-11 Stress vs stain curves of NB/CDN copolymer films.

5-4. Conclusion

Copolymerizations of NB and CDN were achieved by anilinonaphthoquinone-ligated nickel complexes using MMAO as cocatalyst. The catalysts showed good activity even in a long-time duration to give high molecular-weight copolymers with controllable diene contents. The highest BD incorporation of 33 mol% and the highest IP incorporation of 41 mol% were obtained at the NB:CDN ratio of 6:4. The T_g values were controlled in a wide range by differing the CDN contents. The introduction of CDNs improved the brittleness of COCs.

References

1. H. Suzuki, S. Matsumura, Y. Satoh, K. Sogoh, H. Yasuda, *React. Funct. Polym.* **2004**, *59*, 253–266.
2. S. Yamakawa, D. Takeuchi, K. Osakada, S. Takano, S. Kaita, *React. Funct. Polym.* **2019**, *136*, 19–24.
3. N. Yu, M. Nishiura, X. F. Li, Z. F. Xi, Z. M. Hou, *Chem. Asian. J.* **2008**, *3*, 1406–1414.
4. S. Q. Liu, G. X. Du, J. Y. Long, S. W. Zhang, X. F. Li, *Macromolecules* **2014**, *47*, 3567–3573.
5. X. Li, X. F. Ni, Z. Q. Shen, *Chem. J. Chin. Univ.* **2012**, *5*, 1095–1099.
6. J. Meng, X. Li, X. Ni, Z. Shen, *Polym. Int.* **2017**, *66*, 1617–1623.
7. J. Meng, X. Li, X. Ni, Z. Shen, *RSC Adv.* **2016**, *6*, 19351–19356.
8. H. Feng, X. Lu, W. Wang, G. N. Kang, W. J. Mays, *Polymers* **2017**, *9*, 494.
9. L. B. Canto, G. L. Mantovani, E. R. deAzevedo, T. J. Bonagamba, E. Hage, L. A. Pessan, *Polym. Bull.* **2006**, *57*, 513–524.
10. I. W. Cheong, C. M. Fellows, R. G. Gilbert, *Polymer* **2004**, 45, 769–781.

Summary

Catalysts play the key role in olefin polymerization. Especially nickel catalysts have garnered much attention because of their low oxophilicity, and correspondingly, the potential of realizing the copolymerizations of olefin with functionalized comonomers.

With the above point of view, norbornene copolymerization was studied with anilinonaphthoquinone-ligated nickel complexes [Ni($C_{10}H_5O_2NAr$)(Ph)(PPh_3): **1a**, Ar = C_6H_3-2,6-^{i}Pr; **1b**, Ar = C_6H_2-2,4,6-Me; **1c,** Ar = C_6H_5] in presence of activator.

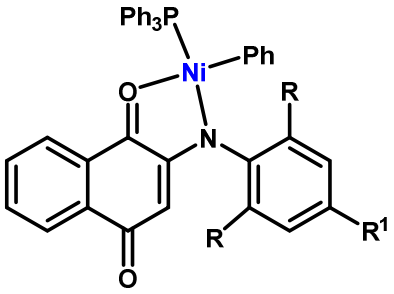

1a, R = $CH(CH_3)_2$, R^1 = H.
1b, R = R^1 = CH_3.
1c, R = R^1 = H.

Chapter I: General introduction

The history of transition metal catalysts for norbornene homo- and copolymerization with their potential application were described.

Chapter II: Copolymerization of Norbornene with Styrene using Anilinonaphthoquinone-Ligated Nickel Complexes

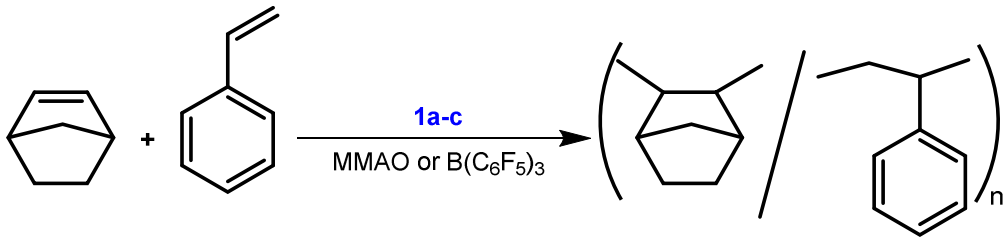

Scheme 6-1. NB/St copolymerization using Ni catalyst.

The nickel complexes **1** showed moderate activity for norbornene (NB)/styrene (St) copolymerization activated with MMAO (**Scheme 6-1**). Complex **1a**, which showed the highest activity in NB polymerization, also showed the highest activity in NB/St copolymerization among the complexes used.

The influence of reaction temperature on NB/St copolymerization was studied using **1**-MMAO at the fixed feeding ratio (NB/St = 4/1 in molar ratio), because the low St feed ratio gave high molecular weight NB/St copolymer. The copolymerization activity decreased with lowering the temperature from 70 to 0 °C. The highest activity around 70 $kg_{polymer}$ mol_{Ni}^{-1} h^{-1} for the copolymerization was achieved at 70 °C in each system. On the other hand, the St content and the M_n value monotonously increased with lowering the

polymerization temperature, and the NB/St copolymer with 32 mol % of St and 61,000 of M_n was obtained at 0 °C by **1c-**MMAO.

The NB/St copolymerization (NB/St = 4/1 in molar ratio) by the **1-**$B(C_6F_5)_3$ system, was conducted at different temperatures (30, 50, and 70 °C). The activity of the $B(C_6F_5)_3$ system was lower than that of the MMAO system but the St incorporation was almost four times higher than the **1-**MMAO system. The highest St incorporations of 51~59% were observed at 30 °C with the M_n values of 43,000~78,000. The addition of the reaction mixture of $^tBu_3Al$ and 2,6-$^tBu_2$-*p*-cresol as a scavenger increased the activity keeping the same St content and the M_n value reached 103,000 in the NB/St copolymerization with **1a**-$B(C_6F_5)_3$. The results indicate the potentiality of **1**-$B(C_6F_5)_3$ for NB/St copolymerization.

The highest T_g value of 329 °C, and the lowest value of 128 °C, were detected for the copolymers with 4 and 59 mol % of St, respectively. The copolymer film showed the transmittance above 85% in the visible light region.

Chapter III: Copolymerization of Norbornene with Substituted Styrenes using Anilinonaphthoquinone-ligated Nickel Complexes

Norbornene (NB)/*p*-substituted styrene (XSt) copolymerizations were carried out using nickel complexes **1** activated by MMAO in toluene with the

NB/XSt feed ratio of 4/1 at the copolymerization temperature from 0 to 70 °C (**Scheme 6-2**).

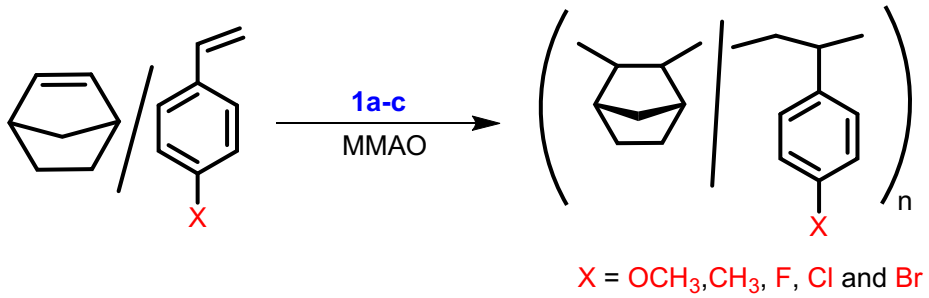

Scheme 6-2. NB/XSt copolymerization using Ni catalyst.

The yield increased with increasing the polymerization temperature and depended on the comonomer XSt as follows irrespective of the Ni complex, BrSt > ClSt > FSt > St ≥ MeSt > MeOSt. The M_n value and the XSt content were depended on the polymerization temperature and increased with lowering the temperatures. The lowest T_g value of 120 °C and the highest value of 365 °C were detected for the copolymers with 73 mol% of MeSt and 5 mol% of BrSt, respectively. All the copolymer films showed high transmittance around 90% in the visible light region (300–800 nm). Despite having a high T_g, the films of the halogenated functional copolymers displayed good flexibility at room temperature. The NB/MeSt copolymer showed low elongation at break, which was improved up to four-fold by the NB/FSt copolymer.

Chapter IV: Copolymerization of Norbornene with Divinylbenzene using Anilinonaphthoquinone-ligated Nickel Complexes

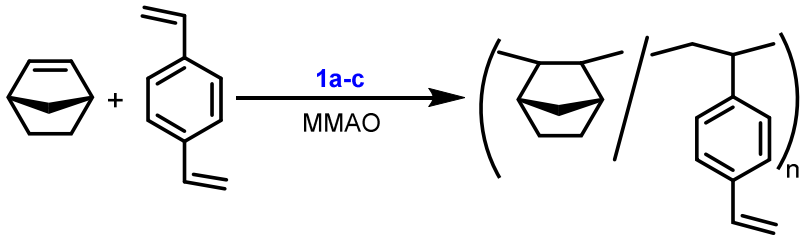

Scheme 6-3. NB/DVB copolymerization using Ni catalyst.

Copolymerization of NB and DVB was carried out using the nickel complexes **1** activated by MMAO (**Scheme 6-3**). The activity increased with decreasing the DVB ratio in feed. The activity of 220 $kg_{polymer}$ mol_{Ni}^{-1} h^{-1} was obtained for NB/DVB copolymerization using **1a** with the DVB ratio of 5 mol% at 70 °C. The activity of NB/DVB copolymerization exhibited a rapid increase with increasing the polymerization temperature from 0 to 70 °C. The M_n value and the DVB content were depended on the polymerization temperature and increased with lowering the temperatures. The copolymer yield increased with increasing the polymerization time from 1 to 3 h without crosslinking.

The styryl group of poly(NB-*co*-DVB) was transferred to epoxy and dihydroxy groups by *m*-CBPA at room temperature and the hydrolysis of the epoxy at 90 °C (**Scheme 6-4**). The functional NB/DVB copolymer showed higher solubility in $CHCl_3$ than the NB/DVB copolymer.

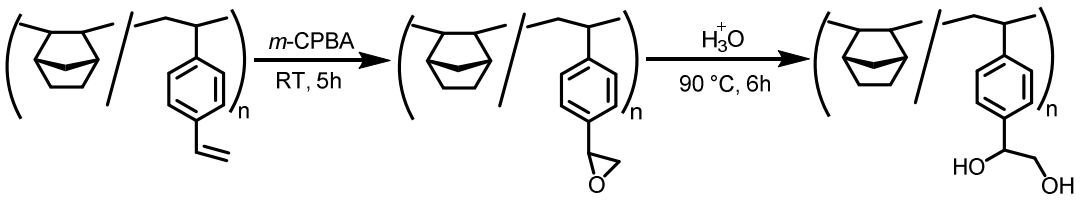

Scheme 6-4. Styryl group modification of poly(NB-*co*-DVB).

The graft polymerization of MMA from poly(NB-*co*-DVB) was achieved by RATRP using AIBN in the presence of $CuCl_2$ and bipyridine (**Scheme 6-5**).

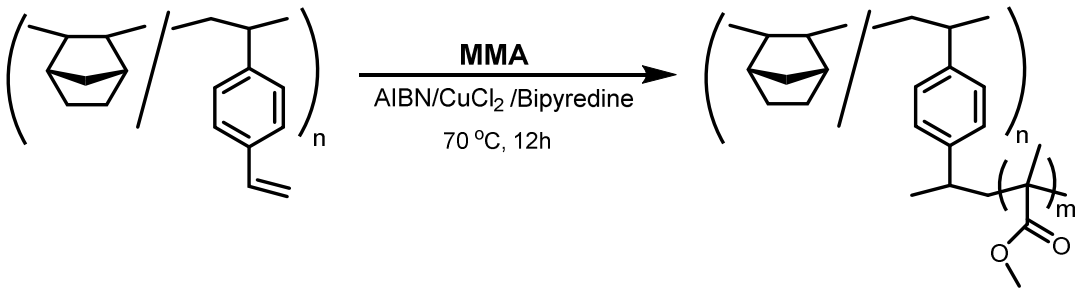

Scheme 6-5. Graft polymerization of MMA from poly(NB-co-DVB) using AIBN.

The films prepared from poly(NB-*co*-DVB) and poly(NB-*co*-DVB)-*graft*-PMMA films showed light transmittance around 85% in the visible light region. Poly(NB-*co*-DVB)-*graft*-PMMA showed lower stress value and higher flexibility than poly(NB-*co*-DVB).

Chapter IV: Copolymerization of Norbornene and Conjugated Dienes using Anilinonaphthoquinone-ligated Nickel Complexes

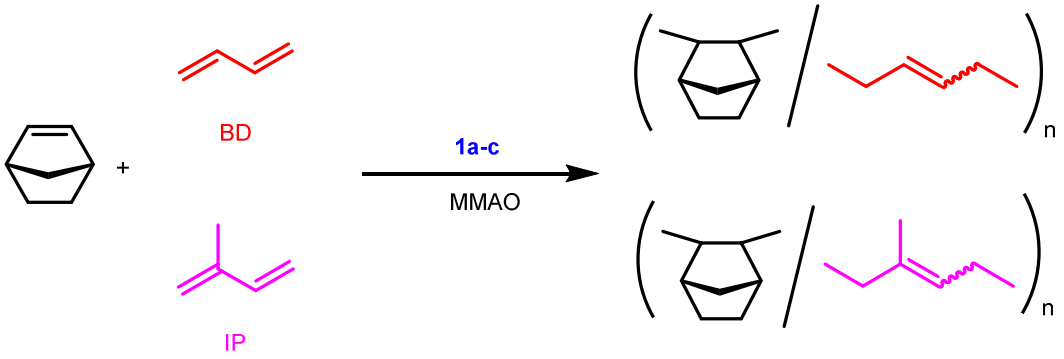

Scheme 6-6. NB/CDN copolymerization using Ni catalyst.

Copolymerizations of NB and CDN (BD or IP) were carried out using the nickel complexes activated by MMAO (**Scheme 6-6**). The yield increased by changing the NB:CDN ratio from 6:4 to 9:1. The yield of NB/CDN copolymerization exhibited a rapid increase with increasing the polymerization temperature from 30 to 70 °C and the conversion of NB/BD copolymerization was higher than that of NB/IP copolymerization.

The M_n value were increased and the CDN content slightly enhanced with lowering the temperatures. The yields of both copolymers were gradually increased with increasing the polymerization time from 1 to 3h. Accompanied by the increases of M_n values with keeping the CDN content and narrow molecular weight distribution. The T_g value was contorted by the CDN content

approximately between 100 and 200 °C. Both copolymer films were transparent in the visible light region (around 90%) and flexible.

The mechanical properties of the copolymers synthesized in this research work is compared and the highest elongation break value was observed for NB/IP copolymers (**Figure 6-1**).

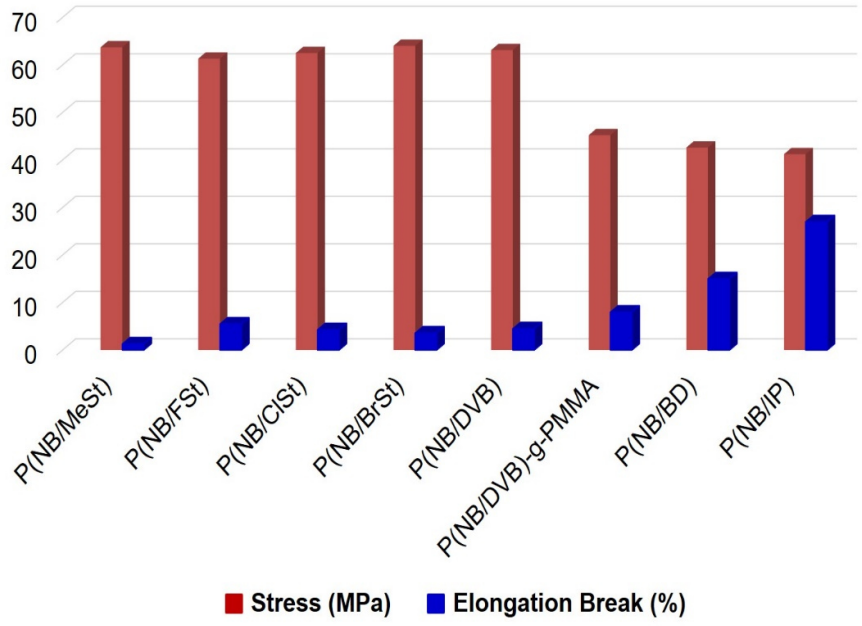

Figure 6-1. Mechanical properties comparison of the synthesized copolymers in this research.

This thesis has shown the potentiality of anilinonaphthoquinone-ligated nickel complexes as a precatalyst for the copolymerization of norbornene with conjugated hydrocarbon monomers, i.e., styrene, *p*-substituted styrene derivatives, butadiene and isoprene, to produce novel copolymers with high molecular weight and improved properties. Judging from the activity and the properties of the copolymers, the norbornene/halogenated styrene copolymers should be the most promising materials among the copolymers obtained. From the viewpoints of the accessibility of comonomer as well as the properties of the copolymers, the norbornene/diene copolymers are also interesting.

Compared with the catalysts for ethylene or propylene polymerization, however, further improvement of the activity is necessary for the copolymerizations. The author hopes that this thesis would give some information for the research to develop the catalysts for the copolymerizations.

List of Publication

Chapter II

Copolymerization of Norbornene and Styrene with Anilinonaphthoquinone-ligated Nickel Complexes

Samiul Islam Chowdhury, Ryo Tanaka, Yuushou Nakayama, Takeshi Shiono

Polymers **2019**, 11, 1100 (1-10)

Chapter III

Coordination-insertion Copolymerization of Norbornene and *p*-Substituted Styrenes using Anilinonaphthoquinone-ligated Nickel Complexes.

Samiul Islam Chowdhury, Ryo Tanaka, Yuushou Nakayama, Takeshi Shiono

Macromolecular Chemistry and Physics **2020**, *221* (5), 1900494 (1-7).

Chapter IV

Copolymerization of Norbornene and Divinylbenzene using Anilinonaphthoquinone-ligated Nickel Complexes and Its Application for Synthesis of Functional Copolymer and Graft Polymerization

Samiul Islam Chowdhury, Ryo Tanaka, Yuushou Nakayama, Takeshi Shiono

Submitted in *Journal of Polymer Science*

Chapter V

Copolymerization of Norbornene and Conjugated Dienes using anilinonaphthoquinone-ligated Nickel Complexes

Samiul Islam Chowdhury, Ryo Tanaka, Yuushou Nakayama, Takeshi Shiono

Polymer **2020**, *187*, 122094 (1-6)

Presentation in Internal Conference

Coordination-insertion Copolymerization of Norbornene and Substituted Styrenes using Anilinonaphthoquinone-ligated Nickel Complexes

Samiul Islam Chowdhury, Ryo Tanaka, Yuushou Nakayama, Takeshi Shiono

The 12th SPSJ International Polymer Conference (IPC2018), **2018**, (Hiroshima, Japan)

Copolymerization of Norbornene and *p*-Substituted Styrenes using Anilinonaphthoquinone-ligated Nickel Complexes

Samiul Islam Chowdhury, Ryo Tanaka, Yuushou Nakayama, Takeshi Shiono

The 8th Asian Polyolefin Workshop, **2019**, (Hiroshima, Japan)

Presentation in Domestic Conference

Copolymerization of Styrene and Norbornene using Anilinonaphthoquinone ligated Nickel Catalysts

Samiul Islam Chowdhury, Ryo Tanaka, Yuushou Nakayama, Takeshi Shiono

Polymer Preprints, Japan Vol. 66, No. 2 (1Pf032) **2017**

Copolymerization of Norbornene with Halogen-substitued Styrenes Catalyzed by Anilinonaphthoquinone-ligated Nickel Complexes

Samiul Islam Chowdhury, Ryo Tanaka, Yuushou Nakayama, Takeshi Shiono

Polymer Preprints, Japan Vol. 67, No. 2 (2B15) **2018**

Copolymerization of Norbornene and Conjugated Dienes using anilinonaphthoquinone-ligated Nickel Complexes

Samiul Islam Chowdhury, Ryo Tanaka, Yuushou Nakayama, Takeshi Shiono

Polymer Preprints, Japan Vol. 68, No. 1 (2Pb002) **2019**

Copolymerization of norbornene and divinylbenzene using anilinonaphthoquinone-ligated nickel complexes and its application for synthesis of graft copolymers

Samiul Islam Chowdhury, Ryo Tanaka, Yuushou Nakayama, Takeshi Shiono

Polymer Preprints, Japan Vol. 68, No. 2 (2Pd006) **2019**

Acknowledgement

The research work presented in this thesis has been carried out at polymer chemistry laboratory, Department of applied Chemistry, Hiroshima University, under the supervision of **Professor Takeshi Shiono.**

First of all, I would like to express my immense gratitude and pleasure to **Professor Takeshi Shiono,** for his sincere guidance and helpful discussion throughout the duration of this research work. Never could this study have been continued without his kind guidance and cooperation.

I convey my heartiest gratitude to Dr. Yuushou Nakayama, Associate Professor and Dr. Ryo Tanaka, Assistant Professor, Hiroshima University, for helpful suggestions and continues support for my research work.

I also owe my deeper gratitude to Professor Tariqul Hasan, Department of chemistry, Rajshahi University, for his kind cooperation.

I greatly acknowledge the assistance provided by all laboratory members of Polymer Chemistry at Hiroshima University for their helpful cooperation.

I am indebted miles and miles to my parents because their praying to Almighty (ALLAH) and blessing has brought me toward today's platform. Finally, this research work has been made possible due to all out sacrifice endured by my wife Lamya Zahir**,** I find no words fit to express my gratitude to her.

January 2020

MD. SAMIUL ISLAM CHOWDHURY